1997

Attenuated poliovirus bacteriophage and bromide transport through a coarse-grained aquifer western Montana

Quinn T. Kiley
The University of Montana

Attenuated Poliovirus, Bacteriophage, and Bromide Transport Through a Coarse-Grained Aquifer, Western Montana.

by

Quinn T. Kiley

B.S., Washington & Lee University, Lexington, Virginia

Presented in partial fulfillment of the requirements for the

degree of Master of Science.

University of Montana

April, 1997

Approved by:

Chairman, Thesis Committee

Dean, Graduate School

5-19-97

Date

Quinn T. Kiley, M.S., April 1997 Geology

Attenuated Poliovirus, Bacteriophage, and Bromide Transport Through a Coarse-Grained Aquifer, Western Montana.

Chairman: Dr. William W. Woessner

Abstract WWW 5-19-97

Microbial contamination of groundwater supply wells causes 50% of the outbreaks associated with waterborne diseases each year. The transport of the bacteriophages MS2, PRD1, ∅X174, the attenuated enterovirus poliovirus type-1 (CHAT strain), and bromide in a cold water, sand and gravel aquifer was studied under natural gradient conditions near Missoula, MT. The average transport velocity for bromide was 25-30m/d. Bacteriophages were observed at concentrations of 10^3 PFU/ml 40.5m from the injection well. After 8 hours of transport approximately 97% of the injected attenuated poliovirus and 35-79% of the bacteriophages adsorbed to the aquifer material. Although adsorption occurs, a portion of the viruses appears to act conservatively creating breakthrough curves similar to bromide, though with long tails. Virus were persistent, as seeded viruses were observed 185 days after injection.

Acknowledgments

I would like to thank the National Water Resources Institute and the US EPA for their joint funding of this research. The Montana State Fish, Wildlife, and Parks Department was instrumental in allowing us access to the Erskine site, without which none of this work would have been possible.

My utmost thanks goes to Bill Woessner for guiding me throughout this project. He gave me a controlling hand at the field site, but was wary of whether or not everything was "under control". Bill's editing, seemingly continuous, I hope has resulted in clear document that truly expresses the breadth and scope of the work we did at the Erskine site. Dan DeBorde, who kept us hydrogeologists from losing sight of the virological aspect of the study, and whose work in the laboratory with PhD. candidate Pat Ball was both laborious, productive, and efficient. Johnnie Moore who served on the committee and in the midst of all of his other commitments was willing to help me through my tenure in Missoula.

I would be doing a great injustice if I did not mention the legions of students who aided me in the field and the laboratory, sampling and analyzing, and instrumenting the sight. Lynn Biegelsen, who was always ready for another tracer test. Loreene Skeel and Judy Fitzner who helped me wade through the bureaucracy and stay afloat for two years.

Table of Contents

List of Figures

List of Tables

List of Appendices

1. Introduction

Microbial contamination of groundwater supplies causes over half the waterborne disease outbreaks in the United States (Keswick and Gerba, 1980). Wellhead protection from microbial contamination, especially viruses, has been a major topic of research in recent years (Welling et al, 1975; Mathess and Pekdeger, 1981; Pekdeger and Mathess, 1983; Bitton et al, 1984; Yates et al, 1985; Jansons et al, 1989a,b; Bales et al, 1995; Rossi et al, 1994). These studies have led to a greater understanding of the physical and chemical factors controlling the transport and survival of viruses in groundwater. Temperature, pH, adsorption, and dispersion have been identified as major controls of virus fate and transport. Lower groundwater temperature allows for greater persistence of viruses (Yahya et al, 1993; Yates and Yates, 1987). Groundwater pH has been reported to influence virus adsorption. Viruses more readily adsorb to sediments when the groundwater pH is less than 5 and adsorb less effectively when the pH is greater than 5 (Goyal and Gerba,1979; Bales et al, 1993). In addition to the varying chemical characteristics in an aquifer, one virus strain will adsorb more strongly to an aquifer matrix than another under identical conditions because of the differences in viral surface properties (Goyal and Gerba, 1979). The mechanism of adsorption as described by Gerba(1984) results from the virus adsorbing ions onto its surface layer and then affixing to an oppositely charged medium, the aquifer material. The lowering of pH decreases the thickness of the layer of ions, allowing van der Waals forces to effectively bond the virus to the dispersive medium (Gerba, 1984).

Though these basic transport and survival processes have been documented for indicator bacteriophages and some strains of poliovirus in laboratory settings, relatively few multiple virus seeding experiments have been conducted at the field scale (Alhajjar et al, 1987; Jansons et al, 1989a,b; Bales et al, 1989; Bales et al, 1995; Rossi et al, 1994). Unfortunately, field assessments often include insufficient hydrogeologic data to allow reasonable transferability of study results to similar hydrogeologic settings. In addition, research completed in well characterized sand and gravel dominated aquifers is costly (weeks of sampling and complex assay procedures). As a result, well documented virus plumes and peaks have been limited to about a 15m travel distance (Bales et al, 1995). These limitations have forced regulators assessing the adequacy of existing and proposed set back distances used to protect groundwater supply wells to extrapolate the available data by applying poorly calibrated predictive models (HydroGeoLogic, 1994a, 1994b; Yates and Yates, 1989; Macler, 1995; Macler and Pontius, 1995; U.S. EPA, 1994).

This work documents the behavior of four viruses seeded into a well characterized cold water, highly conductive, unconfined aquifer. The experiment design and site conditions allowed for: 1) rapid collection of tracer data (72 hr.), 2) control of virus inactivation, 3) detailed resolution of the virus plumes and peak travel times. The hydrogeologic setting was chosen to represent a "worst case" scenario for virus transport through unfractured porous media, permitting direct observation of transport over the suggested 30m separation between a virus source and a water supply well. The field experiment included the simultaneous injection of the bacteriophages MS2, PRD1, and ∅X174, and attenuated poliovirus type-1 (CHAT strain). The CHAT strain of polio is attenuated and not pathogenic. It is similar to the Sabin live vaccine in that it is alive and infectious, but has been altered so as to not cause the disease poliomyelitis. The migration of the viral plume through the sampling well network was monitored for 72hrs. Virus transport was observed over a distance of 40 m, with a 6 log reduction in the titer over that distance.

2.0 Methods

2.1 Site Description

The study was conducted in the grassland flood plain of the Clark Fork River at the Erskine Fishing Access near Missoula, MT. (Figure 1). The shallow, unconfined, flood plain aquifer contains clast supported cobbles and gravel with a medium- to coarse-grained sand matrix to a depth of 6m, where the aquifer material fines and becomes predominantly sand. The hydrologic properties were determined from tracer tests and aquifer tests (Table 1). The water table varied between 2.1 to 2.5m below ground surface. The 10°C groundwater is a calcium bicarbonate type (Appendix B).

2.2 Field Methods

An area of 240m by 285m was instrumented with 89 monitoring wells and 10 staff gauges in low lying areas and sloughs (Appendix C). Seven tracer tests using bromide and rhodamine-wt were used in conjunction with water table maps constructed from monthly head measurements to determine the south westerly flow path in the vicinity of injection well I4 (Appendix D). The multilevel monitoring well network was designed such that the tracer would pass through the arcs of multilevel monitoring wells at distances of 7.5, 19.5, 30, and 40.5 m from injection well I4 (Figure 2). Each multilevel monitoring well was built with 0.5cm diameter high-density polyethylene (HDPE) tubing affixed to a 1.3cm diameter PVC pipe. These sampling ports are 1.8, 2.7, 3.6, and 4.5m below the surface. The tubing

Figure 1. Erskine Research Site near Missoula, MT.

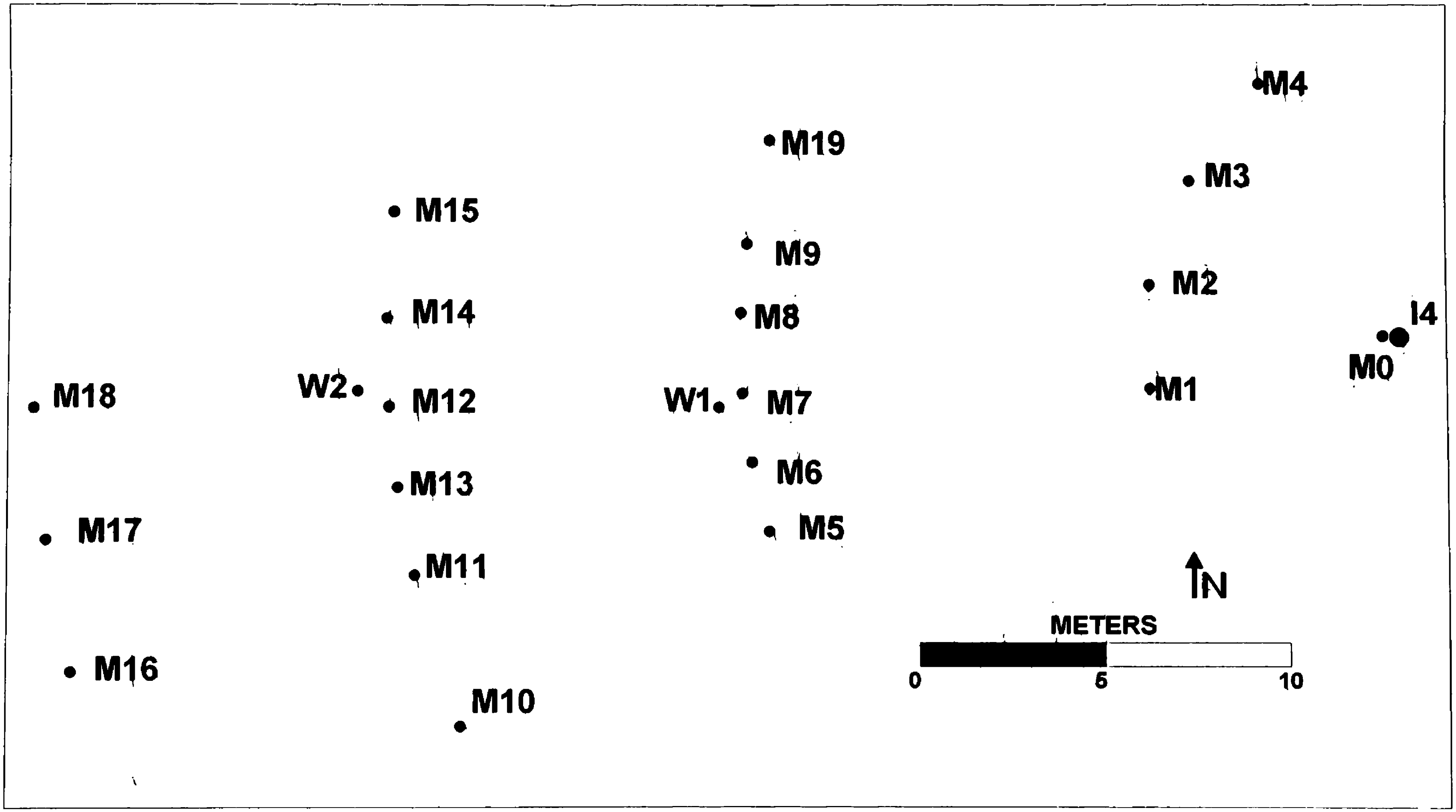

Figure 2. Sampling well network consisting of 20 multilevel wells (M) in arcs 7.5, 19.5, 30, and 40.5m from injection well I4.

Table 1. Aquifer characteristics

Hydrologic Properties			Water Chemistry	
Porosity	0.2		Water Type	Calcium, Bicarbonate
Gradient	0.00043		Spec. Conductivity	288 mS/cm^2
Avg. K (m/d)	400-45,000		DO	3.5 mg/l
GW Velocity (m/d)	27		pH	7.2
			Temp. (C)	10.3

Table 2. initial concentration of injected tracers

MS2	PRD1	ΦX174	Attenuated Polio	Bromide
PFU/ml	PFU/ml	PFU/ml	PFU/ml	mg/l
5.60E+10	5.40E+09	2.90E+07	3.40E+06	1143

was perforated over 5cm and screened with nylon mesh (Appendix C). Flexible tubing was dedicated to each piece of HDPE for use with a peristaltic pump.

The multiple virus seeding was preceded one week by a bromide tracer test. In both tests 18.9 liters of groundwater from a background well up gradient from the injection well were used to create the tracer solution. The solution was gravity drained into injection well I4 over a period of 10 to 12 minutes. Injection well I4 is a 3.18cm diameter steel sand point screened from 2.1 to 2.7m. Initial concentrations of the tracers injected are shown in Table 2. Prior to virus injection, the use of the selected viruses was approved by the University Biohazards Committee, Missoula City-County Health Department, Montana Department of Environmental Quality, and Region 8 EPA. In addition, a Montana Environmental Impact Statement was submitted at the request of the land steward, Montana Department of Fish, Wildlife, and Parks.

Sampling for the tracer experiments covered a 36 hr period for bromide, and a 72 hr period for the virus seeding. Samples were collected with peristaltic pumps from I4 and all 20 multilevel monitoring well ports at the 2.7, 3.6, and 4.5m depths; which corresponded to 0.6, 1.5, and 2.4m below the water table. The sampling schedule was designed to capture expected peak arrivals at each arc of wells. Wells were sampled from expected lowest concentration to expected highest concentration to further reduce the risk of cross contamination. Bromide samples were collected in HDPE 50 ml bottles, filtered (0.45 μm) and analyzed using a standard ion chromatography technique (Pfaff, 1993). An analytical error of 2% was calculated for the ion chromatography technique used. Bromide concentrations were reported in mg/l to an instrument detection limit of 0.01mg/l. Virus samples were collected in sterile 50 ml polypropylene tubes, immediately placed on ice, and transported in ice-filled coolers to the laboratory where they were stored at 4° C.

2.3 Analytical Methods

The coliphages MS2, PRD1, and ∅X174 were assayed using host bacteria specific to each virus. A single layer assaying method was employed to assay all three coliphages because of its relative simplicity and efficiency (Adams, 1959). The single agar procedure was performed as follows: 1) host cultures were grown to mid-log phase and placed on ice to quench any further growth; 2) 1ml of host bacteria was added to 10ml. of sample (groundwater) and placed in a 37° C water bath for 3 to 5 minutes; 3) 11ml. of soft agar was added to the sample and bacteria mixture; 4) 10ml. of the mixture was plated onto each of two 100mm petri dishes. After the agar sets the dishes were inverted in a 37°C incubator. The titer in plaque forming units per milliliter (PFU/ml) was then determined by counting the number of plaques on the plates. The detection limits for the assay of the bacteriophages is 1 virus in 10ml of sample.

Although not reported in the majority of previously published virus transport papers, there is significant error associated with the infectious assay for bacteriophages. Analysis of 10 duplicate samples from a single sampling port permitted error calculations to confidence levels of 95%. A minimum error of 15% was calculated for the assay of bacteriophages. Error was calculated using the standard method for examinations of water and waste water (Eaton et al, 1995).

Prior to assay for attenuated poliovirus, 5 to 7ml. of field sample were filtered through a 0.45 micron filter and diluted in ELAH at a 1:1 dilution. These samples were stored in 15 ml polypropylene tubes at -70° C. The use of controls showed that this procedure had no detrimental effects on the virus recovery and did not lower the titer.

The attenuated poliovirus was assayed on 3 to 5 day old Buffalo Green Monkey Kidney (BGM) cells that were grown in 25 cm^2 tissue culture flasks (Smith and Gerba, 1982). The cells were prepared for the assay with the proper adjustments made to compensate for the difference in the volumes of tissue culture flasks. One ml of sample, diluted one to one with ELAH containing antibiotics without calf serum, was added to BGM cells. The inoculum was exposed to the BGM host cells for 90 minutes at room temperature to initiate viral attachment. The 1 ml inoculum was then removed and 10ml. of an agar-medium overlay was added to the flasks. The agar-medium overlay was held in a 41° C water bath during use. After the overlay was added, the flasks were covered to protect them from light and allowed to harden before they were inverted and put in a 37° C incubator. The flasks were monitored for five days, with plaques counted on a daily basis. The titer was then determined when plaque development was complete. The detection limit of this method is 1 virus in 2ml of sample.

Analytical errors were calculated for the infectious assay of attenuated poliovirus with the same methods used for the bacteriophages. Minimum error is not known, but an estimated minimum of 20% is used here.

A mass balance was performed using the 8 hour data for the virus and bromide plumes. There was no tracer detected at the 3.6m sampling port, 1.5m below the water table. An area bounded by two lines of known concentration was calculated. The concentration of that area was the average of the known concentration boundaries delineating the area. Using an estimated aquifer porosity of 0.20 and assuming the plume was 0.9m thick, the amount of tracer in aqueous phase was determined (Johnson, 1992).

3. Results

A bromide tracer was injected at the water table using well I4 on September 22, 1996. The viruses MS2, PRD1, ∅X174, and attenuated poliovirus type-1 (CHAT strain) were also injected at the water table, one week later on October 2, 1996, using well I4. The plume centers for both injections passed through wells M2, M7, M14, and M17. The transport of viruses through groundwater is controlled by all the hydrologic properties of the aquifer, and the sorptive nature of the virus itself. The viruses moving through the aquifer that are not adsorbed onto the aquifer material are affected by mechanical dispersion. The longitudinal dispersivity was determined to be 0.42m using a Peclet number of 18 based on the breakthrough data for well M2, located 7.5m from well I4 (Sauty, 1980). Transverse spreading properties were not calculated.

Plume sizes and peak concentrations varied partly as a function of initial concentration. The plumes for all viruses and Br^- showed slight vertical migration, with a maximum of 1.8m over 30m of horizontal transport. The lowest sampling port (4.5m depth) was generally below the plume and served to establish a vertical zero concentration boundary. The 2hr sampling frequency and well locations permitted identification of plume distribution, peak arrivals, and determination of transport rates.

Previously observed dispersion of bromide and virus tracers and their resulting distribution and concentrations at this site suggested sampling over a 36hr period for bromide and a 72hr period for viruses would capture the peak arrivals throughout the sampling network. Virus inactivation was determined to be insignificant in this aquifer over the short duration of the test. A vial filled with groundwater from the site and a known concentration of seeded virus was immersed in an unused well for the duration of the experiment. No change in concentration over the 72hr experiment was detectable.

The concentration of virus injected into I4 declined more rapidly than bromide over time (Figure3). The concentration of bromide declined one log in 28hr, where the poliovirus concentration dropped one log in 5hr. The bacteriophage concentrations declined one log in 15-20hr

The sampling plan effectively captured the tracer concentrations as the plumes moved through each arc of wells, and away from I4 (Figure 3). Peak arrival times at a given well were similar for the four viruses. The bromide peak appears to arrive after the virus peaks during the first 7.5m of transport (Table 3; Figure 4). Due to the error associated with measuring tracer concentrations, peak identification can be difficult. At monitoring well M2 definable virus peaks were observed, but the peak arrival time for bromide cannot be accurately identified. Analysis of breakthrough curve data collected at well M2 suggest that poliovirus is transported faster than bromide and the bacteriophages. The peak arrival of attenuated poliovirus occurs two hours prior to the arrival of the bromide and bacteriophage peaks. Peak arrival times for each tracer could not be distinguished due the over lap of error bars at maximum concentrations at wells M7 and M14 (Figure 5, 6). Therefore, a range of transport rates for the peaks was calculated at these wells (Table 3). A similar approach was used to interpret peak arrivals at well M17. Trace concentrations of bromide and attenuated poliovirus were sporadically detected in the wells at the 30m and 40.5m arcs, but breakthrough curves could not be constructed due to paucity of data (Figures 6, 7).

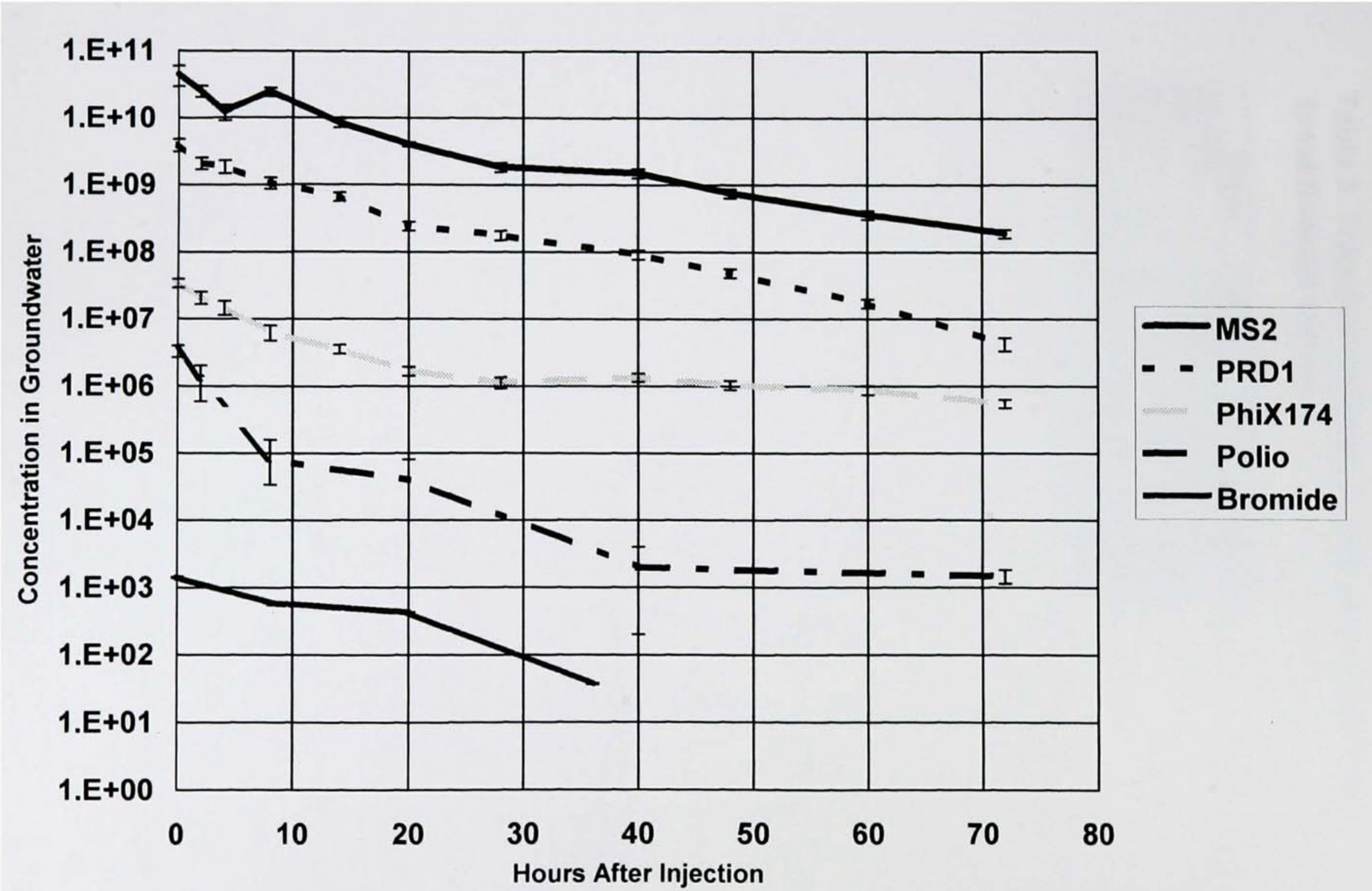

Figure 3. Concentration reduction with time for injection well I4. Virus concentrations in PFU/ml, bromide concentrations in mg/l.

Table 3. Transport velocities (m/d) calculated from breakthrough curves

Tracer	M2 7.5m	M7 19.5m	M14 30m
Bromide	22.5-30	26-29.25	NA
MS2	30	23.4-39	25.7-36
PRD1	30	26-39	36
ΦX174	30	33.4-39	18-36
Attenuated Polio	45	33.4-58.5	NA

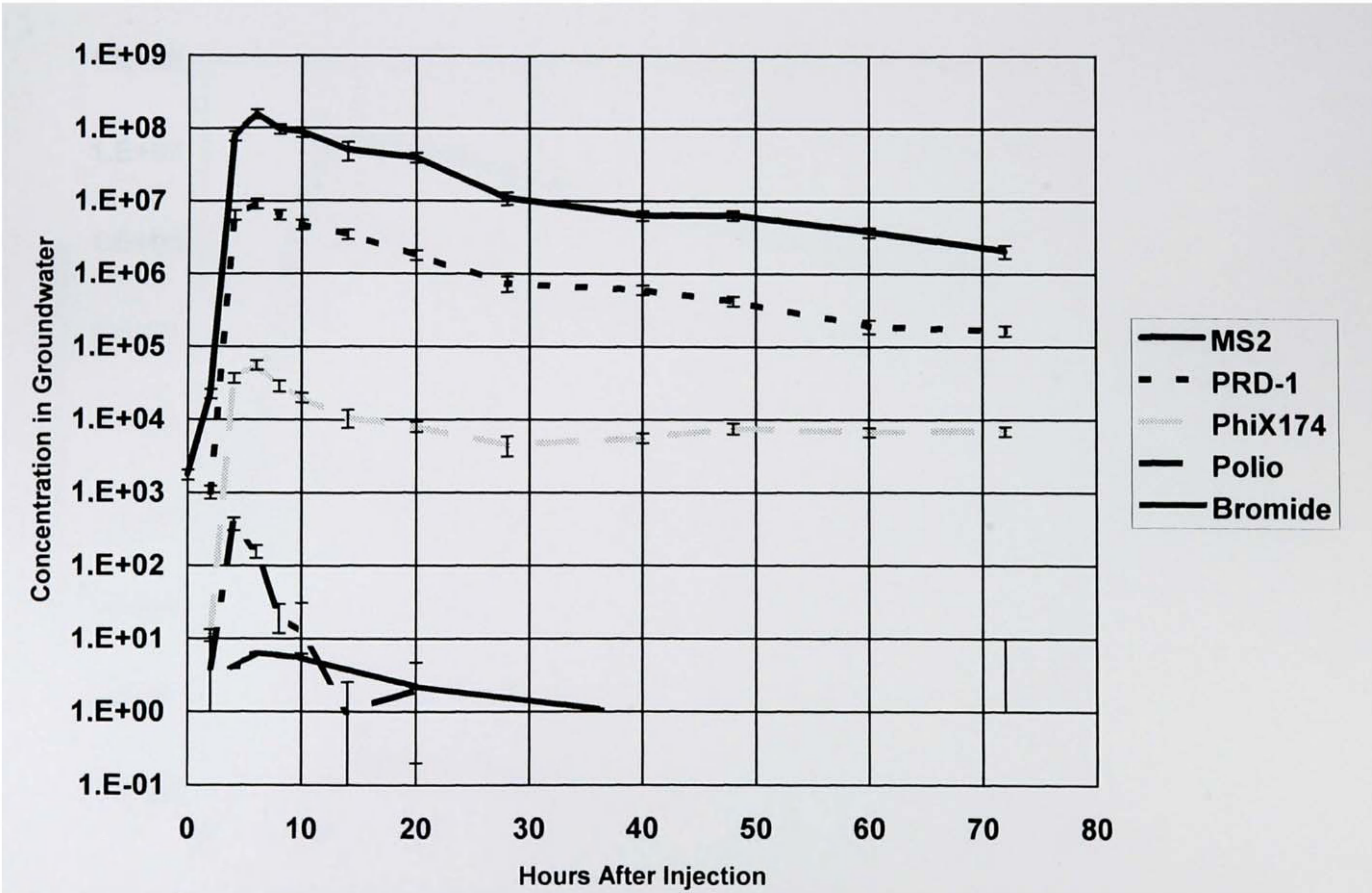

Figure 4. Breakthrough curves for well M-2, 0.6m below water table, 7.5m from I4 . Virus concentrations in PFU/ml, bromide concentrations in mg/l.

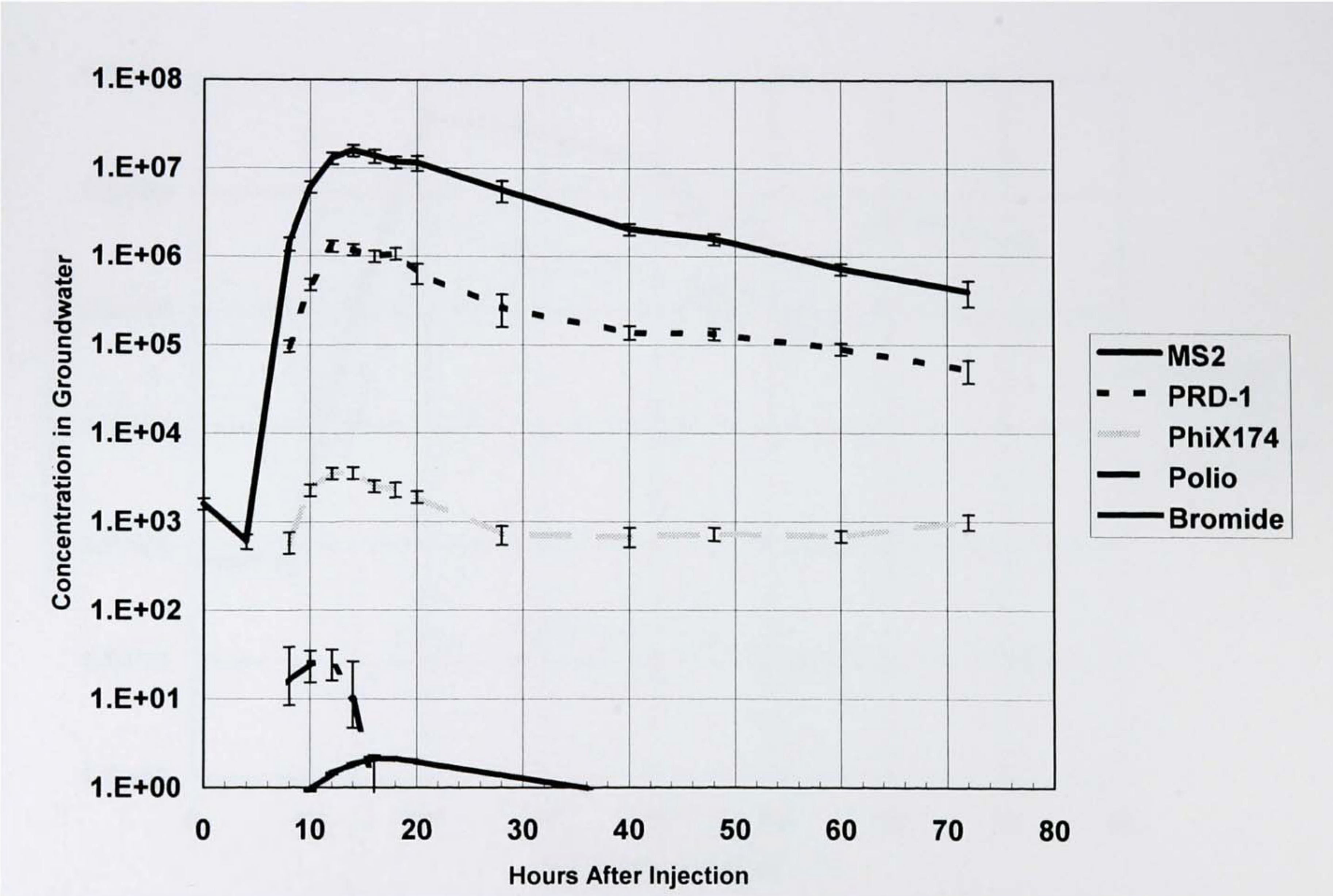

Figure 5. Breakthrough curves for well M-7, 0.6m below water table, 19.5m from I4. Virus concentrations in PFU/ml, bromide concentrations in mg/l.

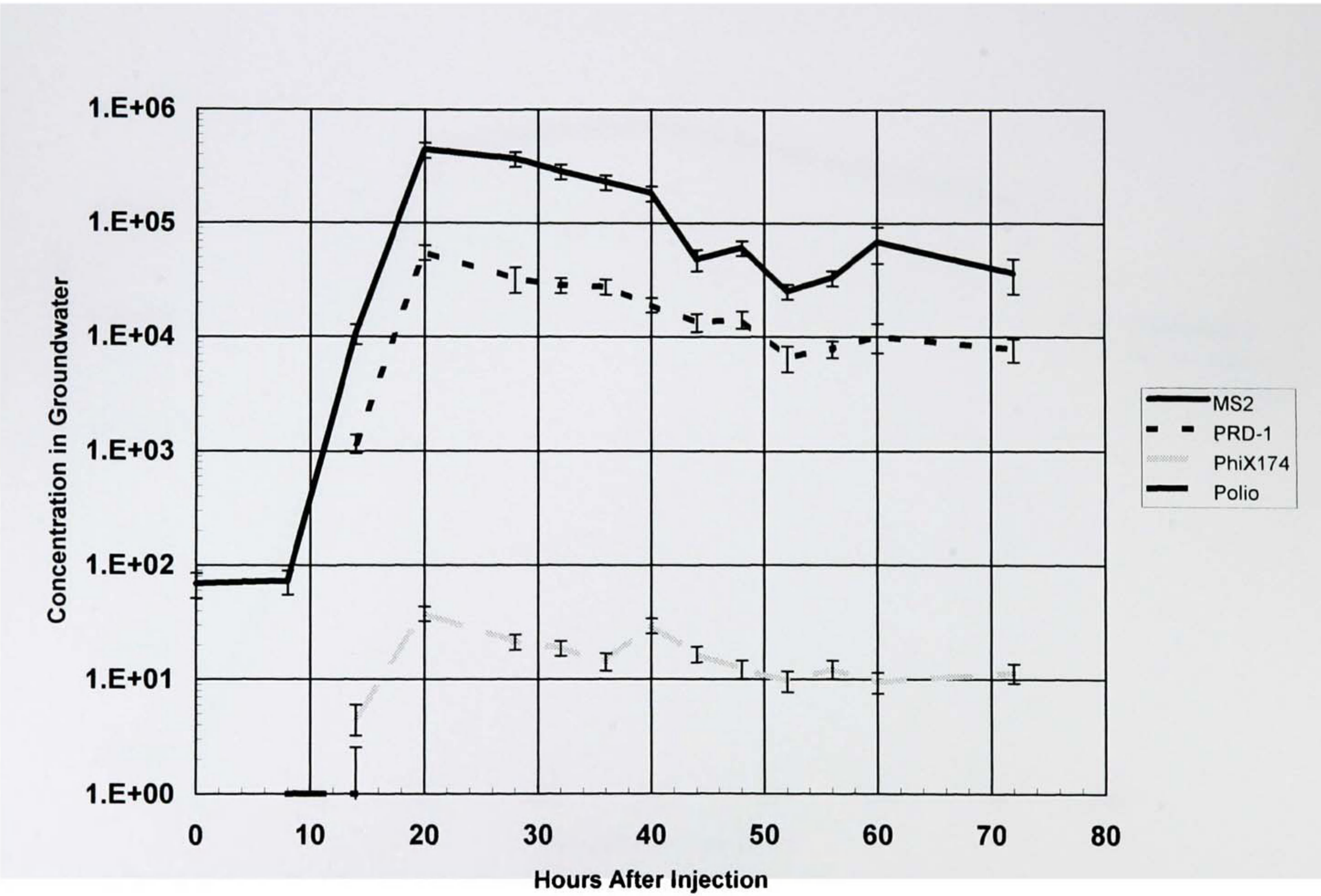

Figure 6. Breakthrough curves for well M-14, 0.6m below water table, 30m from I4. Virus concentrations in PFU/ml, bromide concentration in mg/l.

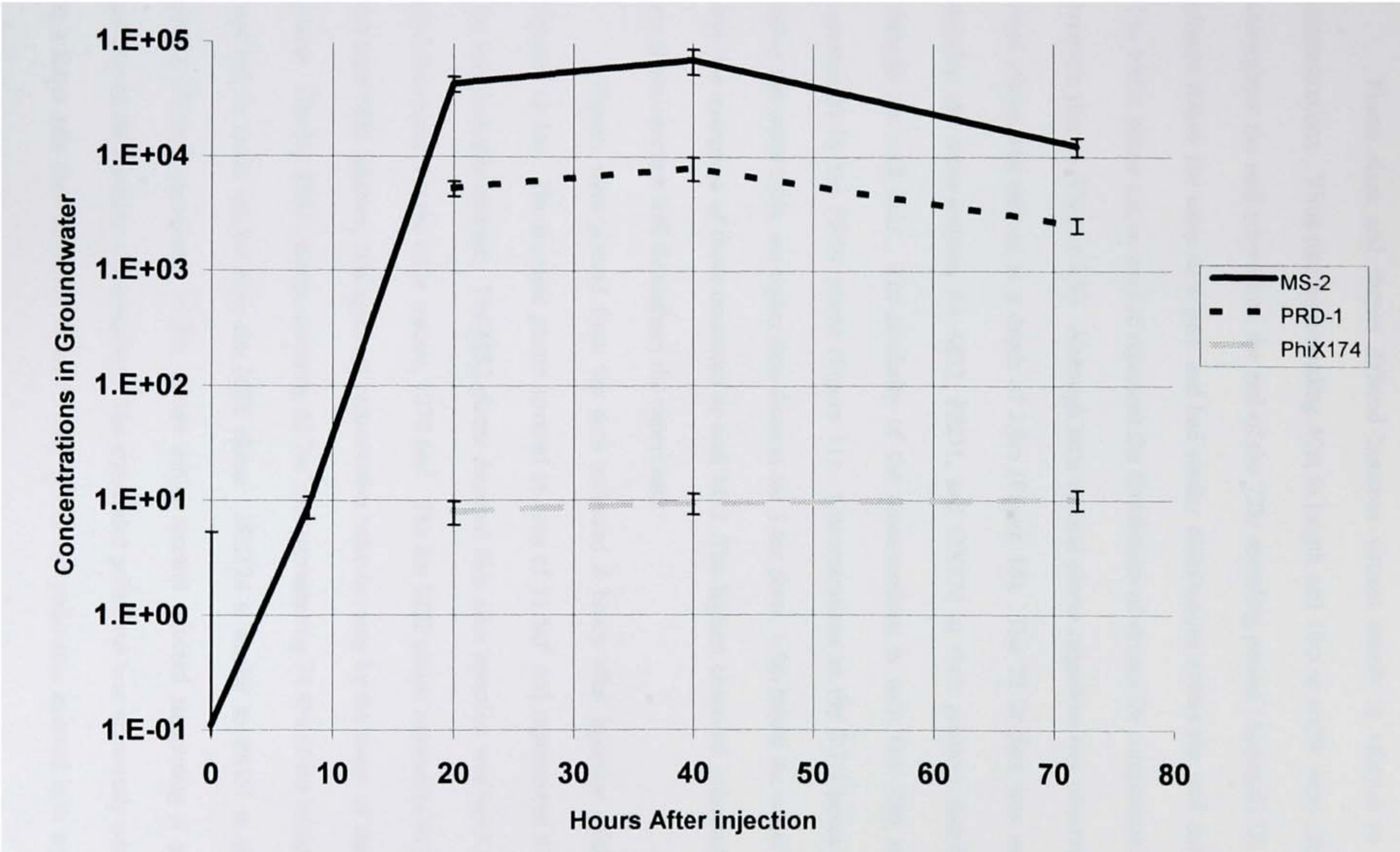

Figure 7. Breakthrough curves for well M-17, 0.6m below water table, 40.5m from I4. Virus concentrations in PFU/ml, bromide concentration in ppm.

Plume sizes and shapes differed between viruses mainly in relation to initial concentrations. Virus plumes exceeding 40m in length and 16m in width were observed throughout the well network at the end of the 72hr sampling period (Appendix D). The plumes follow the same flow path and had similar distributions across the well network. The PRD1 plume can be used to represent the distribution of viruses for comparison to the bromide plumes (Figures 8,9). Although little vertical plume migration was observed, an areal plume was defined at a depth of 3.6m (Figure 10). The 72 hr data was used to develop the cross-sections for MS2, PRD1, and ∅X174 at their greatest distribution through the well field. The similarity of the cross-sections is such that they can be represented by the PRD1 plume (Figure 11). Concentrations at the 2.7m ports, 0.6m below the water table, are higher than those at the 3.6m ports, 1.5m below the water table, with the exception of those measured at well M13. The highest observed concentrations are at the injection well throughout the experiment.

Plumes were plotted from the data collected 8 hours after injection (Table 4; Figures 12-16). The bromide plume covered an area of 51.8m^2 and represented 87% of the total bromide injected. The MS2 plume detected 8hrs after injection was much larger than the plumes for the other tracers, 1270.6m^2. The 8hr MS2 plume represents 64.2% of the total MS2 injected, this apparent conservative behavior may be the cause of the large plume. The 8hr PRD1 plume, covering 62.7m^2 and representing 24.4% of the initial virus injected, is much smaller than the MS2 plume. ∅X174 is similar to PRD1 in that its plume, 71.1m^2, represents 21.2% of the initial amount injected suggesting a greater portion of the injectate was adsorbed. The attenuated poliovirus was apparently adsorbed at a faster rate than the other viruses. Only 3% of the poliovirus injected is in aqueous

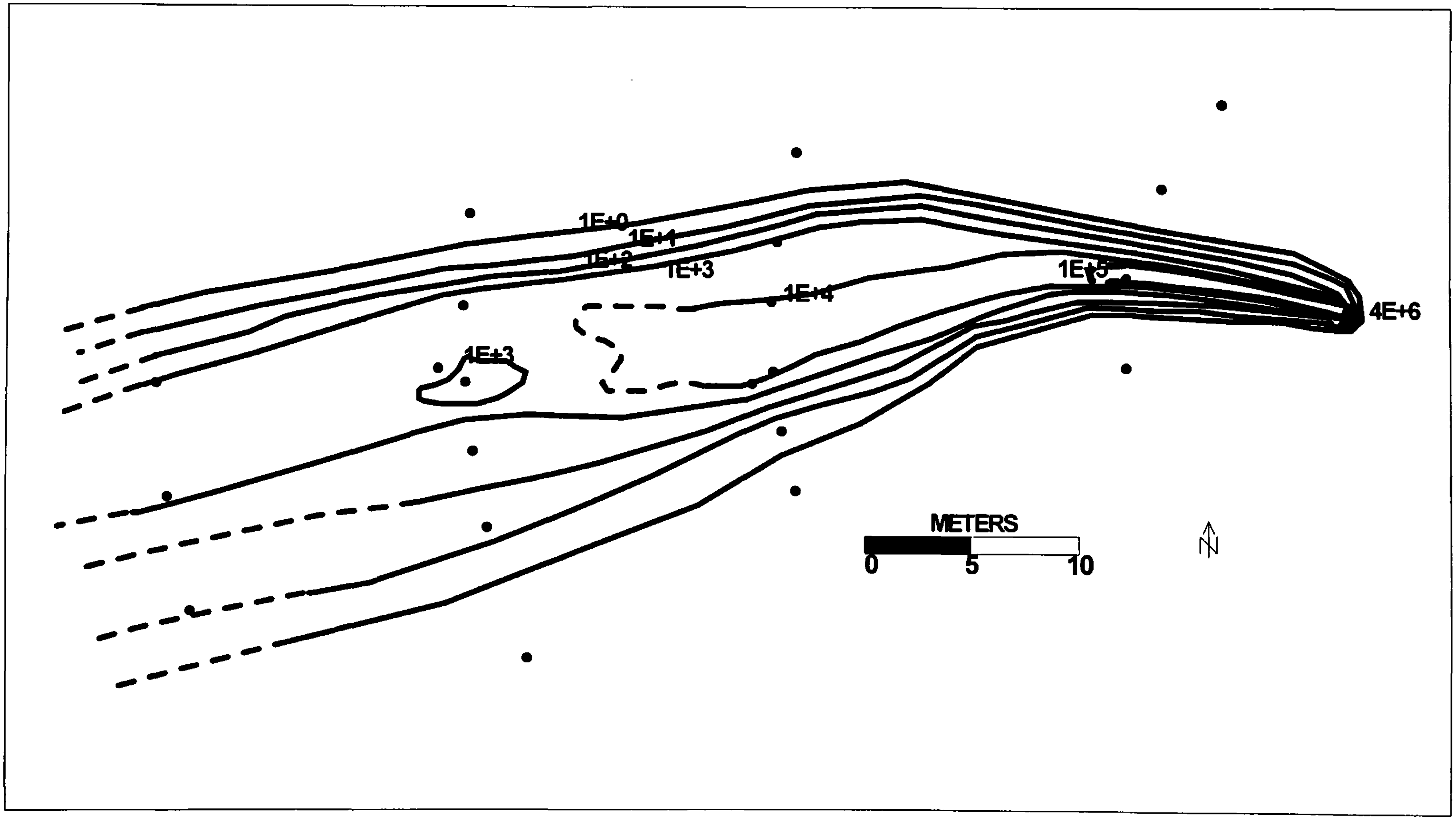

Figure 8. 72hr PRD-1 plume 0.6m below water table from 10/2/96 virus seeding experiment. Groundwater is flowing from east to west.

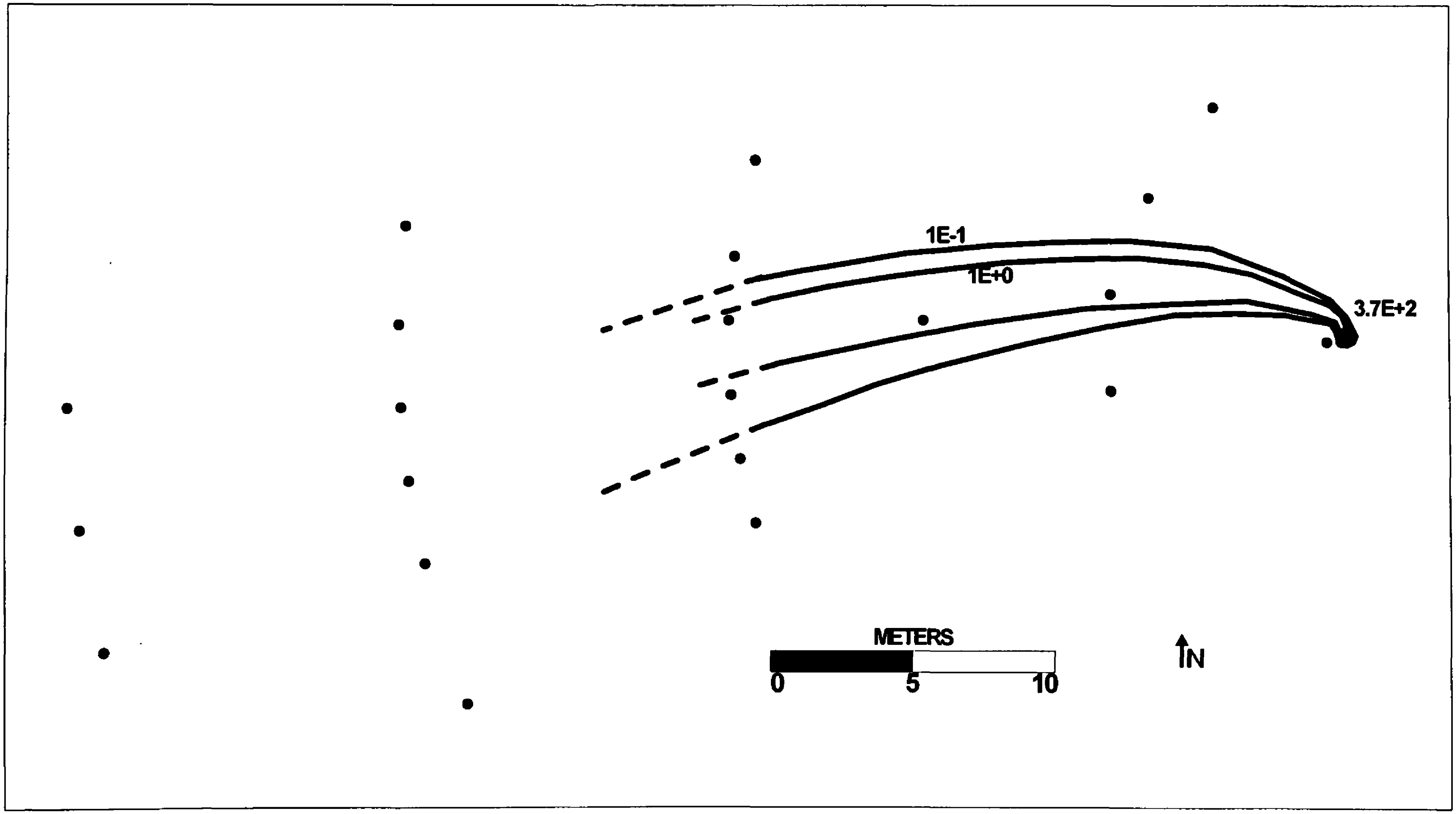

Figure 9. 36hr bromide plume 0.6m below water table from 9/22/96 tracer experiment. Groundwater is flowing from east to west.

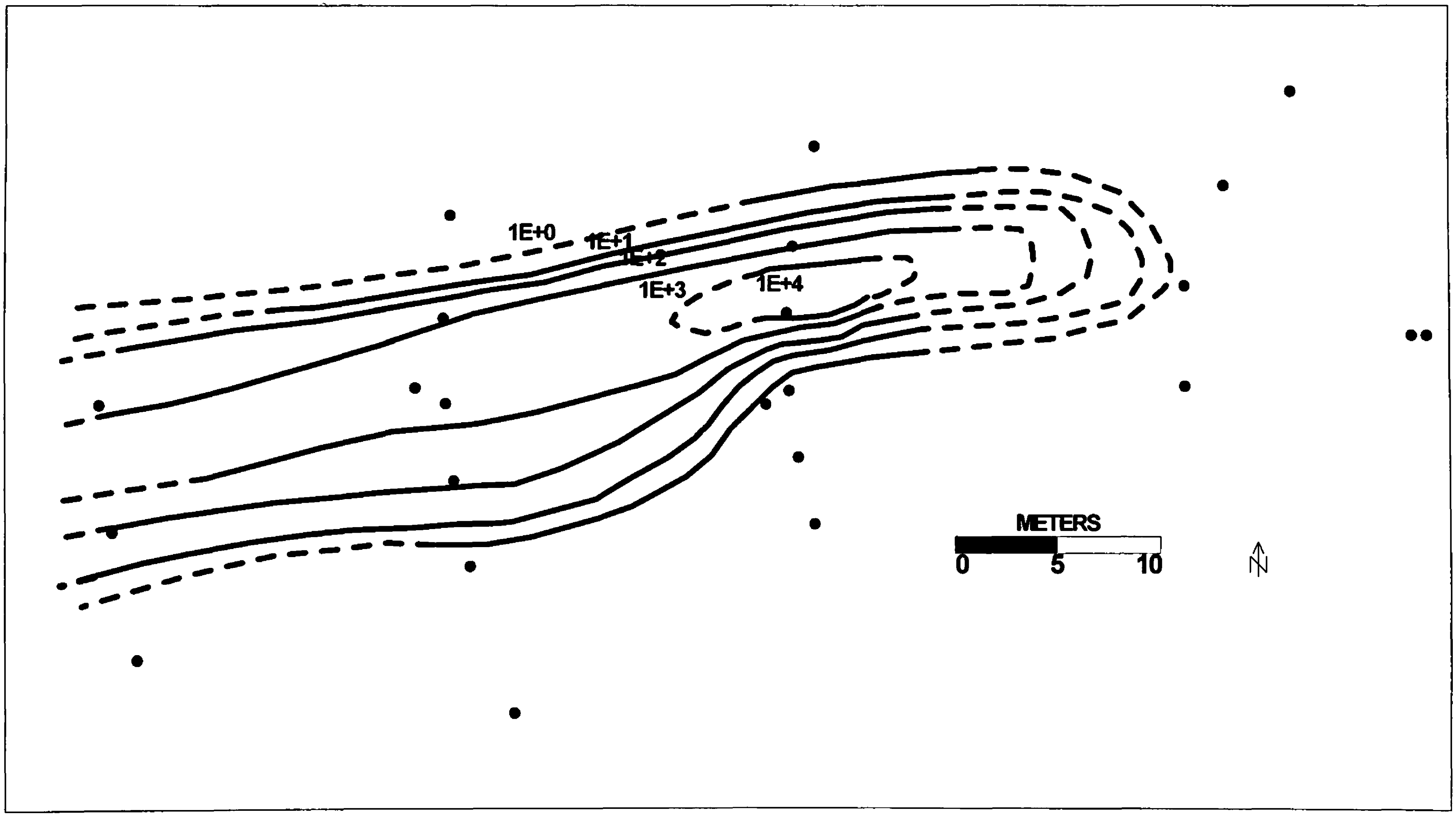

Figure 10. 72hr PRD-1 plume 1.5m below water table from 10/2/96 virus seeding experiment. Groundwater is flowing from east to west.

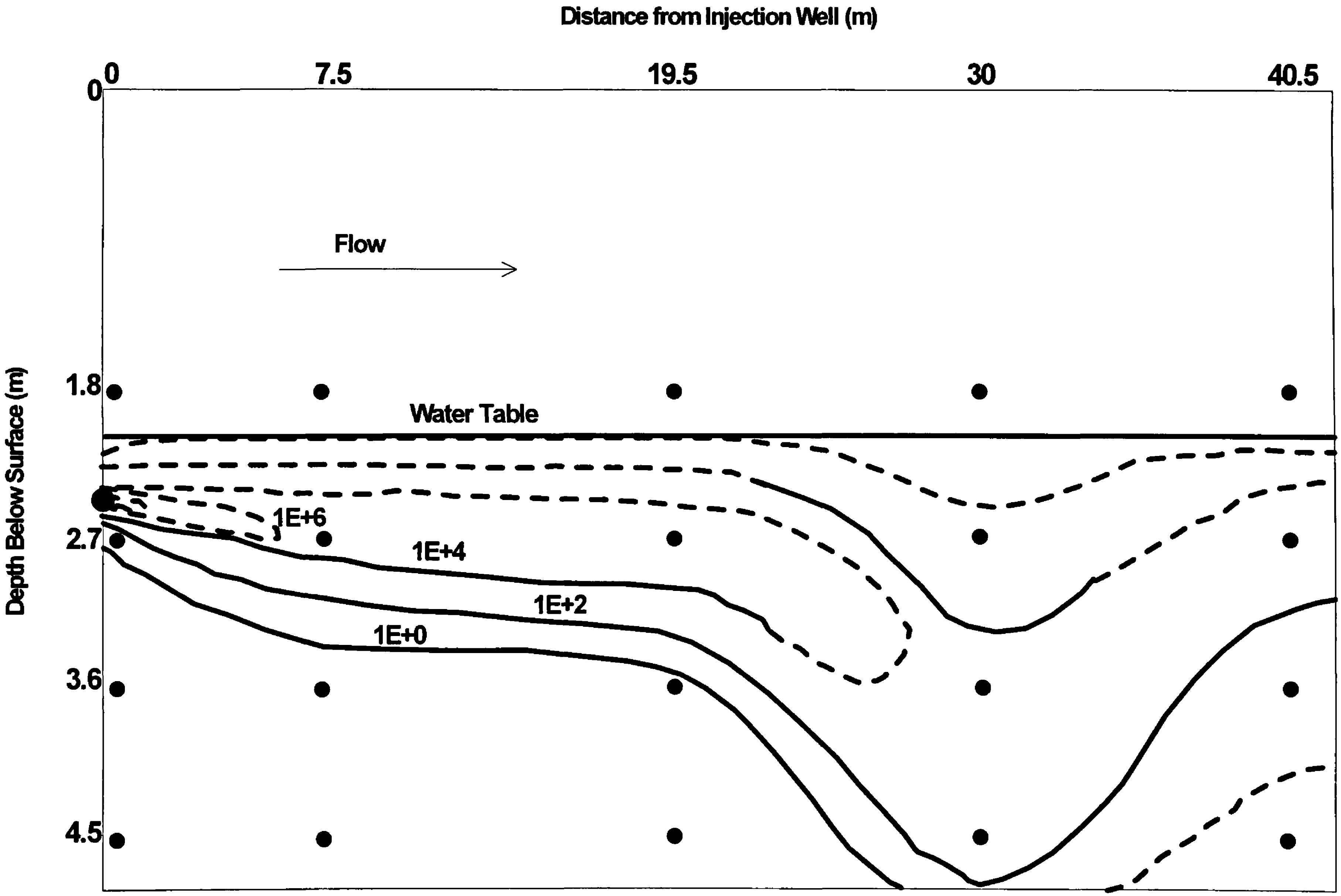

Figure 11. 72hr PRD-1 plume cross-section from 10/2/96 virus seeding experiment. Flow direction is to the west.

Table 4. Percent of tracer adsorbed and in the aqueous phase

Tracer	% Adsorbed	% in Aqueous Phase
Bromide	Conservative	87
MS2	35.8	64.2
PRD1	75.6	24.4
ΦX174	78.8	21.2
Poliovirus	97	3

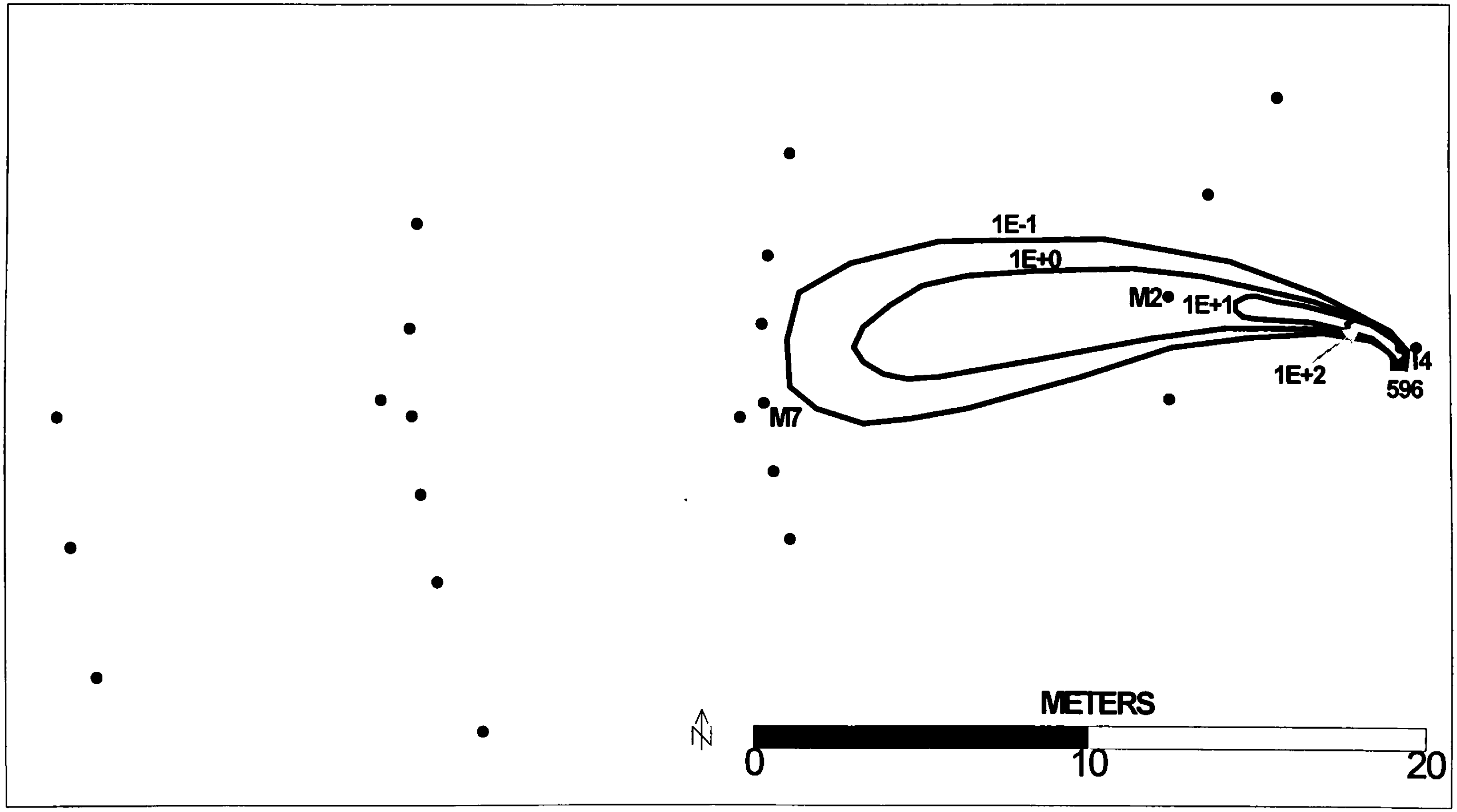

Figure 12. 8hr Bromide plume at 9ft from 9/20/96 tracer test, concentration in mg/l. Flow direction is to the west.

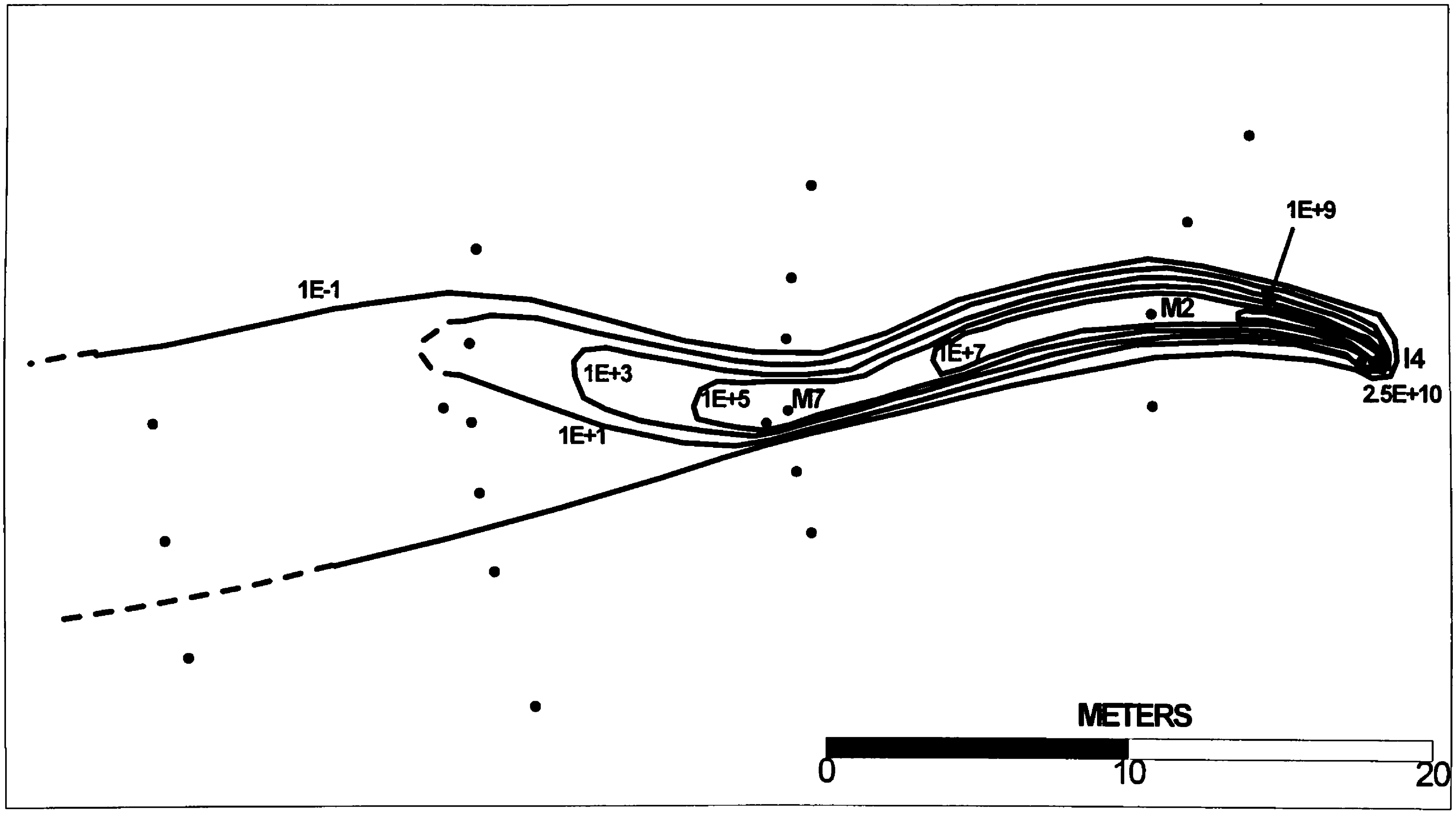

Figure 13. 8hr MS2 plume at 9ft depth from 10/2/96 seeding experiment. Concentration in PFU/ml, flow direction to the west.

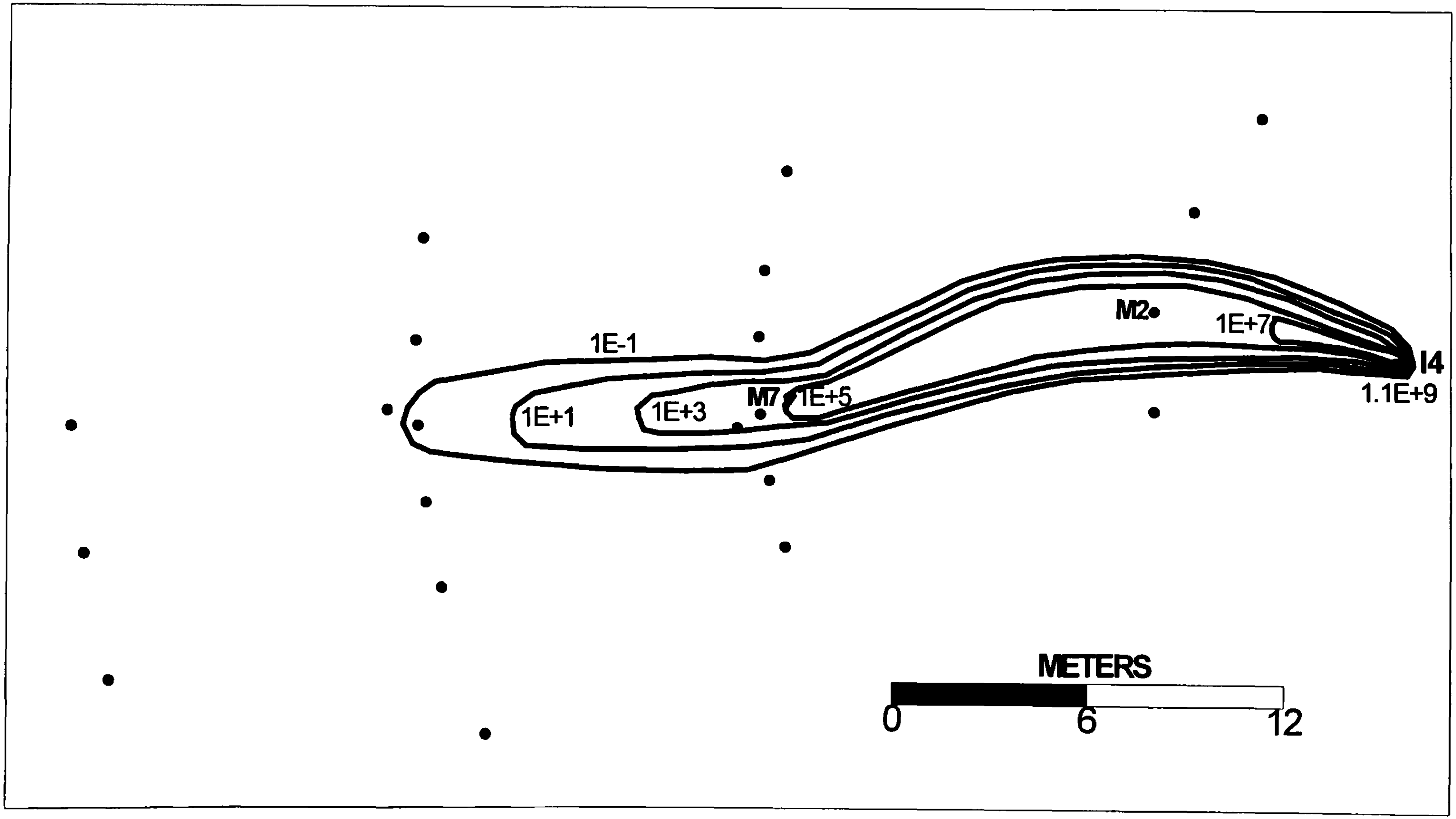

Figure 14. 8hr PRD1 plume at 9ft depth from 10/2/96 seeding experiment. Concentration in PFU/ml, flow direction to the west.

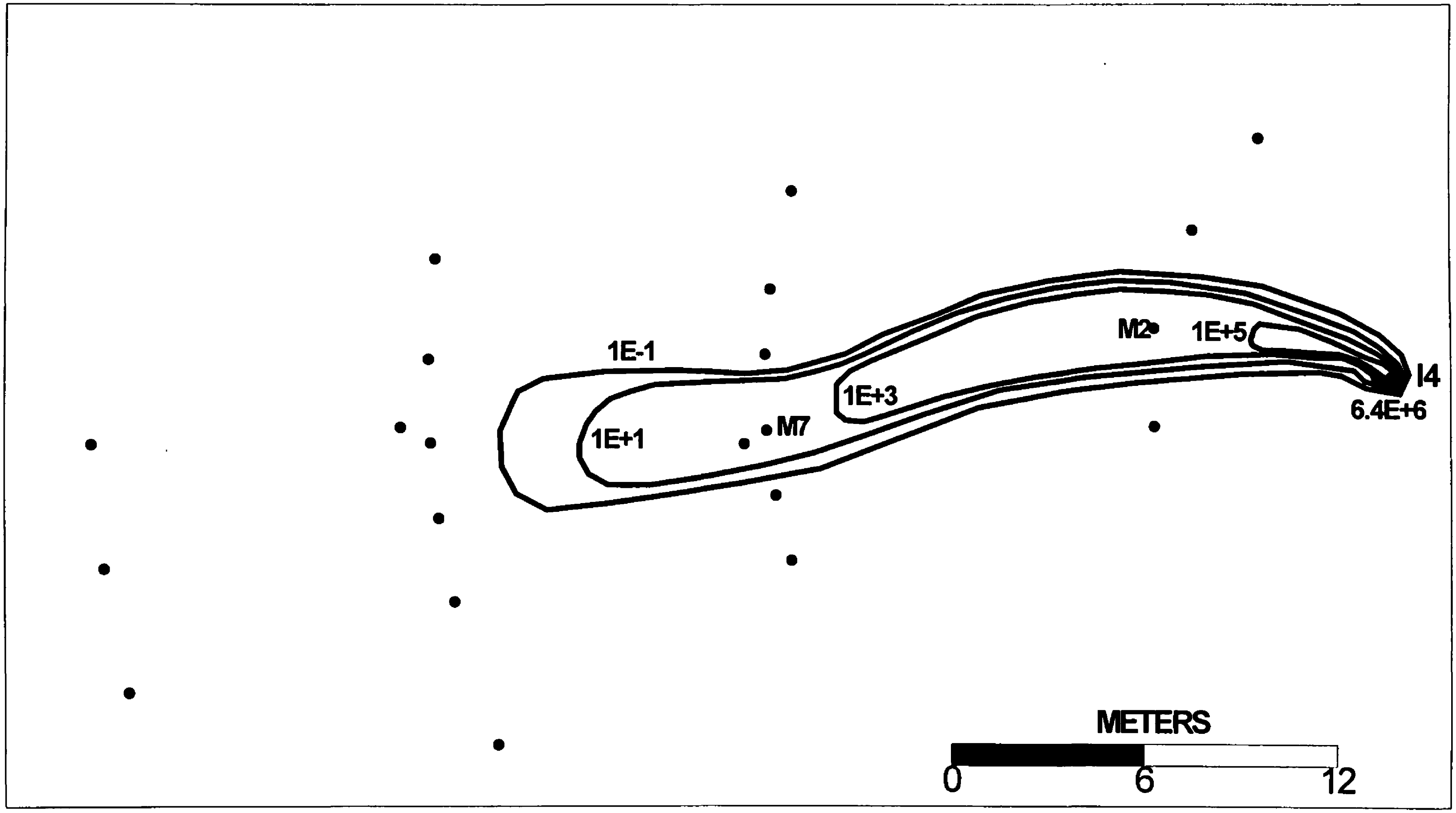

Figure15. 8hr PhiX174 plume at 9ft depth from 10/2/96 seeding experiment. Concentrations in PFU/ml, flow direction to the west.

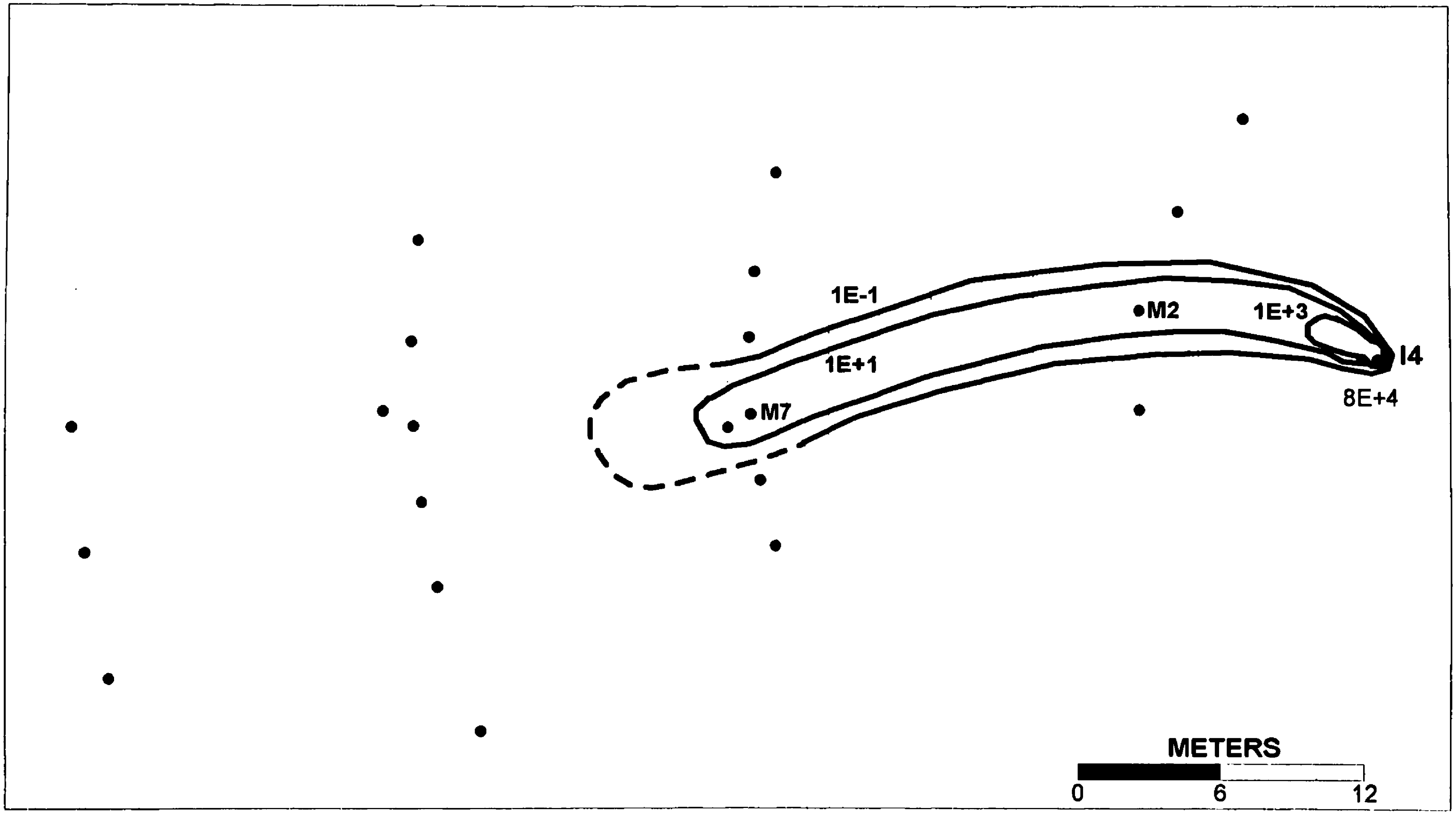

Figure 16. 8hr Polivirus plume at 9ft depth from 10/2/96 seeding experiment. Concentrations in PFU/mi, flow direction to the west

phase 8 hours after injection. The larger plume size, $109.4m^2$, may be a result of the difference between assay techniques used for poliovirus and those used for the bacteriophages.

4.0 Discussion

The highest concentrations of tracers were measured in wells I4, M2, M7, M14, and M17. Tracer tests and aquifer tests performed in the well field suggest that there is zone of extremely high hydraulic conductivity, 13,500m/d, intersecting the injection well I4 and monitoring wells M2 and M7. The cause of this zone could be a very coarse-grained buried channel or gravel bar deposit. The wide range of hydraulic conductivity derived from aquifer tests and the depositional environment suggests a heterogeneous flow field. Flow through the sampling network is controlled by a coarse-grained zone of high hydraulic conductivity. This high velocity zone creates a preferential flow path through the sampling network. Such zones are characteristic of high energy, gravel deposits in this region (Miller, 1991; Smith, 1992).

4.1 Comparison of Virus and Bromide Distribution

While bromide and viruses follow the same flow path; virus plumes are detected over areas much greater than the bromide plume. This is in part a function of our ability to resolve bromide and virus plumes. In an effort to avoid density effects, bromide was injected a 10^3 mg/l and detectable to 0.1mg/l. Bacteriophages were injected at 10^7-10^{10} PFU/ml and detectable to 0.1 PFU/ml, and poliovirus was injected at 10^6 PFU/ml and detectable to 0.5 PFU/ml. This suggests that the use of bromide as a predictive tracer for viral contamination may not be appropriate. The use of bromide to predict virus transport would most likely underestimate the areal extent of viral contamination. However, this study illustrates the utility of the use of bromide to predict virus flow paths and peak transport rates.

4.2 Conservative Virus Sub-Population

Based on breakthrough curve analyses, a portion of the injected viruses were observed to be traveling at average rates similar to the conservative bromide ion. This group of virus have not been retarded by adsorbing to the aquifer material, and appear to behave conservatively. The reasons for this conservative behavior are unknown, but there are several possibilities. There may be a genetic sub-population of viruses that express their genetic differences in their protein coats, yielding different adsorptive properties. This sub-population may be less likely to adsorb to the aquifer material and thus are transported in a conservative manner (Goyal and Gerba, 1979). Another possibility is that the portion of viruses that moves conservatively down gradient may be adsorbing to colloidal material in the groundwater. The viruses could then "piggy back" through the aquifer. These viruses would not be adsorbing differently than those attached to the aquifer material, but would appear to be acting conservatively.

4.3 Comparison of Transport Rates

Virus peaks appear to move at or faster than the average groundwater flow velocity as defined by bromide. This phenomenon has been observed by other workers. Bales et al (1989) documented the bacteriophages MS2 and f2 traveling at 1.6 to 1.9 times the velocity of conservative tracers through sand columns in the laboratory. Bales et al (1995) reported bromide and PRD1 moving at the same rate in a sand and gravel aquifer. If the viruses represented by the peaks identified in the breakthrough curves are behaving conservatively and moving faster than the bromide, further explanation is needed. A difference in effective flow path length for viruses and bromide could account for this disparity. Tortuosity (T) is the relative difference between the observed straight line flow path (L) and the actual interpore flow path (L_e), such that $T = L_e / L$ (Fetter, 1993). L is the same for bromide and viruses, however L_e may be quite different. Bromide is an ion 1.96 angstroms in diameter, and therefore it is subject to flow through tortuous pathways and pore sizes down to the molecular level. Viruses are between 20 and 300nm in diameter and are subject to pore size exclusion (Pekdeger and Mathess, 1983). Some pores that the bromide ion can enter are smaller than the diameter of viruses. The effect of pore size exclusion on an individual virus is macropore flow and lower tortuosity. Pore size exclusion, or filtration, has been identified as a major control of microbial flow (Wood and Ehrlich, 1978; Pekdeger and Mathess, 1983). Viruses flow is thus concentrated through larger pores that may have a shorter effective flow path length (L_e). This would result in the virus peak arriving before the bromide peak. If viruses are adsorbed onto colloidal material, they too would be affected by pore size exclusion.

The hypothesis of pore size exclusion is based on the premise that viruses are indeed being transported through the aquifer faster than the average groundwater flow velocity as defined with bromide. By plotting error bars on the breakthrough curves it becomes obvious that distinct transport velocities cannot be differentiated. Responsible reporting of the data results in ranges of transport velocities that overlap, and therefore one cannot assert that the rates are any different (Table 3).

The exception to this statement is the comparison of transport rates for bromide and attenuated poliovirus. Poliovirus peaks arrive before bromide peaks at wells M2 and M7, 7.5 and 19.5m from injection well I4. The use of standard solute transport analysis would result in a calculated average transport rate for polioviruses that is faster than that calculated for bromide. A plausible mechanism for this faster transport has been previously discussed, however pore size exclusion should affect all the viruses not just poliovirus. Although the attenuated poliovirus peak does arrive before the bromide peak, an alternative explanation is that the poliovirus transport is not actually faster than bromide transport.

Poliovirus adsorbs more readily than the other viruses, as represented by relative concentration plots and mass balances (Figure 17). The breakthrough curves for poliovirus also indicate different adsorptive properties for poliovirus. The tailing effect observed for the bacteriophages is not present in the polio curve. A sharp decline in concentration after the peaks suggests that the poliovirus is adsorbing more completely to the aquifer material than the bacteriophages, and the adsorbed mass of poliovirus is not desorbing as fast as the mass of adsorbed bacteriophages. The strong adsorptive characteristics of attenuated poliovirus manifests itself in the peaks identified in the breakthrough curves. The high percentage of poliovirus adsorbed to the aquifer material and the rapid rate at which it adsorbs limits the amount of attenuated poliovirus in the aqueous phase. If bromide concentration is being affected only by mechanical dispersion, then the differences in plots of C/Co for bromide and poliovirus are due to the rate of poliovirus adsorption. This rate, expressed as C/Co vs. time and plotted as negative values for clarity, is illustrated by the adsorption function in Figure 18. The non-linear rate of poliovirus adsorption vs. Its transport rate would result in a truncation of the breakthrough curve shifting the peak towards the left. The resulting earlier peak will be misinterpreted as an overall faster rate of transport. Without better resolution of virus

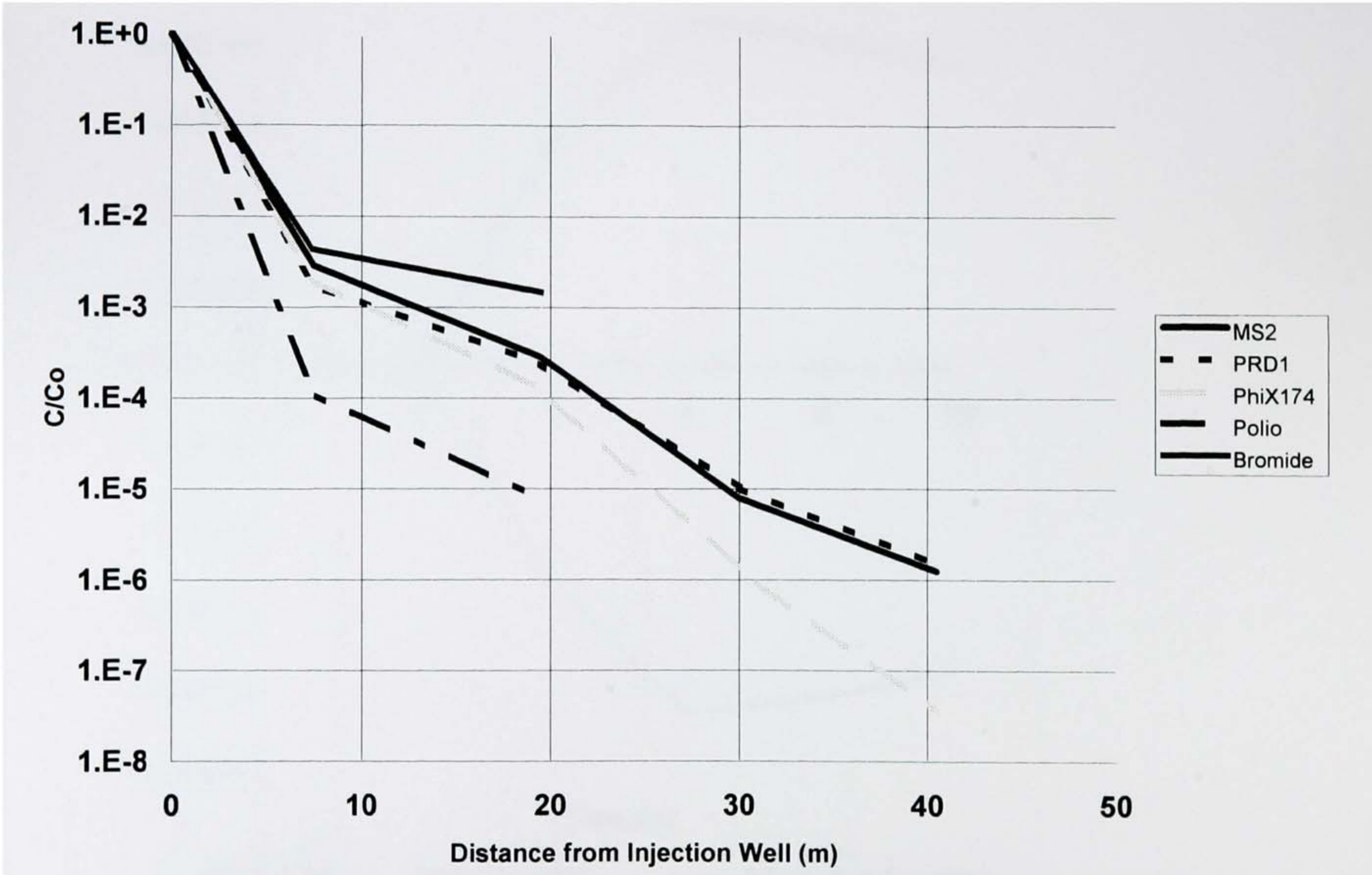

Figure 17. Plot of relative concentration (C/Co) v. distance from injection well I4, 0.6m below water table in wells I4, M2, M7, M14, and M17.

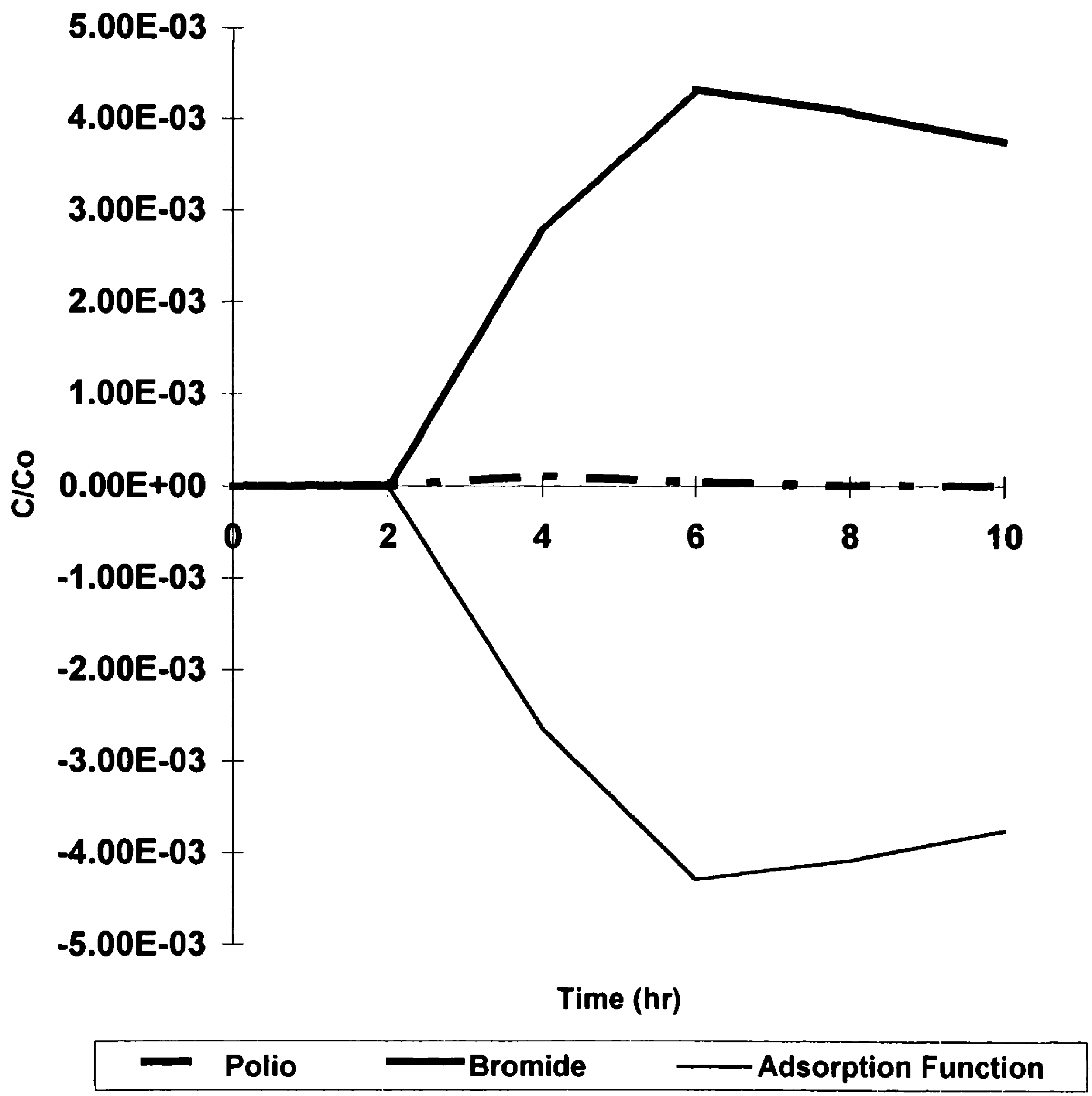

Figure 18. Relative concentration of attenuated poliovirus and bromide over time, observed at well M2. The adsorption funtion is the difference between the two curves.

breakthrough curves, it seems more likely the poliovirus is moving at an average rate typical of the bacteriophages.

5.0 Conclusion

A preferential flow path identified in the sampling network appears to result from a coarse-grained zone of high hydraulic conductivity. In addition to allowing average transport rate over 30m/d the cold groundwater negated virus die off, allowing it to remain infectious for at least 185 days in the system.

The use of four viruses and bromide to evaluate virus behavior and transport in a sand and gravel aquifer has yielded some interesting findings: 1) the average rate of transport for a portion of seeded virus is as fast as the average groundwater flow velocity defined with bromide; 2) the adsorption and desorption of viruses at different rates may affect observed virus peak arrival times; 3) to properly interpret virus transport the error inherent in infectious assays must be analyzed and reported; 4) each virus demonstrated different adsorptive properties. But perhaps most importantly, the research at the Erskine site has defined the difference between peak arrival times and solute transport rates in respect to viruses. The application of standard solute transport analysis to determine solute transport rates may be inappropriate for virus transport. The use of the breakthrough curve to calculate average transport rate for the solute assumes that the peak represents the average transport of the entire mass. That peak represents a portion of the total virus injected, and in the case of poliovirus it may not properly represent its rate of transport.

This "worst-case" scenario at the Erskine research site documents viruses being transported at faster rates and higher concentrations over distance than has been previously reported. A portion of viruses seeded into this groundwater system moved at an average rate of over 30 m/d. Long tails seen in breakthrough data imply re-release of sorbed virus for large periods of time. This re-release of sorbed viruses affects the virus peaks and contributes to long term survival of the viruses seeded into this system. Hydrogeologically based natural disinfection distances (source well separation distances) would need to exceed the traditional 30m values in this coarse-grained system. The results further suggest that the use of bromide to assess the threat posed by viral contamination would insufficiently represent virus transport in a coarse-grained aquifer.

References Cited

Adams, M.H., 1959, *Bacteriophages*, Wiley-Interscience, New York.

Alhajjar, B.J., S.L. Stamer, D.O. Cliver, and J.M. Harkin, 1988, Transport Modeling of Biological Tracers from Septic Systems, Water Research, v22, n7, p907-915.

Alhajjar, B.J., J.M. Harkin, D.O. Cliver, and S.L. Streamer, 1987, Biological Tracer Plumes from Septic Systems, 4th Annual Eastern Regional Ground Water Conference, July 14-17, p247-277.

Bales, R.C. and Shimn Li, 1993, MS2 and Poliovirus Transport in Porous Media; Hydrophobic Effects and Chemical Perturbations, WRR, v29, n4, p957-963.

Bales, R.C., C.P. Gerba, G.H. Grondin, and S.L. Jensen, 1989, Bacteriophage Transport in Sandy Soil and Fractured Tuff, Applied and Environmental Microbiology, v55, n8, p2061-2067.

Bales, R.C., S. Li, K.M. Maguire, M.T. Yahya, C.P. Gerba, and R.W. Harvey, 1995, Virus and Bacteria Transport in a Sandy Aquifer, Cape Cod, MA., Ground Water, v33, n4, July-August, p653-661.

Bitton, G, S.R., Farrah, R.H. Ruskin, J. Butner, and Y.J. Chou, 1983, Survival of Pathogenic and Indicator Organisms in Ground Water, Ground Water, v21, n4, July-August, p405-410.

Davis, S.N., G.M. Thompson, H.W. Bentley, and G. Stiles, 1980, Ground-Water Tracers - A Short Review, Ground Water, 18:1, pp14-23.

Driscoll, F.G., 1986, Groundwater and Wells, 2nd ed., Johnson Filtration Systems, Inc. St. Paul, MN, 1108pp.

Ed. Eaton, A.D., , L.S. Clesceri, and A.E. Greenberg, 1995, *Standard Methods for Examination of Water and Waste Water*, American Public Health Association, p9-58.

Fetter, C.W., 1993, *Contaminant Hydrogeology*, Prentice-Hall, Inc., 458 p.

Gerba, C.P., D.K. Powelson, M.T. Yahya, L.G. Wilson, G.L. Amy, 1991, Fate of Viruses in Treated Sewage Effluent During Soil Aquifer Treatment Designed for Wastewater Reclamation and Reuse, Water Science Technology, v24, n9, p95-102.

Gerba, C.P., 1984, Applied and Theoretical Aspects of Virus Adsorption to Surfaces, Advances in Applied Microbiology, v30, p133-168.

Gilbert, R.G., C.P. Gerba, R.C., Rice, H. Bouwer, C. Wallis, and J.L. Melnick, 1976, Virus and Bacteria Removal from Wastewater by Land Treatment, Applied Environmental Microbiology, v32, n3, Sept., p333-338.

Goyal, S.M. and C.P. Gerba, 1979, Comparative Adsorption of Human Enteroviruses, Simian Rotavirus, and Selected Bacteriophages to Soils, *Applied and Environmental Microbiology*, 38:2, pp241-47.

HydroGeoLogic, Inc., 1994a, Viralt, Version 3.0, Documentation and User's Guide, 130p.

HydroGeoLogic, Inc., 1994b, Canvas, Version 2.0, Documentation and User's Guide, 132p.

Isotok, J.D. and M.D. Humphrey, 1995, Laboratory Investigation of Buoyancy-Induced Flow (Plume Sinking) During Two-Well Tracer Tests, Ground Water, 33:4, pp.597-604.

Jansons, J., L.W. Edmonds, B. Speight, and M.R. Bucens, 1989a, Movement of Viruses After Artificial Recharge, Water Research, v23, n3, p293-299.

Jansons, J., L.W. Edmonds, B. Speight, and M.R. Bucens, 1989b, Survival of Viruses in Groundwater, Water Research, v23, n3, p301-306.

Johnson, A.I., 1992, Specific Yield - Compilation of Specific Yields for Varioous Materials, USGS Water-Supply Paper 1662-D.

LeBlanc, D.R., S.P. Garabedian, K.M. Hess, L.W. Gelhar, R.D. Quadri, K.G. Stollerwerk, and W.W. Wood, 1991, Large-Scale Natural Gradient Tracer Test in Sand and Gravel, Cape Cod, Massachusetts: 1. Experimental Design and Observed Tracer Movement, Water Resources Research, 27:5, pp.895-910.

Levine, A.J., 1992, *Viruses*, Scientific American Library, New York, 240p.

Macler, B.A., 1995, Developing a National Drinking Water Regulation for Disinfection of Ground Water, Ground Water Monitoring and Remediation, p77-84.

Macler, B.A and F.W. Pontius, In Publication, Update on the Groundwater Disinfection Rule, JAWWA.

Mathess, G. and A. Pekdeger, 1985, Survival and Transport of Pathogenic Bacteria and Viruses in Ground Water, Ground Water Quality, John Wiley & Sons, New York, pp.472-82.

Mills, W.B., S. Lui, and F.K. Fong, 1991, Literature Review and Model (COMET) for Colloid/Metals Transport in Porous Media, Ground Water, v29, n2, April, p199, 208.

Miller, Ross D., 1991, A Numerical Flow Model of the Missoula Aquifer: Interpretation of Aquifer Properties and River Interaction, Master's Thesis, University of Montana, Missoula.

Pekdeger, A. and G. Mathess, 1983, Factors of Bacteria and Virus Transport in Groundwater, *Environmental Geology*, 5:2, pp.49-52.

Pfaff, J.D., 1993, Method 300.0, Determination of Inorganic Anions by Ion Chromatography, Office of Research and Development, US EPA, August, 30 p.

Rossi, P., A. De Carvalho-Dill, I, Müller, and M. Aragno, 1994, Comparative tracing Experiments in a Porous Aquifer Using Bacteriophages and Fluorescent Dye on a Test Field Located at Wilerwald (Switzerland) and Simultaneously Surveyed in Detail on a Local Scale by Radio-magneto-tellury (12-240 kHz), Environmental Geology, v23, p192-200.

Sauty, J.P., 1980, An Analysis of Hydrodispersive Transfer in Aquifers, *Ground Water*, 16:1, pp.145-58.

Smart, P.L. and L.M.S. Laidlaw, 1977, An Evaluation of Some Fluorescent Dyes for Water Tracing, Water Resources Research, 13:1, pp15-32.

Smith, Clifford, 1992, *The Hydrogeology of the Central and Northwestern Missoula Valley*, Master's Thesis, University of Montana, Missoula.

Smith, E.M. and C.P. Gerba, 1982, Laboratory Methods for Growth and Detection of Animal Viruses, *Methods in Environmental Virology*, Marcel Dekker, New York, pp15-47.

Stramer, S.L., and D.O. Cliver, 1984, Septage Treatments to Reduce the Numbers of Bacteria and Polioviruses, Applied and Environmental Microbiology, v48, n3, September, p566-572.

Tim, U.S. and S Mostaghimi, 1991, Model for Predicting Virus Movement Through Soils, Ground Water, v29, n2, p251-259.

US EPA, VIRALT Version 3.0: Documentation and User's Guide, Office of Drinking Water, Washington, D.C.

US EPA, Groundwater Disinfection Rule, Workshop on Predicting Microbial Contamination of Groundwater Systems, July 10-11, 1996, Proceedings Report, September, 1996.

Wellings, F.M., A.L. Lewis, C.W. Mountain, and L.V., Pierce, 1975, Demonstration of Virus in Groundwater after Effluent Discharge onto Soil, Applied Microbiology, v29, n6, p751-757.

Wood, W.W. and Ehrlich, 1978, Use of Baker's Yeast to Trace Microbial Movement in Ground Water, *Ground Water*, 16, pp.398-403.

Yahya, M.T., L. Galsomies. C.P. Gerba, and R.C. Bales, 1993, Survival of Bacteriophages MS-2 and PRD-1 in Ground Water, Water Science Technology, v27, n3-4, p409-412.

Yates, M.V., C.P. Gerba, and L.M. Kelley, 1985, Virus Persistence in Groundwater, Applied and Environmental Biology, v49, n4, April, p778-781.

Yates, M.V. and S.R. Yates, 1987, A Comparison of Geostatistical Methods for Estimating Virus Inactivation Rates in Ground Water, Water Research, v21, n9, p1119-1125.

Yates, M.V. and S.R. Yates, 1989, Septic Tank Setback Distances: A way to minimize Virus Contamination of Drinking Water, Ground Water, v27, n2, p202-208.

Appendix A

Viruses and Health Risks

Viruses are microorganisms, 20 to 300nm in diameter, composed of a genetic core containing RNA or DNA and surrounded by a protein coat, with more complex viruses encased in lipids (Levine, 1992). Viruses can only reproduce in living host cells that they have infected. Viruses can infect animals, plants, and bacteria (bacteriophages). Bacteriophages, first identified by Frederick Twort in 1912, infect and reproduce in bacteria. Three bacteriophages were injected into the aquifer to study virus transport in groundwater. The "phages" pose no threat to human health because they are infectious to bacteria, not animal cells.

Attenuated poliovirus type-1 (CHAT strain) was also used as a viral tracer. An attenuated virus is still infectious, but does not produce a pathology or disease in an infected organism. The strain used in this experiment is similar to, but weaker than, the Sabin live vaccine. Because this attenuated virus is still infectious, cautions were taken in the field to limit exposure to virus laden groundwater. All groundwater pumped during the experiment was collected and chlorinated on site with chlorine bleach.

Modeling

Several attempts to model virus transport have been made (Mills et al, 1991; Alhajjar et al, 1988; Tim and Mostaghimi, 1991). These models have had limited success. Mills et al (1991) developed a colloid transport model, COMET. Viruses range in size from 20 to 300nm, well within the range of colloids, and the model COMET although directed towards solid waste, is still applicable to viruses. Mills work despite being only a few years old, points out the lack of knowledge about colloidal attachment to solids. This is important because attachment is believed to be a major control of virus and colloid transport. COMET deals primarily with predicting the transport of contaminants adsorbed onto colloids, and the mechanisms used in the models may affect viruses and their transport in water. Therefore, COMET may be useful for predicting virus transport. A stochastic model focused on biological tracers was developed by Alhajjar et al (1988). The researchers hoped to use indicator bacteria fecal streptococci and total and fecal coliforms as indicators for the presence of viruses. Field studies demonstrated that these indicators did not travel or survive in a similar fashion to poliovirus, which was also introduced into the system. This study is important because it illustrates the fact that viruses behave differently than other biological tracers. Modeling efforts must specifically geared towards viruses for them to be accurate. VIROTRANS, CANVAS, and VIRALT are models specific to virus transport and use numeric solutions to model virus laden waste water percolating through soils (Tim and Mostaghimi, 1991; HydrGeoLogic, 1994a, 1994b). These models, although designed for virus transport are severely limited by the lack of knowledge about how viruses are transported in varying hydrogeologic settings. Very few common characteristics have been identified that can be applied to different virus types, in fact the behavior of a single virus type may vary from system to system. .

Appendix B

Water Table Variations

The Erskine Fishing Access near Frenchtown, MT. lies in the flood plain of the Clark Fork River. The close proximity of the site to a major river results in a shallow water table that is under the influence of the river stage. To monitor the water table fluctuations, determine direction of flow, and observe the surface water influence on the shallow aquifer, water levels were measured periodically during the study in 44 wells and 10 staff gauges. The wells and staff gauges are noted on each potentiometric map, and can be seen in Figure B1. A typical potentiometric map generated from these measurements illustrates a westerly flow direction and low gradient (Figure B2). The combination of a continuous water level recorder and periodic water level measurements produced a hydrograph for the Erskine site (Figure B3). Water level measurements were taken from November 1995 to September 1996 and are relative to a 100ft elevation datum on the surface (Table B1).

Hydrologic Properties

The hydrologic properties of the aquifer were derived by two methods including bromide tracer tests and aquifer tests. The tracer tests are described in Appendix D. The data from the September 1996 bromide tracer tests were used to calculate hydraulic conductivity (K) using the equation:

$$K = VI/n$$

where V is velocity, n is estimated porosity, and I is measured hydraulic gradient (Table B2). Aquifer test data was subjected to time-drawdown, recovery, and steady state analysis. Steady state calculations used a version of the Thiem equation:

$$K = [Q \log(r_2/r_1)] \div [1.366(h_2^2 - h_1^2)]$$

where K is in m/d, Q is pumping rate in m^3/d, r_1 and h_1 are the radial distance in meters and the head in meters measured from the bottom of the aquifer, during pumping, for a near monitoring well, and r_2 and h_2 are for a distant monitoring well (Table B2) (Driscoll, 1986). This equation was used for steady state data from the pumping of well W1 and W2. Another version of the Thiem equation from Driscoll (1986) was used to analyze steady state drawdown in the pumping well for well W0 and W3:

$$K = [Q \log(R/r)] \div [1.366(H^2 - h^2)]$$

where the variables are as described above and H is the static head in meters measured from the bottom of the aquifer, h is the head in meters measured from the bottom of the aquifer while pumping, R is the radius of the cone of depression (estimated to be 30m) and r is the radius of the pumping well, all in meters (Table B2).

Time-drawdown data was analyzed using Driscoll's version of the Theis equation rearranged to yield K in m/d:

$$K = (0.183\ Q) \div (\Delta s\ b)$$

where Δs is drawdown in meters over one log-cycle of time, and b is aquifer thickness in meter (Table B3-6, Figures B4-24).

The final analysis on this pumping data focused on water level recovery in the pumping wells W1, W2, and W3. Using the Theis concepts, Driscoll's equation is as follows:

$$K = (0.183\ Q) \div (s-s')\ b$$

where ***(s-s')*** is the difference between the pumping water level and the recovered water level in meters.

The results of these analyses indicate a heterogeneous flow field over the study site. However, the correlation of the calculated ***K*** from the tracer data and the aquifer test at W1 suggest that the hydraulic conductivity between the injection well I4 and W1 is approximately 13,200 m/d. In an attempt to generalize the hydrologic properties of the site, the results from all methods of calculation were pooled. The average ***K*** over the entire site is 4,000 m/d, with a median value of 1,000 m/d. The ***K*** calculated for the area from I4 to W1 is likely a zone of high conductivity, closer to the maximum for the site 13,000 m/d than the minimum of 120 m/d.

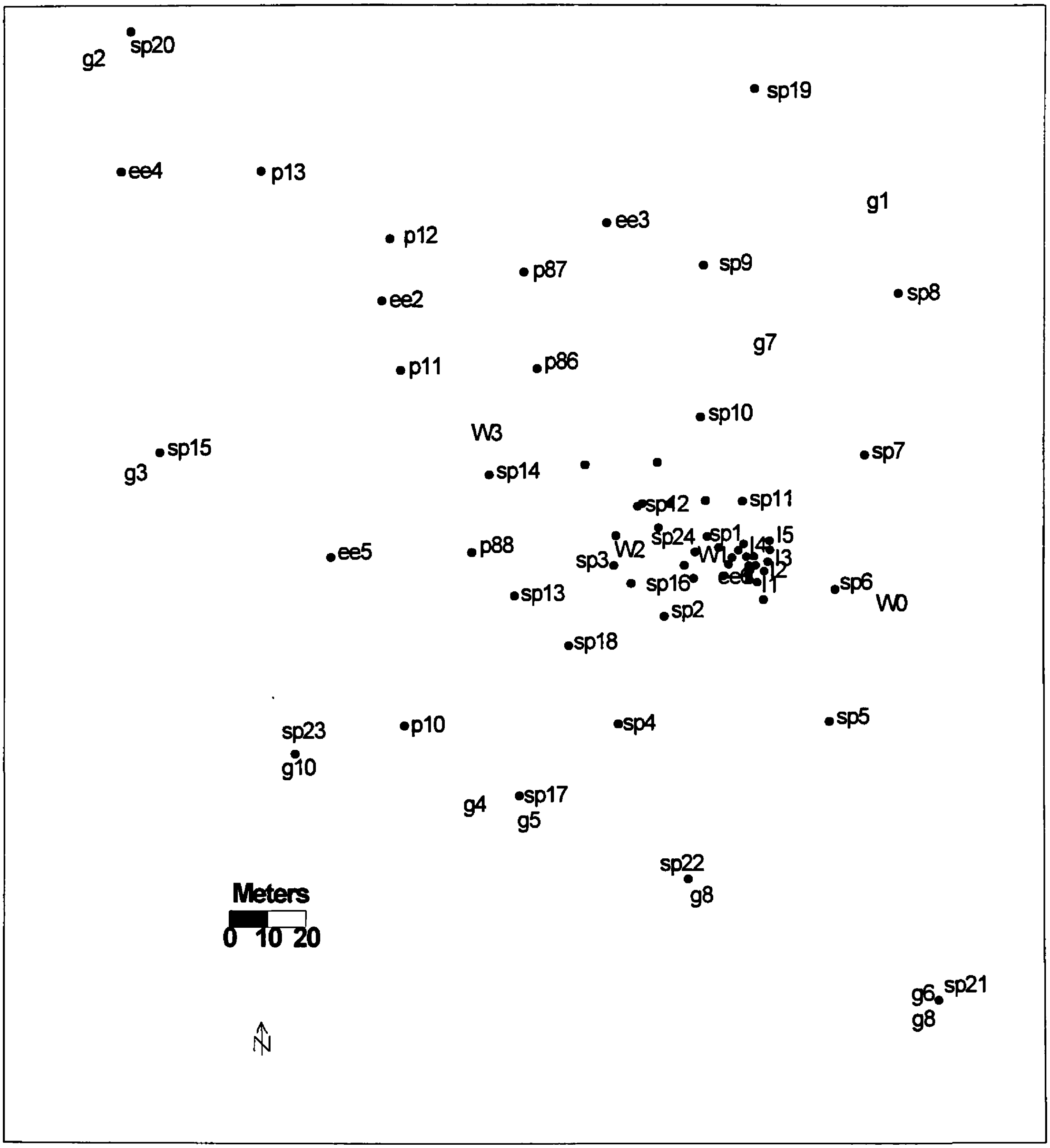

Figure B1: Wells and staff gauges used in water level measurments

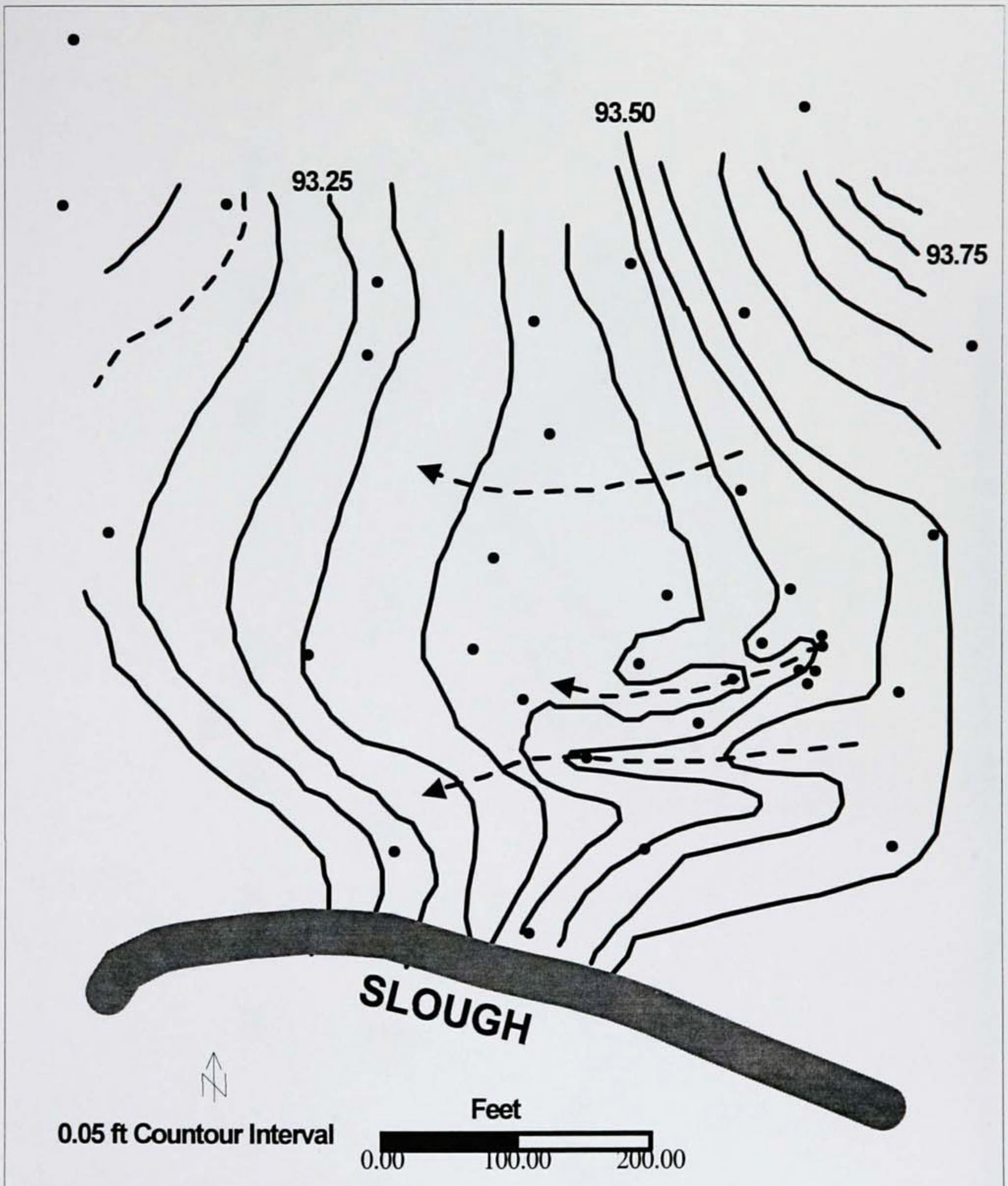

Figure B2. Potentiometric map for 9/24/96 with flow lines, 0.05 countour interval relative to a 100 ft datum.

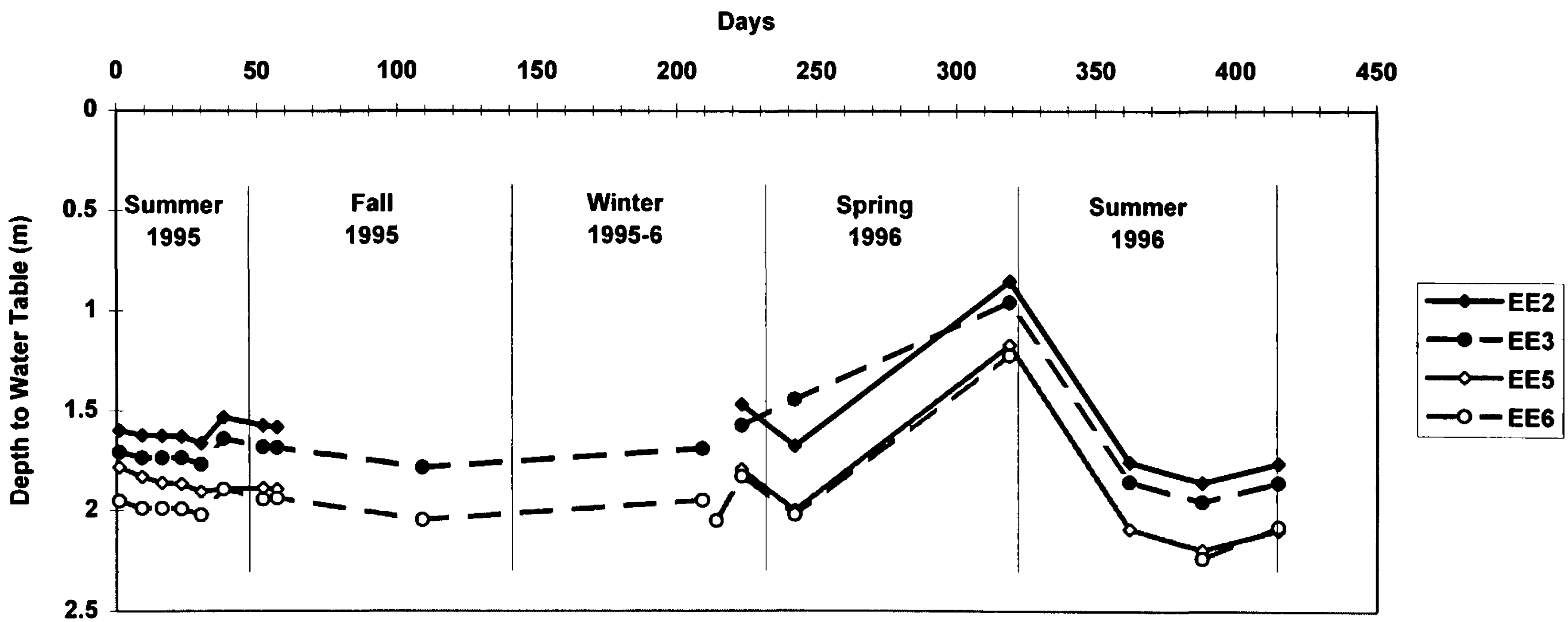

Figure B3. Hydrograph illustrating yearly water table fluctuation at Erskine site.

Table B1. Water levels measured at the Erskine Site, 11/95 to 3/97

Water Levels	11/11/95				
Note: Most wells inaccessible due to snow cover.					
East	North	Water Table	Water Depth	Elevation	Well
1219.568	874.648	93.67	6.82	100.489	ee6
918.547	739.817	93.49	8.65	102.141	p10
792.682	1221.803	93.30	5.95	99.251	p13
905.245	1163.351	93.41	5.45	98.862	p12
914.848	1049.168	93.62	6.10	99.718	p11
1094.061	1177.213	93.67	5.95	99.616	ee3
Water Levels	03/01/96				
Note: Some well caps were frozen to casing and wells could not be measured.					
East	North	Water Table	Water Depth	Elevation	Well etc.
1225.707	864.441	94.16	7.64	101.803	i1
1231.516	874.006	94.00	7.20	101.204	i2
1234.793	882.396	94.02	6.99	101.011	i3
1236.548	892.545	94.03	6.60	100.627	i4
1236.159	900.458	94.05	6.48	100.526	i5
1219.568	874.648	93.99	6.50	100.489	ee6
918.547	739.817	93.76	8.38	102.141	p10
792.682	1221.803	93.67	5.58	99.251	p13
905.245	1163.351	93.80	5.06	98.862	p12
977.175	890.369	93.95	7.96	101.906	p88
1034.129	1050.801	93.93	6.31	100.236	p86
1094.061	1177.213	93.98	5.64	99.616	ee3
1103.073	905.007	93.00	7.70	100.697	p37
1224.489	879.406	92.91	7.34	100.254	p23
1218.305	873.538	92.93	6.95	99.878	p7
1217.773	871.124	93.03	6.85	99.876	p22
1219.025	866.452	93.08	6.70	99.78	p21
1216.230	886.691	92.87	7.25	100.122	p40
1196.364	869.961	92.88	6.83	99.713	p28
1200.810	880.029	93.06	6.56	99.617	p27
1209.500	892.306	93.16	6.75	99.907	p25
1213.913	897.854	92.73	7.38	100.11	p24
1162.498	879.049	93.12	7.43	100.55	p30
1171.965	890.739	93.14	6.92	100.056	p31
1182.469	904.202	92.73	6.73	99.462	p32
1180.937	935.710	92.91	6.99	99.896	p33
1149.977	932.964	92.76	6.60	99.362	p34
1125.994	933.070	94.16	7.30	101.455	p85
1138.914	969.006	92.07	7.98	100.045	p38
1075.786	966.912	92.79	6.62	99.41	p39
Water Levels	03/06/96				
East	North	Water Table	Water Depth	Elevation	Well etc.
1225.707	864.441	94.39	7.41	101.803	i1
1231.516	874.006	93.80	7.40	101.204	i2
1236.548	892.545	93.75	6.88	100.627	i4
1236.159	900.458	93.73	6.80	100.526	i5
1219.568	874.648	93.65	6.84	100.489	ee6

Table B1. Water levels measured at the Erskine Site, 11/95 to 3/97

918.547	739.817	93.59	8.55	102.141	p10
792.682	1221.803	93.41	5.84	99.251	p13
905.245	1163.351	93.52	5.35	98.862	p12
977.175	890.369	94.16	7.75	101.906	p88
1034.129	1050.801	93.65	6.59	100.236	p86
1103.073	905.007	92.72	7.98	100.697	p37
1224.489	879.406	92.83	7.42	100.254	p23
1218.305	873.538	92.65	7.23	99.878	p7
1217.773	871.124	92.76	7.12	99.876	p22
1219.025	866.452	92.81	6.97	99.78	p21
1216.230	886.691	92.71	7.42	100.122	p40
1196.364	869.961	92.62	7.10	99.713	p28
1200.810	880.029	90.40	9.22	99.617	p27
1209.500	892.306	92.93	6.98	99.907	p25
1213.913	897.854	92.45	7.66	100.11	p24
1162.498	879.049	92.36	8.19	100.55	p30
1171.965	890.739	92.92	7.14	100.056	p31
1182.469	904.202	92.48	6.98	99.462	p32
1180.937	935.710	92.64	7.26	99.896	p33
1149.977	932.964	92.47	6.89	99.362	p34
1125.994	933.070	94.02	7.44	101.455	p85
1138.914	969.006	91.81	8.24	100.045	p38
1075.786	966.912	92.49	6.92	99.41	p39
671.185	1221.394	93.36	4.80	98.159	ee4
1139.948	911.955	92.28	7.85	100.132	p35
1116.401	863.672	92.39	8.11	100.501	p36
Water Levels	**03/15/96**				
East	**North**	**Water Table**	**Water Depth**	**Elevation**	**Well etc.**
1219.568	874.648	94.39	6.10	100.489	ee6
918.547	739.817	94.20	7.94	102.141	p10
792.682	1221.803	94.05	5.20	99.251	p13
905.245	1163.351	94.20	4.66	98.862	p12
977.175	890.369	94.34	7.57	101.906	p88
1034.129	1050.801	94.36	5.88	100.236	p86
1103.073	905.007	93.42	7.28	100.697	p37
1196.364	869.961	93.31	6.40	99.713	p28
1200.810	880.029	93.48	6.14	99.617	p27
1209.500	892.306	95.89	4.02	99.907	p25
1213.913	897.854	93.15	6.96	100.11	p24
1182.469	904.202	93.17	6.29	99.462	p32
1180.937	935.710	93.35	6.55	99.896	p33
1149.977	932.964	93.30	6.06	99.362	p34
1125.994	933.070	93.85	7.61	101.455	p85
1138.914	969.006	92.47	7.58	100.045	p38
1075.786	966.912	93.19	6.22	99.41	p39
671.185	1221.394	94.02	4.14	98.159	ee4
1094.061	1177.213	94.37	5.25	99.616	ee3
1022.218	1134.289	94.29	4.88	99.167	p87
1203.937	885.997	93.38	6.23	99.606	p26
854.066	886.200	94.29	5.99	100.276	ee5

Table B1. Water levels measured at the Erskine Site, 11/95 to 3/97

898.149	1109.307	94.25	4.90	99.153	ee2
Water Levels	**04/03/96**				
East	**North**	**Water Table**	**Water Depth**	**Elevation**	**Well**
1219.568	874.648	93.75	6.74	100.489	ee6
918.547	739.817	93.58	8.56	102.141	p10
792.682	1221.803	94.01	5.24	99.251	p13
905.245	1163.351	93.54	5.33	98.862	p12
977.175	890.369	93.67	8.24	101.906	p88
1034.129	1050.801	90.80	9.44	100.236	p86
1103.073	905.007	92.69	8.01	100.697	p37
1209.500	892.306	92.94	6.97	99.907	p25
1213.913	897.854	92.59	7.52	100.11	p24
1125.994	933.070	93.82	7.64	101.455	p85
671.185	1221.394	93.34	4.82	98.159	ee4
1094.061	1177.213	93.69	5.93	99.616	ee3
854.066	886.200	93.61	6.67	100.276	ee5
898.149	1109.307	93.55	5.60	99.153	ee2
1225.707	864.441	93.89	7.91	101.803	i1
1231.516	874.006	93.72	7.48	101.204	i2
1234.793	882.396	93.71	7.30	101.011	i3
1236.548	892.545	93.73	6.90	100.627	i4
1236.159	900.458	93.78	6.75	100.526	i5
1171.965	890.739	92.91	7.15	100.056	p31
1116.401	863.672	92.39	8.11	100.501	p36
Water Levels	**04/29/96**				
East	**North**	**Water Table**	**Water Depth**	**Elevation**	**Well**
1176.399	1008.644	95.172	5.440	100.612	sp10
1121.854	930.621	95.098	5.770	100.868	sp12
1101.197	879.184	95.113	6.060	101.173	sp3
1062.006	809.544	95.149	6.750	101.899	sp18
1018.782	678.859	94.971	6.030	101.001	sp17
1009.840	655.506	97.635	2.276	99.911	g5
1104.939	741.457	95.127	6.470	101.597	sp4
1393.880	502.552	97.148	2.240	99.388	g6
1287.557	743.596	95.284	5.350	100.634	sp5
1292.828	858.144	95.209	5.940	101.149	sp6
1225.707	864.441	95.183	6.620	101.803	i1
1231.516	874.006	95.164	6.040	101.204	i2
1234.793	882.396	95.181	5.830	101.011	i3
1236.548	892.545	95.187	5.440	100.627	i4
1236.159	900.458	95.196	5.330	100.526	i5
1219.568	874.648	94.999	5.490	100.489	ee6
1212.873	935.155	95.182	5.740	100.922	sp11
1192.176	894.811	95.172	5.170	100.342	sp1
1170.461	867.896	95.075	6.430	101.505	sp16
1145.109	834.939	95.136	6.590	101.726	sp2
1014.553	852.758	95.092	6.040	101.132	sp13
918.547	739.817	94.981	7.160	102.141	p10

Table B1. Water levels measured at the Erskine Site, 11/95 to 3/97

965.795	668.214	98.467	1.823	100.29	g4
854.066	886.200	94.996	5.280	100.276	ee5
704.938	977.757	94.828	6.190	101.018	sp15
668.469	958.624	98.557	2.760	101.317	g3
671.185	1221.394	94.669	3.490	98.159	ee4
629.841	1330.282	93.603	2.448	96.051	g2
679.076	1343.180	94.388	4.340	98.728	sp20
792.682	1221.803	94.781	4.470	99.251	p13
905.245	1163.351	94.942	3.920	98.862	p12
898.149	1109.307	94.913	4.240	99.153	ee2
992.385	958.430	95.099	5.440	100.539	sp14
977.175	890.369	95.106	6.800	101.906	p88
1034.129	1050.801	95.126	5.110	100.236	p86
1022.218	1134.289	95.027	4.140	99.167	p87
1094.061	1177.213	95.066	4.550	99.616	ee3
1221.998	1293.534	95.290	4.570	99.86	sp19
1312.709	1194.455	95.832	2.250	98.082	g1
1346.346	1115.699	95.404	5.170	100.574	sp8
1214.864	1068.079	95.298	2.385	97.683	g7
1178.298	1140.265	95.172	4.240	99.412	sp9
1318.114	975.460	95.234	4.665	99.899	sp7
Water Levels	**05/05/96**				
East	**North**	**Water Table**	**Water Depth**	**Elevation**	**Well**
1176.399	1008.644	94.852	5.760	100.612	sp10
1121.854	930.621	94.768	6.100	100.868	sp12
1101.197	879.184	94.803	6.370	101.173	sp3
1062.006	809.544	94.829	7.070	101.899	sp18
1018.782	678.859	94.631	6.370	101.001	sp17
1009.840	655.506	97.536	2.375	99.911	g5
1104.939	741.457	94.797	6.800	101.597	sp4
1393.880	502.552	97.044	2.344	99.388	g6
1287.557	743.596	94.954	5.680	100.634	sp5
1292.828	858.144	94.879	6.270	101.149	sp6
1225.707	864.441	94.853	6.950	101.803	i1
1231.516	874.006	94.824	6.380	101.204	i2
1234.793	882.396	94.841	6.170	101.011	i3
1236.548	892.545	94.857	5.770	100.627	i4
1236.159	900.458	94.846	5.680	100.526	i5
1219.568	874.648	94.779	5.710	100.489	ee6
1212.873	935.155	94.862	6.060	100.922	sp11
1192.176	894.811	94.842	5.500	100.342	sp1
1170.461	867.896	94.755	6.750	101.505	sp16
1145.109	834.939	94.806	6.920	101.726	sp2
1014.553	852.758	94.762	6.370	101.132	sp13
918.547	739.817	94.661	7.480	102.141	p10
965.795	668.214	96.683	1.927	98.61	g4
854.066	886.200	94.666	5.610	100.276	ee5
704.938	977.757	94.508	6.510	101.018	sp15
671.185	1221.394	94.349	3.810	98.159	ee4
629.841	1330.282	94.004	2.672	96.676	g2

Table B1. Water levels measured at the Erskine Site, 11/95 to 3/97

679.076	1343.180	94.108	4.620	98.728	sp20
792.682	1221.803	94.471	4.780	99.251	p13
905.245	1163.351	94.622	4.240	98.862	p12
898.149	1109.307	94.593	4.560	99.153	ee2
992.385	958.430	94.729	5.810	100.539	sp14
1034.129	1050.801	94.806	5.430	100.236	p86
1022.218	1134.289	94.737	4.430	99.167	p87
1094.061	1177.213	94.746	4.870	99.616	ee3
1221.998	1293.534	95.030	4.830	99.860	sp19
1312.709	1194.455	95.182	2.500	97.682	g1
1346.346	1115.699	95.104	5.470	100.574	sp8
1214.864	1068.079	94.901	2.682	97.583	g7
1178.298	1140.265	94.862	4.550	99.412	sp9
1318.114	975.460	94.909	4.990	99.899	sp7
Water Levels	**05/17/96**				
East	**North**	**Water Table**	**Water Depth**	**Elevation**	**Well**
1176.399	1008.644	95.85	4.76	100.612	sp10
1121.854	930.621	95.81	5.06	100.868	sp12
1101.197	879.184	95.84	5.33	101.173	sp3
1062.006	809.544	95.87	6.03	101.899	sp18
1018.782	678.859	96.06	4.94	101.001	sp17
1009.840	655.506	99.39	0.52	99.911	g5
1104.939	741.457	95.86	5.74	101.597	sp4
1393.880	502.552	98.95	0.44	99.388	g6
1287.557	743.596	96.04	4.59	100.634	sp5
1292.828	858.144	95.91	5.24	101.149	sp6
1225.707	864.441	95.88	5.92	101.803	i1
1231.516	874.006	95.86	5.34	101.204	i2
1234.793	882.396	95.88	5.13	101.011	i3
1236.548	892.545	95.87	4.76	100.627	i4
1236.159	900.458	95.88	4.65	100.526	i5
1219.568	874.648	95.82	4.67	100.489	ee6
1212.873	935.155	95.86	5.06	100.922	sp11
1192.176	894.811	95.88	4.46	100.342	sp1
1170.461	867.896	95.81	5.70	101.505	sp16
1145.109	834.939	95.86	5.87	101.726	sp2
1014.553	852.758	95.80	5.33	101.132	sp13
918.547	739.817	95.91	6.23	102.141	p10
965.795	668.214	100.25	0.04	100.29	g4
854.066	886.200	95.74	4.54	100.276	ee5
704.938	977.757	94.52	6.50	101.018	sp15
671.185	1221.394	95.33	2.83	98.159	ee4
629.841	1330.282	93.80	2.25	96.051	g2
679.076	1343.180	94.80	3.93	98.728	sp20
792.682	1221.803	95.42	3.83	99.251	p13
905.245	1163.351	95.53	3.33	98.862	p12
898.149	1109.307	95.83	3.32	99.153	ee2
992.385	958.430	95.76	4.78	100.539	sp14
1034.129	1050.801	95.76	4.48	100.236	p86
1022.218	1134.289	95.60	3.57	99.167	p87

Table B1. Water levels measured at the Erskine Site, 11/95 to 3/97

1094.061	1177.213	95.62	4.00	99.616	ee3
1221.998	1293.534	95.48	4.38	99.86	sp19
1312.709	1194.455	95.85	2.23	98.082	g1
1346.346	1115.699	95.96	4.61	100.574	sp8
1214.864	1068.079	95.60	2.08	97.683	g7
1178.298	1140.265	95.72	3.69	99.412	sp9
1318.114	975.460	95.88	4.02	99.899	sp7
Water Levels	**06/03/97**				
East	**North**	**Water Table**	**Water Depth**	**Elevation**	**Well**
1176.399	1008.644	95.95	4.66	100.612	sp10
1121.854	930.621	95.89	4.98	100.868	sp12
1101.197	879.184	95.91	5.26	101.173	sp3
1062.006	809.544	95.94	5.96	101.899	sp18
1018.782	678.859	95.79	5.21	101.001	sp17
1009.840	655.506	97.68	2.23	99.911	g5
1104.939	741.457	95.92	5.68	101.597	sp4
1393.880	502.552	97.62	1.77	99.388	g6
1287.557	743.596	96.02	4.61	100.634	sp5
1292.828	858.144	95.51	5.64	101.149	sp6
1225.707	864.441	95.94	5.86	101.803	i1
1231.516	874.006	95.92	5.28	101.204	i2
1234.793	882.396	95.95	5.06	101.011	i3
1236.548	892.545	95.95	4.68	100.627	i4
1236.159	900.458	95.96	4.57	100.526	i5
1219.568	874.648	95.88	4.61	100.489	ee6
1212.873	935.155	95.96	4.96	100.922	sp11
1192.176	894.811	95.95	4.39	100.342	sp1
1170.461	867.896	95.87	5.64	101.505	sp16
1145.109	834.939	95.93	5.80	101.726	sp2
1014.553	852.758	95.89	5.24	101.132	sp13
918.547	739.817	95.78	6.36	102.141	p10
965.795	668.214	98.52	1.77	100.29	g4
854.066	886.200	95.82	4.46	100.276	ee5
704.938	977.757	95.70	5.32	101.018	sp15
668.469	958.624	99.25	2.06	101.317	g3
671.185	1221.394	95.58	2.58	98.159	ee4
629.841	1330.282	94.59	1.46	96.051	g2
679.076	1343.180	95.35	3.38	98.728	sp20
792.682	1221.803	95.61	3.64	99.251	p13
905.245	1163.351	95.74	3.12	98.862	p12
898.149	1109.307	95.77	3.38	99.153	ee2
992.385	958.430	95.86	4.68	100.539	sp14
977.175	890.369	95.86	6.05	101.906	p86
1022.218	1134.289	95.87	3.30	99.167	p87
1094.061	1177.213	95.87	3.75	99.616	ee3
1221.998	1293.534	96.01	3.85	99.86	sp19
1312.709	1194.455	96.62	1.46	98.082	g1
1346.346	1115.699	96.11	4.46	100.574	sp8
1214.864	1068.079	96.08	1.60	97.683	g7
1178.298	1140.265	95.97	3.44	99.412	sp9

Table B1. Water levels measured at the Erskine Site, 11/95 to 3/97

1318.114	975.460	96.01	3.89	99.899	sp7
Water Levels	**06/20/96**				
East	**North**	**Water Table**	**Water Depth**	**Elevation**	**Well**
1176.399	1008.644	96.52	4.09	100.612	sp10
1121.854	930.621	96.44	4.43	100.868	sp12
1101.197	879.184	96.45	4.72	101.173	sp3
1062.006	809.544	96.49	5.41	101.899	sp18
1018.782	678.859	96.29	4.71	101.001	sp17
1009.840	655.506	97.91	2.00	99.911	g5
1104.939	741.457	96.45	5.15	101.597	sp4
1393.880	502.552	97.46	1.93	99.388	g6
1287.557	743.596	96.52	4.11	100.634	sp5
1292.828	858.144	96.51	4.64	101.149	sp6
1225.707	864.441	96.47	5.33	101.803	i1
1231.516	874.006	96.46	4.74	101.204	i2
1234.793	882.396	96.49	4.52	101.011	i3
1236.548	892.545	96.49	4.14	100.627	i4
1236.159	900.458	96.51	4.02	100.526	i5
1219.568	874.648	96.41	4.08	100.489	ee6
1212.873	935.155	96.51	4.41	100.922	sp11
1192.176	894.811	96.49	3.85	100.342	sp1
1170.461	867.896	96.40	5.11	101.505	sp16
1145.109	834.939	96.45	5.28	101.726	sp2
1014.553	852.758	96.43	4.70	101.132	sp13
918.547	739.817	96.35	5.79	102.141	p10
965.795	668.214	98.77	1.52	100.29	g4
854.066	886.200	96.37	3.91	100.276	ee5
704.938	977.757	96.26	4.76	101.018	sp15
668.469	958.624	99.37	1.95	101.317	g3
671.185	1221.394	96.00	2.16	98.159	ee4
629.841	1330.282	95.09	0.96	96.051	g2
679.076	1343.180	95.84	2.89	98.728	sp20
792.682	1221.803	96.18	3.07	99.251	p13
905.245	1163.351	96.33	2.53	98.862	p12
898.149	1109.307	96.31	2.84	99.153	ee2
992.385	958.430	96.41	4.13	100.539	sp14
977.175	890.369	96.32	5.59	101.906	p86
1022.218	1134.289	96.53	2.64	99.167	p87
1094.061	1177.213	96.43	3.19	99.616	ee3
1221.998	1293.534	96.59	3.27	99.86	sp19
1312.709	1194.455	97.29	0.79	98.082	g1
1346.346	1115.699	96.64	3.93	100.574	sp8
1214.864	1068.079	96.71	0.97	97.683	g7
1178.298	1140.265	96.53	2.88	99.412	sp9
1318.114	975.460	96.56	3.34	99.899	sp7
Water Levels	**08/02/96**				
East	**North**	**Water Table**	**Water Depth**	**Elevation**	**Well**
1176.399	1008.644	93.48	7.13	100.612	sp10

Table B1. Water levels measured at the Erskine Site, 11/95 to 3/97

1121.854	930.621	93.38	7.49	100.868	sp12
1101.197	879.184	93.41	7.76	101.173	sp3
1062.006	809.544	93.48	8.42	101.899	sp18
1018.782	678.859	93.27	7.73	101.001	sp17
1104.939	741.457	93.40	8.20	101.597	sp4
1287.557	743.596	93.53	7.10	100.634	sp5
1292.828	858.144	93.51	7.64	101.149	sp6
1225.707	864.441	93.45	8.35	101.803	i1
1231.516	874.006	92.44	8.76	101.204	i2
1234.793	882.396	93.47	7.54	101.011	i3
1236.548	892.545	93.48	7.15	100.627	i4
1236.159	900.458	93.48	7.05	100.526	i5
1212.873	935.155	93.47	7.45	100.922	sp11
1192.176	894.811	93.46	6.88	100.342	sp1
1170.461	867.896	93.37	8.14	101.505	sp16
1145.109	834.939	93.41	8.32	101.726	sp2
1014.553	852.758	93.39	7.74	101.132	sp13
854.066	886.200	93.31	6.97	100.276	ee5
704.938	977.757	93.19	7.83	101.018	sp15
671.185	1221.394	93.08	5.08	98.159	ee4
679.076	1343.180	92.99	5.74	98.728	sp20
792.682	1221.803	93.11	6.14	99.251	p13
905.245	1163.351	93.26	5.60	98.862	p12
898.149	1109.307	93.29	5.86	99.153	ee2
992.385	958.430	93.38	7.16	100.539	sp14
977.175	890.369	93.36	8.55	101.906	p88
1022.218	1134.289	93.37	5.80	99.167	p87
1094.061	1177.213	93.43	6.19	99.616	ee3
1221.998	1293.534	93.82	6.04	99.86	sp19
1346.346	1115.699	93.82	6.75	100.574	sp8
1178.298	1140.265	93.56	5.85	99.412	sp9
1318.114	975.460	93.53	6.37	99.899	sp7
1379.751	486.204	95.07	26.50	97.277	g8
1165.415	606.592	94.07	4.50	98.567	sp22
1172.071	602.542	95.06	19.50	96.687	g9
823.199	715.475	92.89	5.36	98.247	sp23
820.553	719.268	94.26	24.50	96.297	g10
Water Levels	**08/28/96**				
East	**North**	**Water Table**	**Water Depth**	**Elevation**	**Well**
1176.399	1008.644	93.12	7.49	100.612	sp10
1121.854	930.621	93.01	7.86	100.868	sp12
1101.197	879.184	93.04	8.13	101.173	sp3
1018.782	678.859	92.89	8.11	101.001	sp17
1009.840	655.506	98.40	2.78	98.631	g5
1104.939	741.457	93.04	8.56	101.597	sp4
1287.557	743.596	93.14	7.49	100.634	sp5
1292.828	858.144	93.10	8.05	101.149	sp6
1225.707	864.441	93.09	8.71	101.803	i1
1231.516	874.006	93.41	7.79	101.204	i2
1236.548	892.545	93.12	7.51	100.627	i4

Table B1. Water levels measured at the Erskine Site, 11/95 to 3/97

1219.568	874.648	93.03	7.46	100.489	ee6
1212.873	935.155	93.08	7.84	100.922	sp11
1192.176	894.811	93.11	7.23	100.342	sp1
1170.461	867.896	92.99	8.52	101.505	sp16
1145.109	834.939	93.03	8.70	101.726	sp22
1014.553	852.758	93.04	8.09	101.132	sp13
918.547	739.817	92.93	9.21	102.141	p10
965.795	668.214	98.37	2.84	98.61	g4
854.066	886.200	92.96	7.32	100.276	ee5
671.185	1221.394	92.77	5.39	98.159	ee4
792.682	1221.803	92.85	6.40	99.251	p13
905.245	1163.351	92.99	5.87	98.862	p12
898.149	1109.307	92.95	6.20	99.153	ee2
992.385	958.430	93.02	7.52	100.539	sp14
1034.129	1050.801	93.10	7.14	100.236	p86
1022.218	1134.289	93.08	6.09	99.167	p87
1094.061	1177.213	93.10	6.52	99.616	ee3
1221.998	1293.534	93.51	6.35	99.86	sp19
1346.346	1115.699	93.45	7.12	100.574	sp8
1178.298	1140.265	93.21	6.20	99.412	sp9
1318.114	975.460	93.18	6.72	99.899	sp7
1165.415	606.592	93.71	4.86	98.567	sp22
1172.071	602.542	96.56	1.50	96.687	g9
Water Levels	**09/24/96**				
East	**North**	**Water Table**	**Water Depth**	**Elevation**	**Well**
1176.399	1008.644	93.43	7.18	100.612	sp10
1121.854	930.621	93.34	7.53	100.868	sp12
1101.197	879.184	93.38	7.79	101.173	sp3
1062.006	809.544	93.45	8.45	101.899	sp18
1018.782	678.859	93.19	7.81	101.001	sp17
1009.840	655.506	95.96	32.00	98.631	g5
1104.939	741.457	93.35	8.25	101.597	sp4
1287.557	743.596	93.47	7.16	100.634	sp5
1292.828	858.144	93.42	7.73	101.149	sp6
1225.707	864.441	93.42	8.38	101.803	i1
1231.516	874.006	93.35	7.85	101.204	i2
1236.548	892.545	93.40	7.23	100.627	i3
1236.159	900.458	93.43	7.10	100.526	i5
1219.568	874.648	93.56	6.93	100.489	ee6
1212.873	935.155	93.44	7.48	100.922	sp11
1192.176	894.811	93.41	6.93	100.342	sp1
1170.461	867.896	93.33	8.18	101.505	sp16
1145.109	834.939	93.37	8.36	101.726	sp2
1014.553	852.758	93.36	7.77	101.132	sp13
918.547	739.817	93.19	8.95	102.141	p10
965.795	668.214	96.40	26.52	98.61	g4
854.066	886.200	93.29	6.99	100.276	ee5
704.938	977.757	93.19	7.83	101.018	sp15
671.185	1221.394	93.13	5.03	98.159	ee4
679.076	1343.180	93.10	5.63	98.728	sp20

Table B1. Water levels measured at the Erskine Site, 11/95 to 3/97

792.682	1221.803	93.10	6.15	99.251	p13
905.245	1163.351	93.26	5.60	98.862	p12
898.149	1109.307	93.27	5.88	99.153	ee2
992.385	958.430	93.35	7.19	100.539	sp14
977.175	890.369	93.33	8.58	101.906	p88
1034.129	1050.801	93.35	6.89	100.236	p86
1022.218	1134.289	93.33	5.84	99.167	p87
1094.061	1177.213	93.42	6.20	99.616	ee3
1221.998	1293.534	93.85	6.01	99.86	sp19
1346.346	1115.699	93.83	6.74	100.574	sp8
1178.298	1140.265	93.55	5.86	99.412	sp9
1318.114	975.460	93.50	6.40	99.899	sp7
1165.415	606.592	94.04	4.53	98.567	sp22
1172.071	602.542	95.06	19.50	96.687	g9
Water Levels	**03/26/97**				
East	**North**	**Water Table**	**Water Depth**	**Elevation**	**Well**
1176.399	1008.644	95.07	5.54	100.612	sp10
1121.854	930.621	95.01	5.86	100.868	sp12
1101.197	879.184	95.01	6.16	101.173	sp3
1292.828	858.144	95.09	6.06	101.149	sp6
1225.707	864.441	95.07	6.73	101.803	i1
1231.516	874.006	95.04	6.16	101.204	i2
1234.793	882.396	95.06	5.95	101.011	i3
1236.548	892.545	95.07	5.56	100.627	i4
1236.159	900.458	95.08	5.45	100.526	i5
1219.568	874.648	95.00	5.49	100.489	ee6
1212.873	935.155	95.08	5.84	100.922	sp11
1192.176	894.811	95.07	5.27	100.342	sp1
1170.461	867.896	94.98	6.53	101.505	sp16
1145.109	834.939	95.03	6.70	101.726	sp2
1014.553	852.758	94.99	6.14	101.132	sp13
992.385	958.430	94.96	5.58	100.539	sp14
1321.603	850.607	100.84	6.25	101.357	W0
1169.418	885.477	101.55	7.09	102.137	W1
1133.689	887.152	101.33	6.88	101.907	W2
969.008	991.922	100.68	6.24	101.197	W3

Table B2. Hydraulic conductivity calculated using steady state analysis.

Hydraulic conductivity calculated from bromide tracer test on 09/20/96.

N=.20 I=.00043

	x(ft)	t(hr)	v(fpd)	K(fpd)	K(mpd)
M2-9	25	6	100	46512	13953
M7-9	65	17	92	42681	12804
		Avg.	**96**	**44,596**	**13,379**

Hydraulic conductivity calculated in a monitoring well using the steady state Thiem equation.

Pumping W1

Aquifer Bottom=80.254 Q=98gpm

Well	X	Y	Elev	Final WL	R	H	K(ft/d)	K(m/d)
W1	1169.418	885.4768	102.137	8.68	0.166667	13.203	pumping well	
W2	1133.689	887.1522	101.907	8.44	35.76788	13.213	121987.2	36596.15
sp1	1192.176	894.811	100.342	6.85	24.59806	13.238	32392.39	9717.716
SP24	1152.932	848.2309	101.097	7.61	40.73134	13.233	41615.08	12484.52
M5	1174.388	873.2601	101.027	7.52	13.1891	13.253	19833.75	5950.124
M6	1172.742	880.0665	101.197	7.68	6.350024	13.263	13759.13	4127.74
M7	1171.795	886.873	101.427	7.95	2.75721	13.223	31865.9	9559.769
M9	1172.181	901.6203	100.417	6.94	16.37818	13.223	52100	15630
						Avg K	**44,793**	**13,438**

Pumping W2

Aquifer Bottom = 80.254ft Q=77gpm Saturated Thickness=13.093

Well	X	Y	Elev	Final WL	R	H	K(ft/d)	K(m/d)
W2	1133.689	887.1522	101.907	8.74	0.166667	12.913	umping well	
M15	1137.293	904.7617	100.907	7.49	17.97454	13.163	3386.095	1015.829
M14	1136.563	894.2902	101.127	7.72	7.694922	13.153	2888.976	866.6929
M13	1136.792	885.564	101.157	7.79	3.485312	13.113	2754.541	826.3624
M12	1137.646	877.7105	101.897	8.51	10.23751	13.133	3388.997	1016.699
M11	1139.311	868.9843	101.777	8.38	19.01788	13.143	3727.764	1118.329
M10	1143.83	854.1497	101.577	8.12	34.52526	13.203	3321.02	996.306
SP24	1152.932	848.2309	101.097	7.71	43.41827	13.133	4578.098	1373.429
SP3	1101.197	879.184	101.173	7.78	33.45493	13.139	4246.73	1274.019
						Avg K	**3,537**	**1,061**

Hydraulic conductivity calculated in the pumping well using the Thiem equation.

Pumping W3

Q	H	h	R	r	K(ft/d)	K(m/d)
102.0667	14.403	14.023	100	0.166667	**3,702**	**1,111**

Pumping W0

Q	H	h	R	r	K(ft/d)	K(m/d)
61.625	13.368	10.913	100	0.17	**404**	**121**

Hydraulic conductivity calculated with the Theis equation using recovery data.

WO

Drawdown	Q	b	T(ft^2/D)	K(ft/d)	K(m/d)
0.1	98	13.368	258720	**2,587**	**776**

Table B2. Hydraulic conductivity calculated using steady state analysis.

W1

Drawdown	Q	b	T(ft^2/D)	K(ft/d)	K(m/d)
0.1	98	13.193	258720	**2,621**	**786**

W2

Drawdown	Q	b	T(ft^2/D)	K(ft/d)	K(m/d)
0.28	77	13.193	72600	**736**	**221**

W3

Drawdown	Q	b	T(ft^2/D)	K(ft/d)	K(m/d)
0.38	102.0667	14.403	70909.47	**658**	**197**

Table B4. Time-dradown data from aquifer test of W1.

Pumping W1				W1		SP1		M7		M8		M9		M5		M6		SP16		SP24		W2	
hrs	min	sec	t(min)	s	WL	s	WL	s	WL	s	WL	s	WL	s	WL	s	WL	s	WL	s	WL	s	WL
0	0	0	0.010	0.000	8.560	0.000	6.740	0.000	7.820	0.000	7.200	0.000	6.850	0.000	7.510	0.000	7.610	0.000	8.030	0.000	7.540	0.000	8.350
0	0	36	0.600	0.030	8.590																		
0	0	50	0.833					0.060	7.880														
0	1	20	1.333	0.040	8.600																		
0	1	25	1.417					0.060	7.88														
0	1	55	1.917	0.040	8.600																		
0	2	25	2.417					0.060	7.880														
0	3	10	3.167	0.050	8.610																		
0	4	15	4.250	0.060	8.620																		
0	4	30	4.500					0.080	7.900														
0	5	30	5.500	0.060	8.620																		
0	6	30	6.500	0.070	8.630																		
0	6	30	6.500					0.080	7.900														
0	7	10	7.167	0.070	8.630																		
0	7	50	7.833					0.080	7.900														
0	8	10	8.167	0.070	8.630																		
0	9	0	9.000					0.080	7.900														
0	10	15	10.250					0.085	7.905														
0	10	55	10.917	0.080	8.640																		
0	11	20	11.333					0.090	7.910														
0	12	30	12.500			0.065	6.805																
0	13	15	13.250																	0.050	7.590		
0	13	45	13.750																			0.070	8.420
0	14	30	14.500			0.070	6.810																
0	15	10	15.167	0.080	8.640																		
0	28	30	28.500			0.090	6.830																
0	29	15	29.250																	0.070	7.610		
0	29	40	29.667																			0.070	8.420
0	30	30	30.500	0.100	8.660																		
0	31	15	31.250					0.110	7.930														
0	45	10	45.167			0.100	6.840																
0	45	40	45.667	0.110	8.670																		
0	46	15	46.250					0.130	7.950														
0	46	55	46.917																	0.080	7.620		
0	47	20	47.333																			0.100	8.450
1	12	0	72.000			0.110	6.850																
1	13	0	73.000	0.120	8.680																		
1	15	0	75.000					0.130	7.950														
1	16	0	76.000																	0.080	7.620		
1	16	30	76.500																			0.100	8.450
1	32	0	92.000			0.110	6.850																
1	33	0	93.000	0.120	8.680																		
1	34	0	94.000					0.130	7.950														
1	35	0	95.000																	0.080	7.620		
1	36	0	96.000																			0.100	8.450
2	1	0	######			0.110	6.850																
2	2	0	######															0.090	8.120				
2	3	0	######	0.120	8.680																		
2	4	0	######									0.090	6.940										
2	6	0	######							0.130	7.330												
2	7	0	######					0.130	7.950														
2	8	0	######													0.070	7.680						
2	10	0	######											0.010	7.520								
2	12	0	######																	0.080	7.620		
2	13	0	######																			0.100	8.450

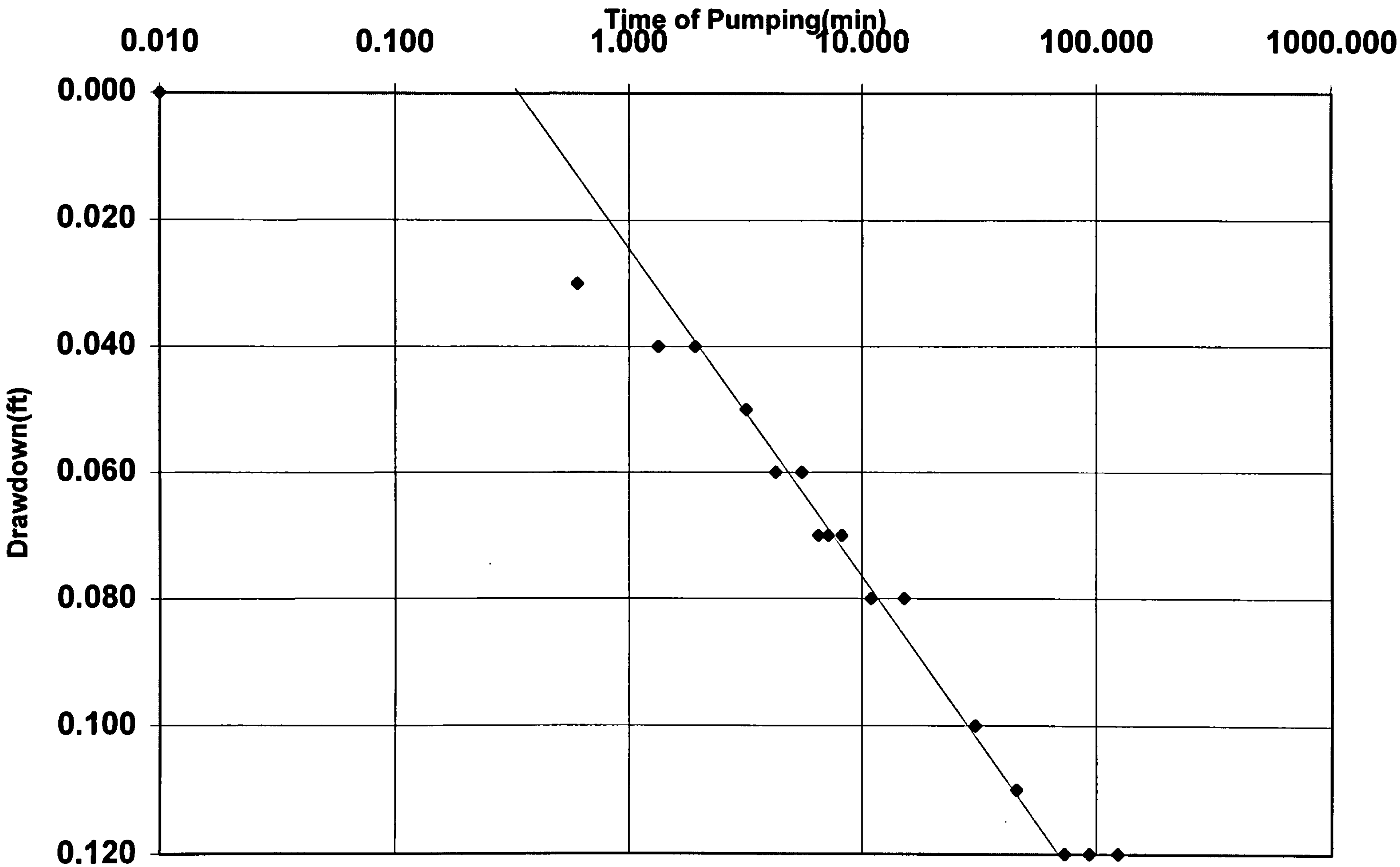

Figure B4. Time-drawdown plot observed in W1, pumping W1.

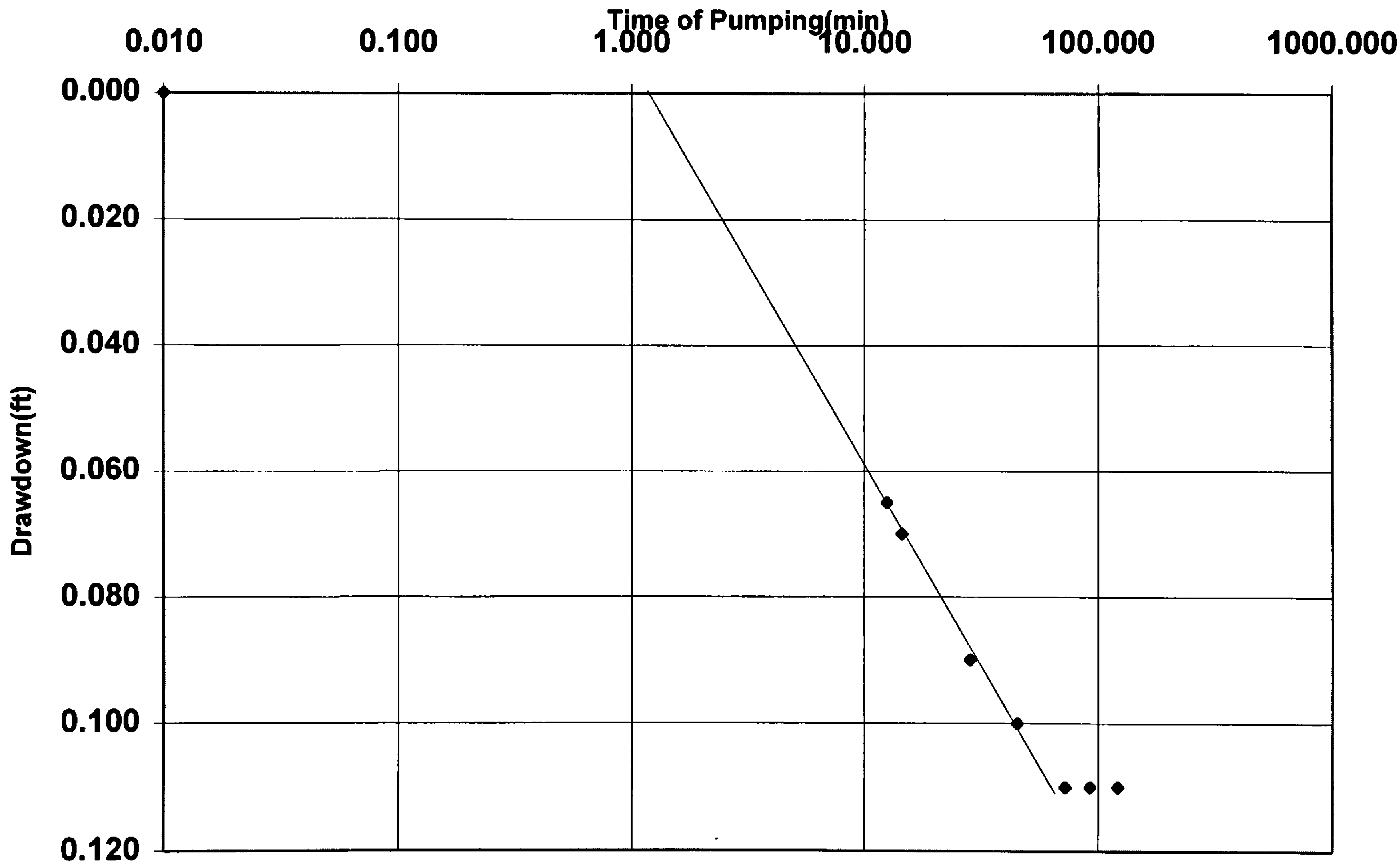

Figure B5. Time-drawdown plot observed in SP1, pumping W1.

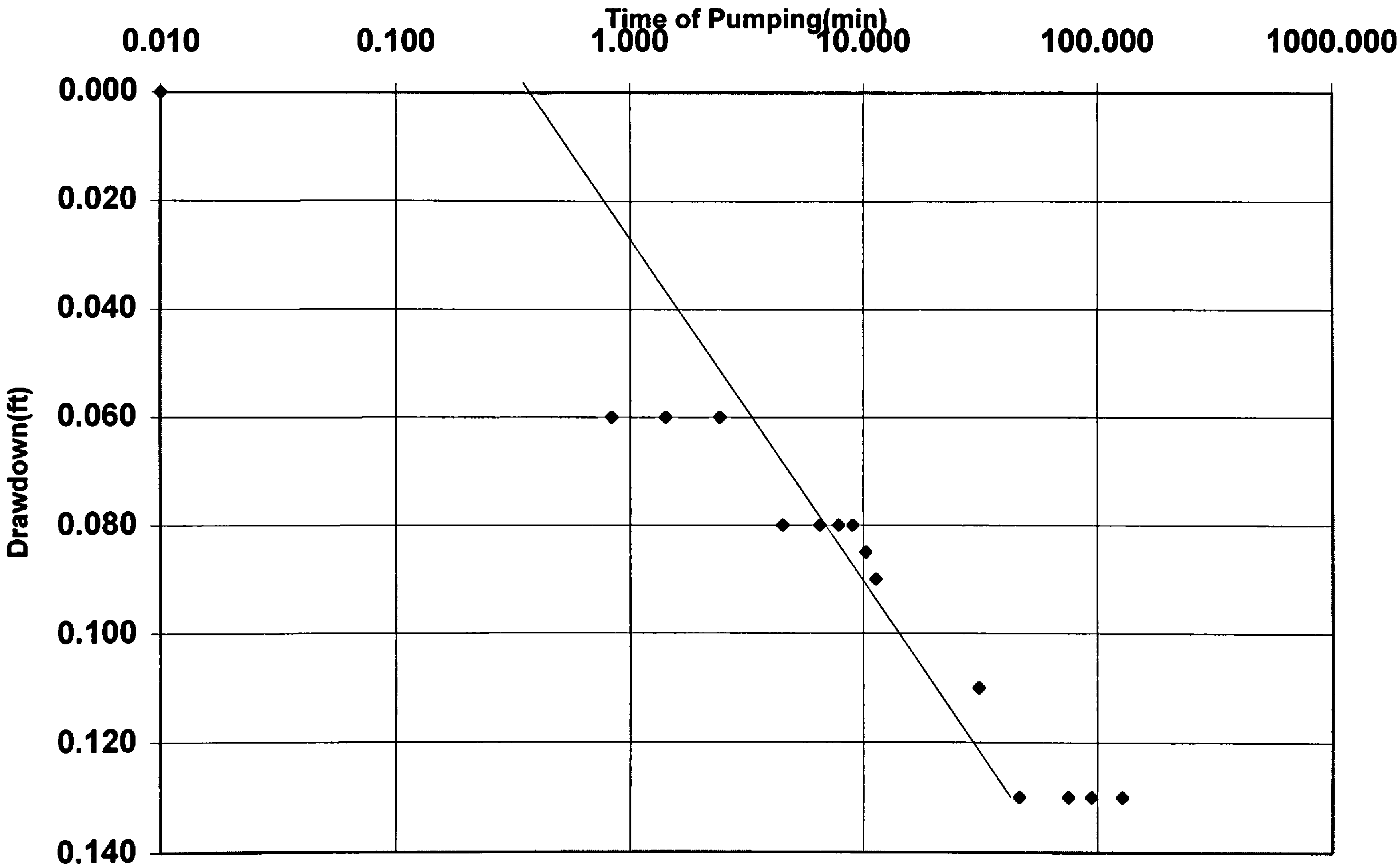

Figure B6. Time-drawdown plot observed in M7, pumping W1.

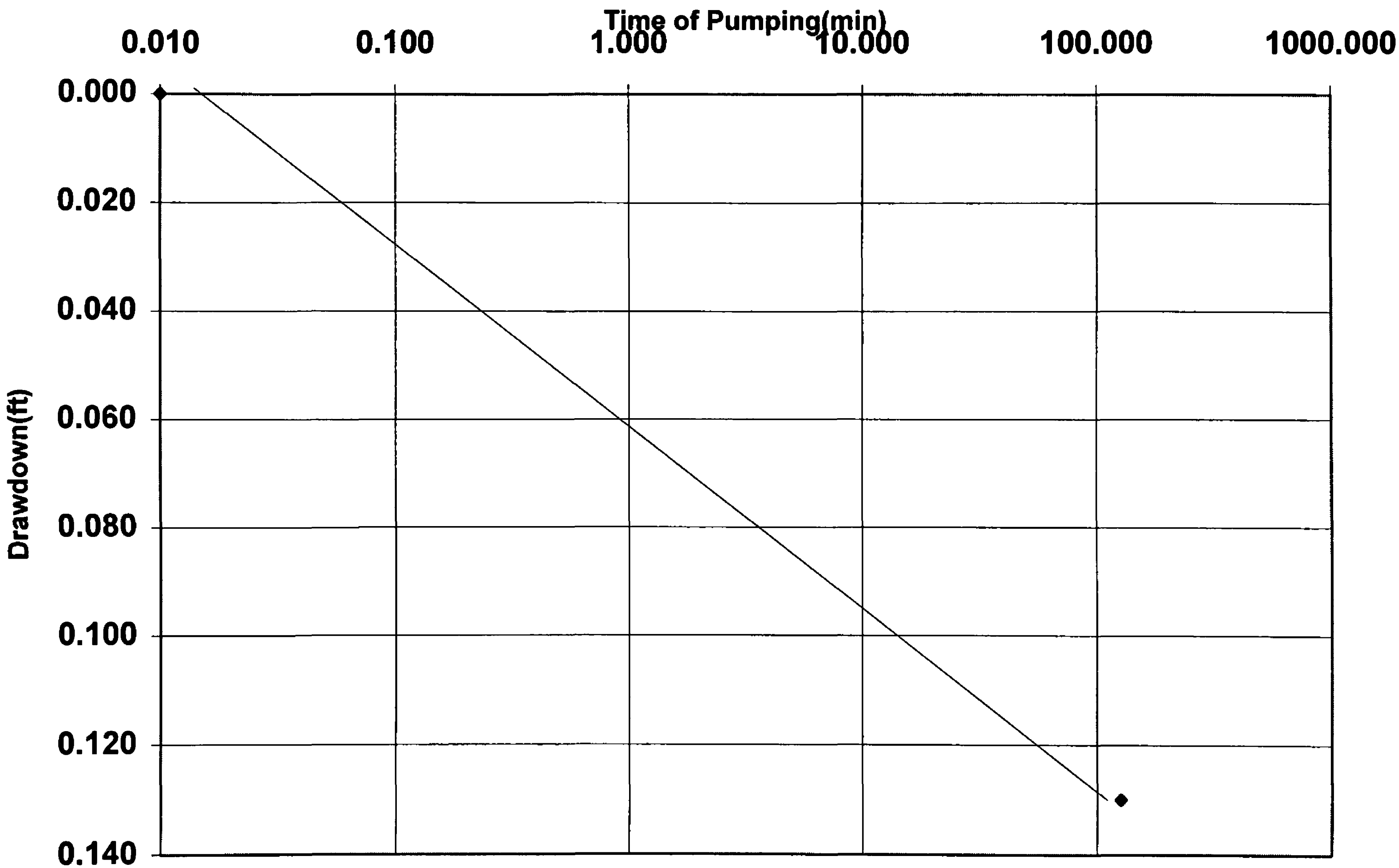

Figure B7. Time-drawdown plot observed in M8, pumping W1.

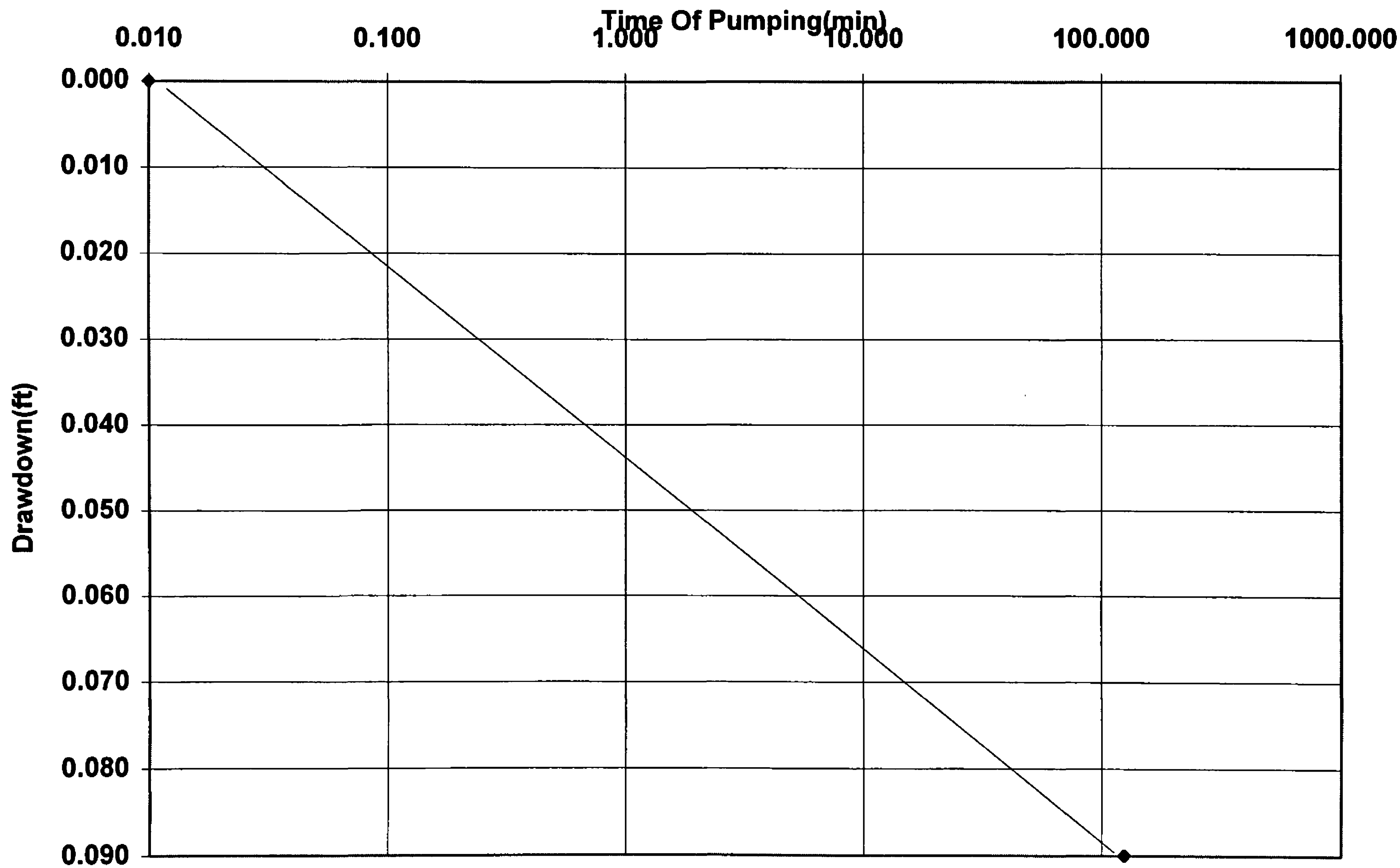

Figure B8. Time-drawdown plot observed in M9, pumping W1.

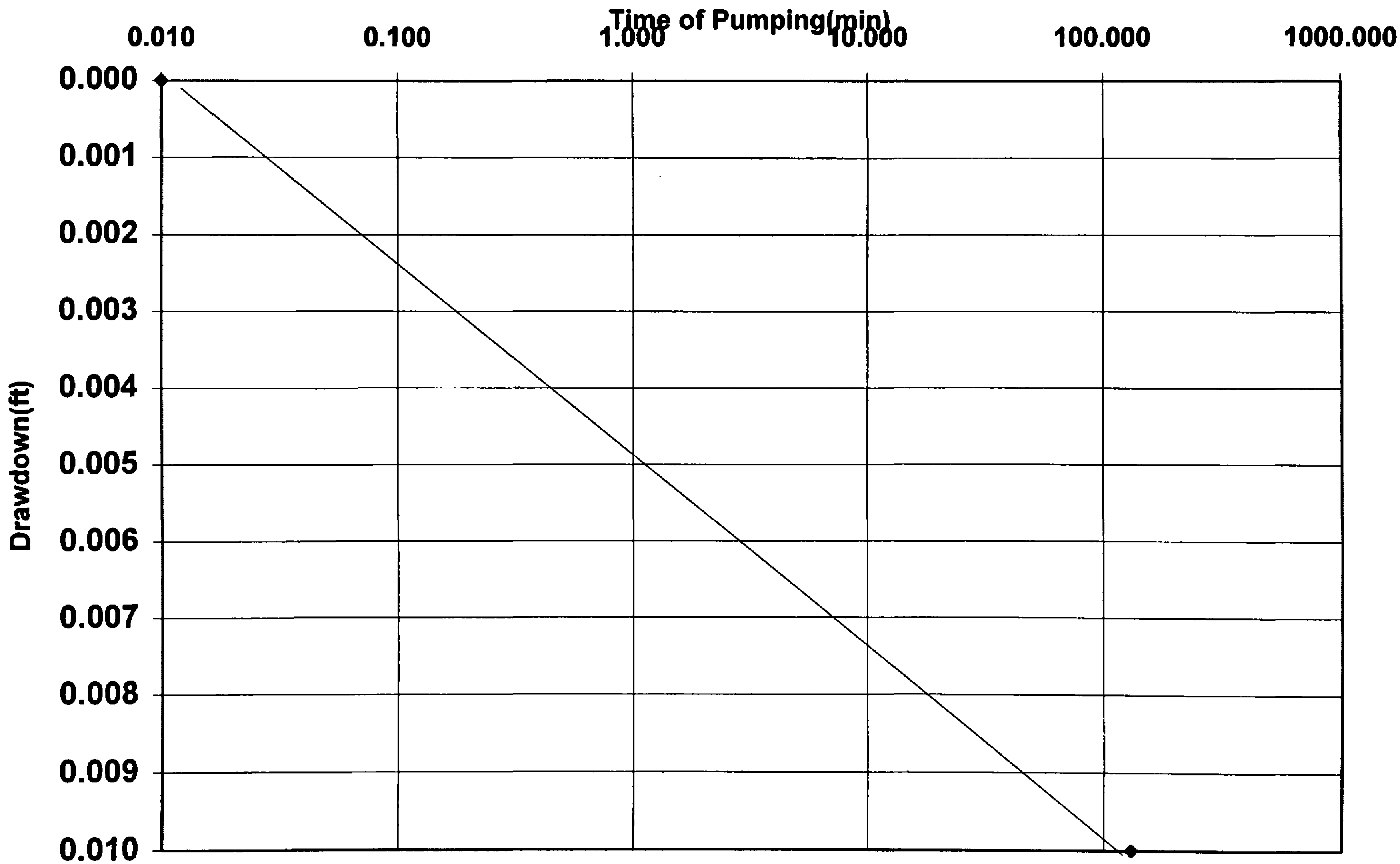

Figure B9. Time-drawdown plot observed in M5, pumping W1.

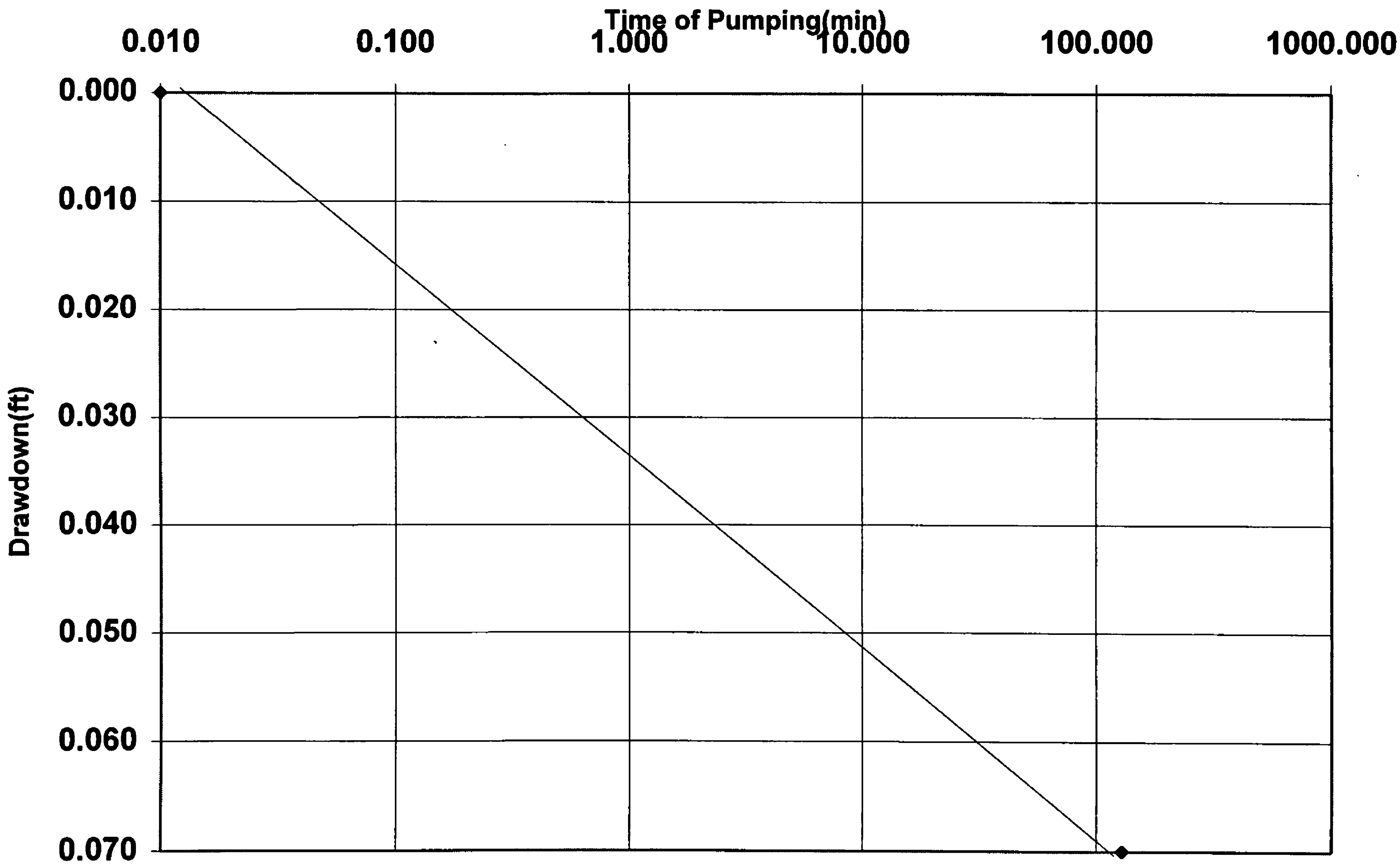

Figure B10. TIme-drawdown plot observed in M6, pumping W1.

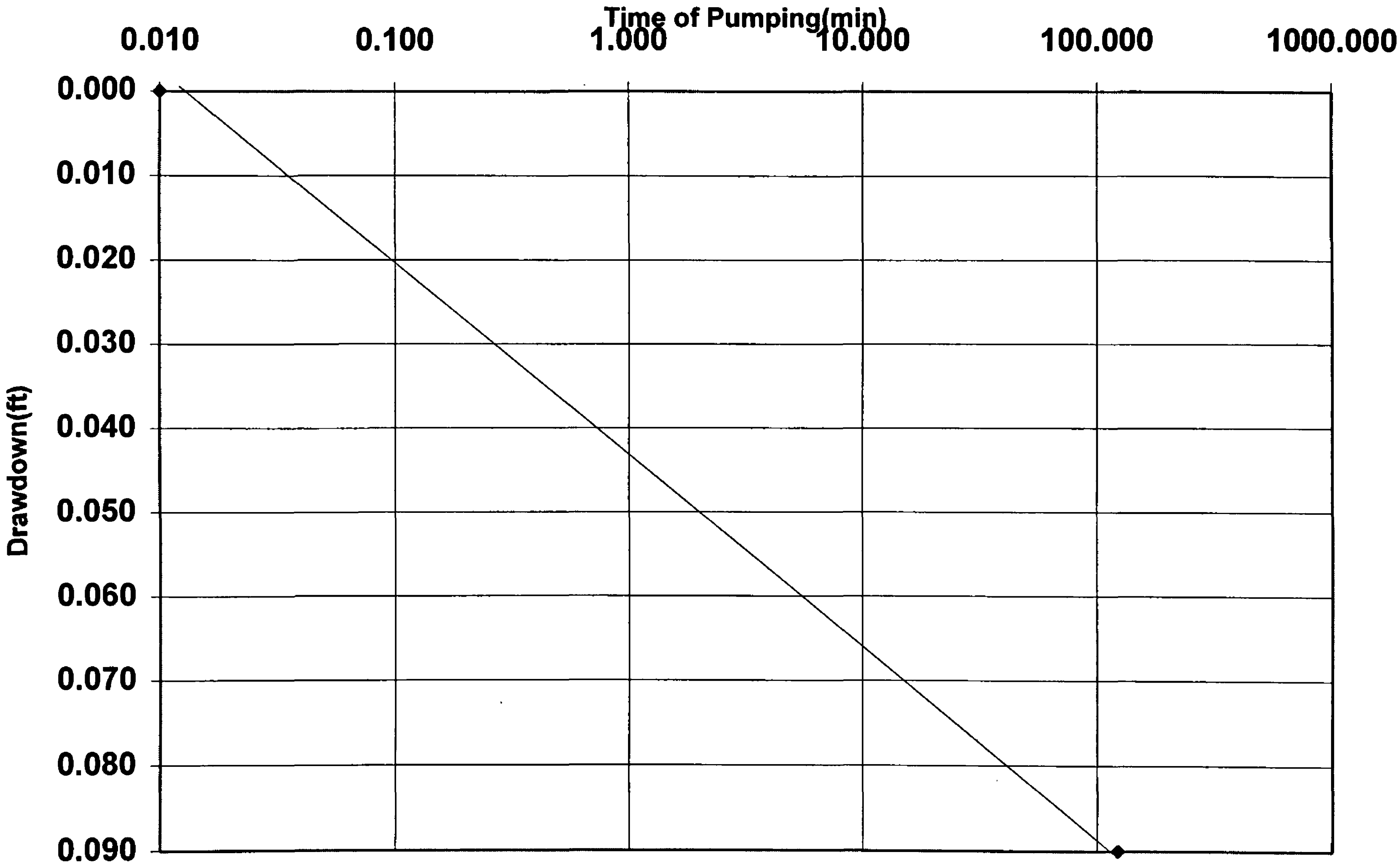

Figure B11. Time-drawdown plot observed in SP16, pumping W1.

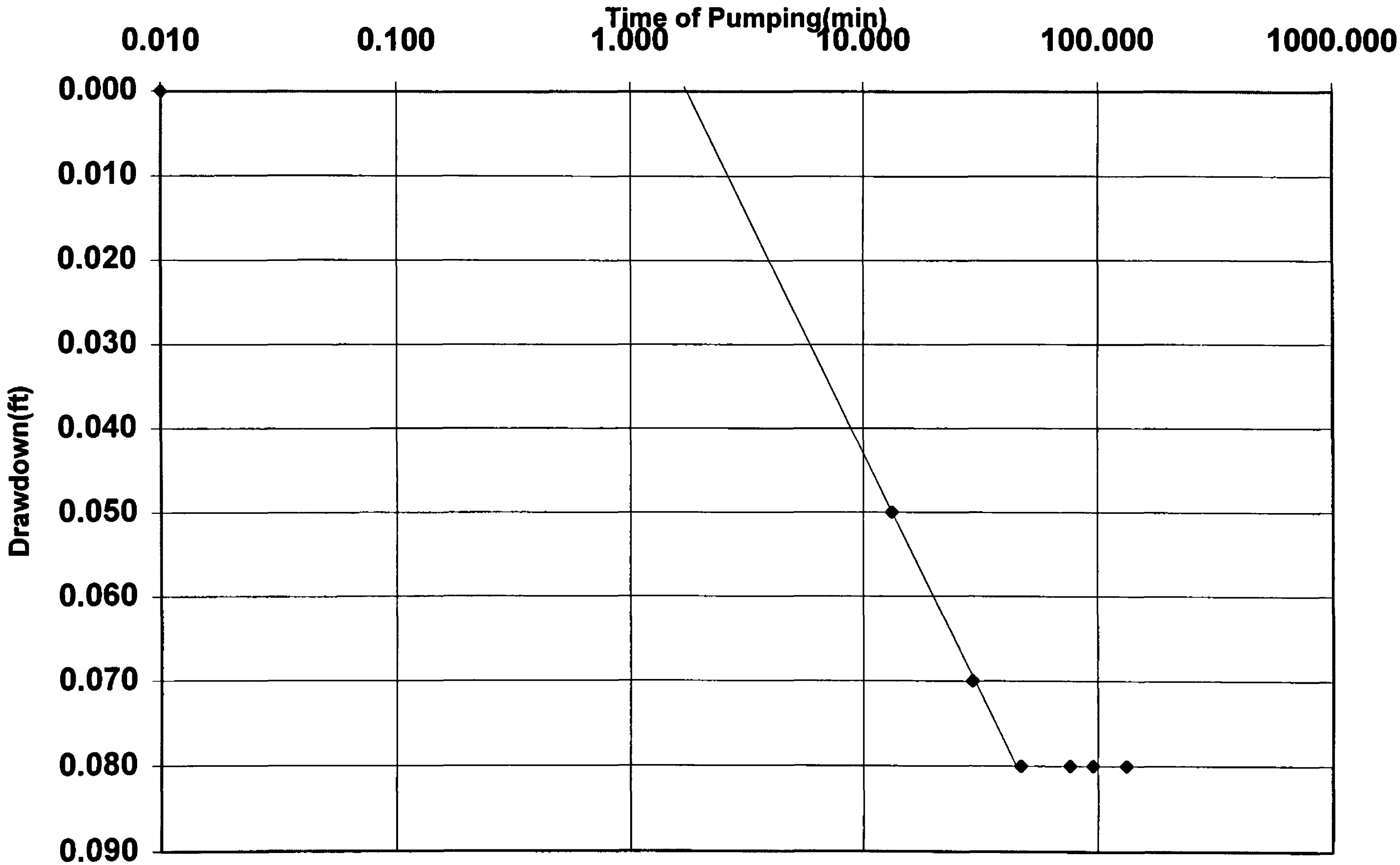

Figure B12. Time-drawdown plot observed in SP24, pumping W1.

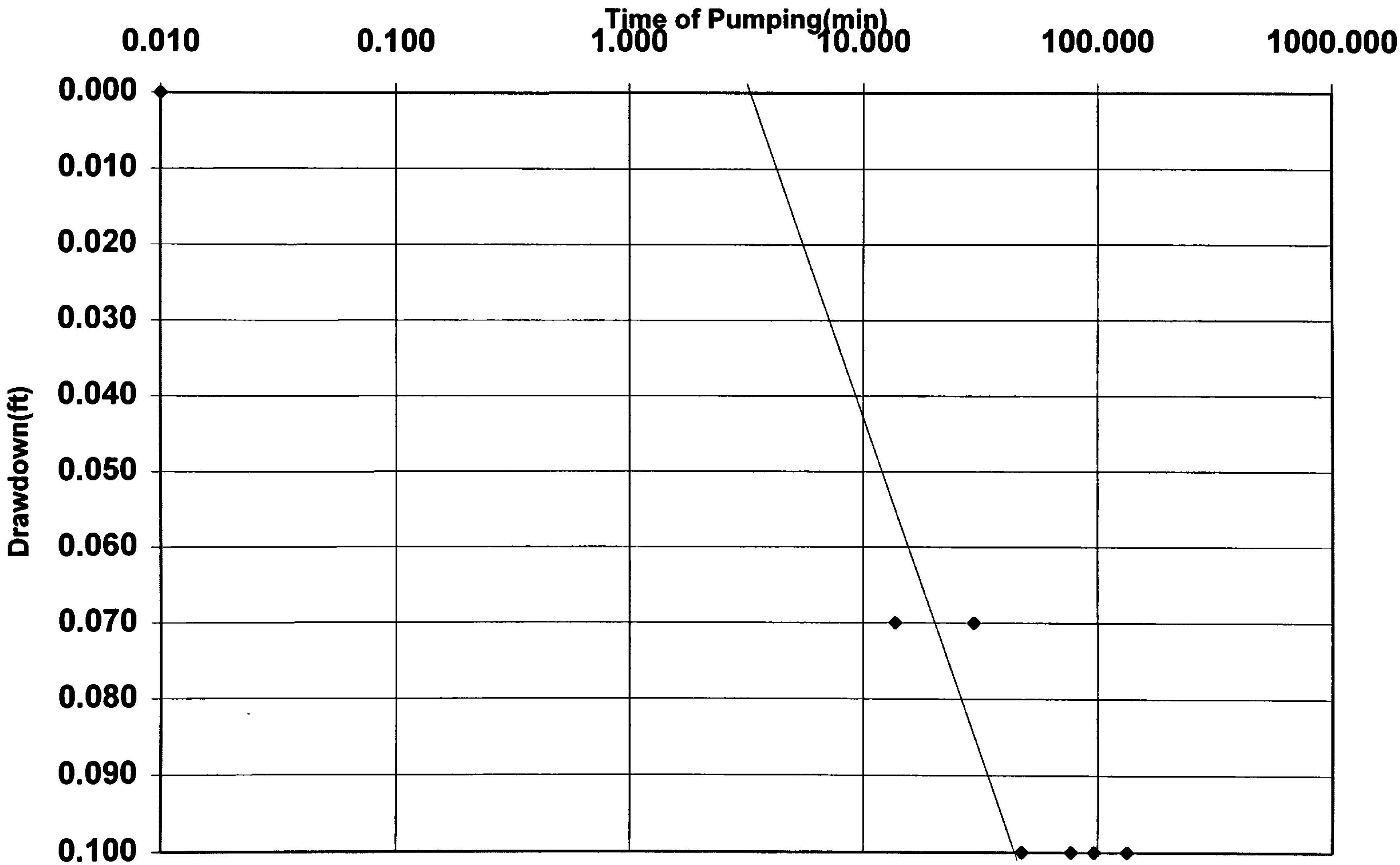

Figure B13. Time-drawdown plot observed in W2, pumping W1.

Table B5. Time-drawdown data from aquifer test of W2.

Pumping W2				W2		SP24		SP3		W1		M10		M11		M12		M13		M14		M15	
hrs	min	sec	t(min)	s	WL	s	WL	s	WL	s	WL	s	WL	s	WL	s	WL	s	WL	s	WL	s	WL
0	0	0	0.010	0.000	8.440	0.000	7.660	0.000	7.720	0.000	8.660	0.000	8.080	0.000	8.310	0.000	8.320	0.000	7.700	0.000	7.650	0.000	7.450
0	0	14	0.233			0.000	7.660																
0	0	42	0.700			0.000	7.660																
0	1	0	1.000			0.000	7.660																
0	1	20	1.333			0.000	7.660																
0	1	42	1.700			0.000	7.660																
0	2	10	2.167	0.240	8.680																		
0	2	49	2.817			0.010	7.670																
0	3	20	3.333			0.010	7.670																
0	4	10	4.167			0.020	7.680																
0	5	13	5.217			0.030	7.690																
0	5	48	5.800	0.260	8.700																		
0	6	55	6.917			0.030	7.690																
0	8	30	8.500			0.030	7.690																
0	10	40	10.667	0.290	8.730																		
0	11	55	11.917													0.180	8.500						
0	13	25	13.417			0.030	7.690																
0	15	20	15.333															0.100	7.800				
0	23	10	23.167			0.040	7.700																
0	23	50	23.833	0.300	8.740																		
0	25	0	25.000					0.060	7.780														
0	26	0	26.000							0.070	8.730												
0	52	55	52.917	0.300	8.740																		
0	53	55	53.917			0.050	7.710																
0	55	45	55.750							0.070	8.730												
1	30	30	90.500			0.050	7.710																
1	31	0	91.000	0.300	8.740																		
1	31	30	91.500					0.060	7.780														
1	32	0	92.000							0.070	8.730												
1	55	0	######							0.070	8.730												
1	55	30	######			0.050	7.710																
1	56	0	######					0.060	7.780														
1	56	30	######	0.300	8.740																		
1	58	30	######									0.040	8.120										
2	2	0	######											0.070	8.380								
2	5	0	######													0.190	8.510						
2	11	0	######															0.100	7.800				
2	12	0	######																	0.070	7.720		
2	14	0	######																			0.040	7.490

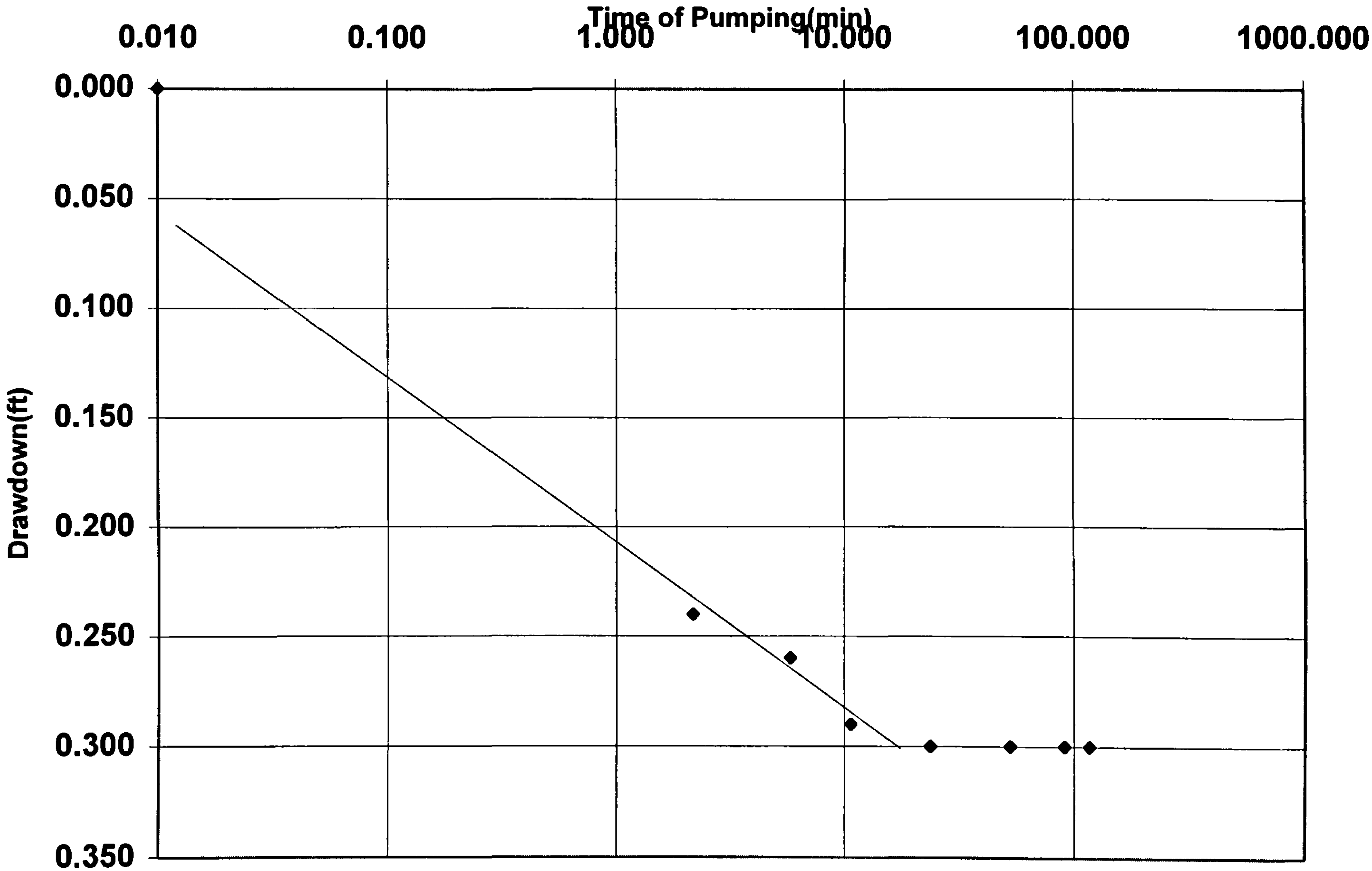

Figure B14. Time-drawdown plot observed in pumping well W2.

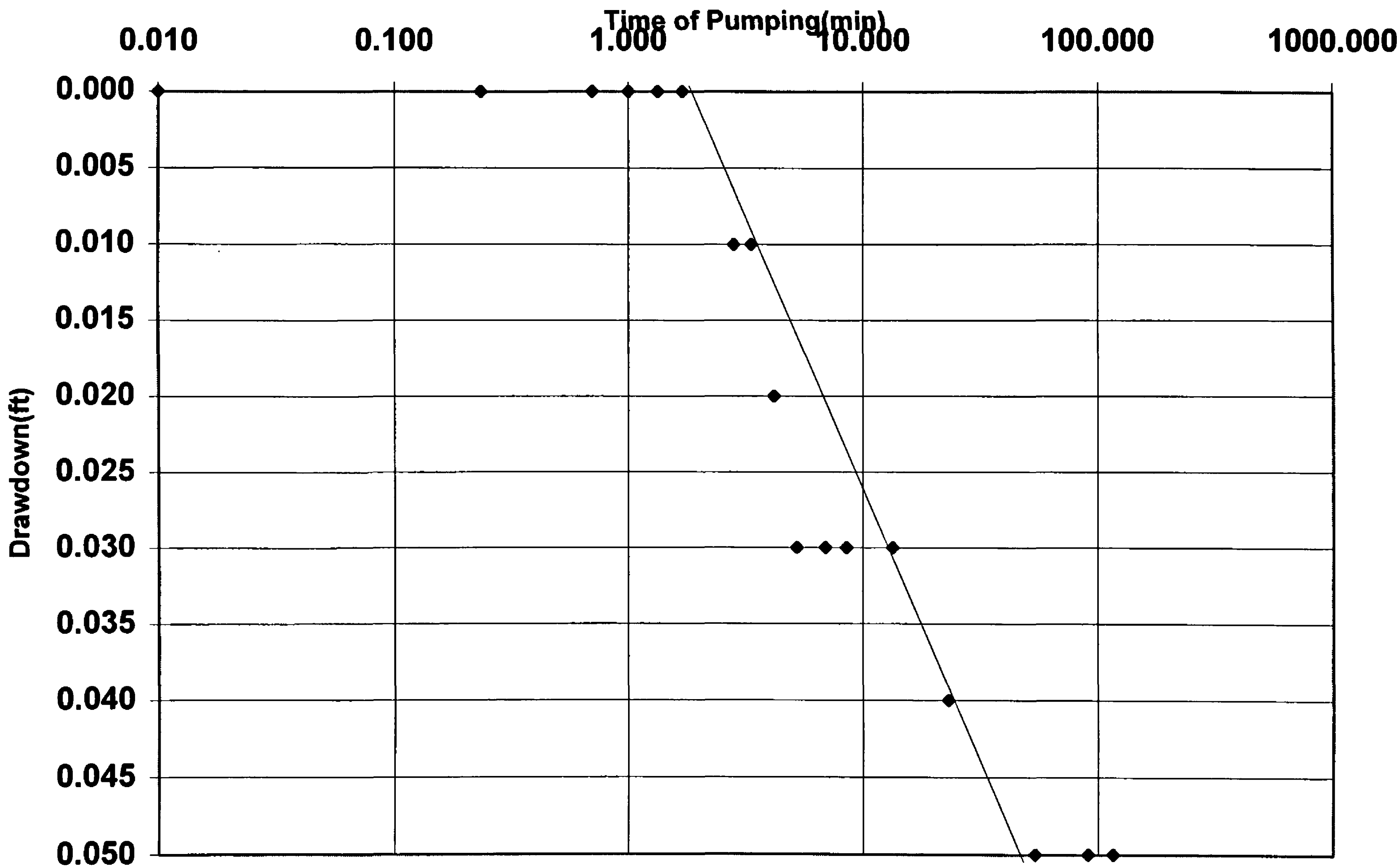

Figure B15. Time-drawdown plot observed in SP24, pumping W2.

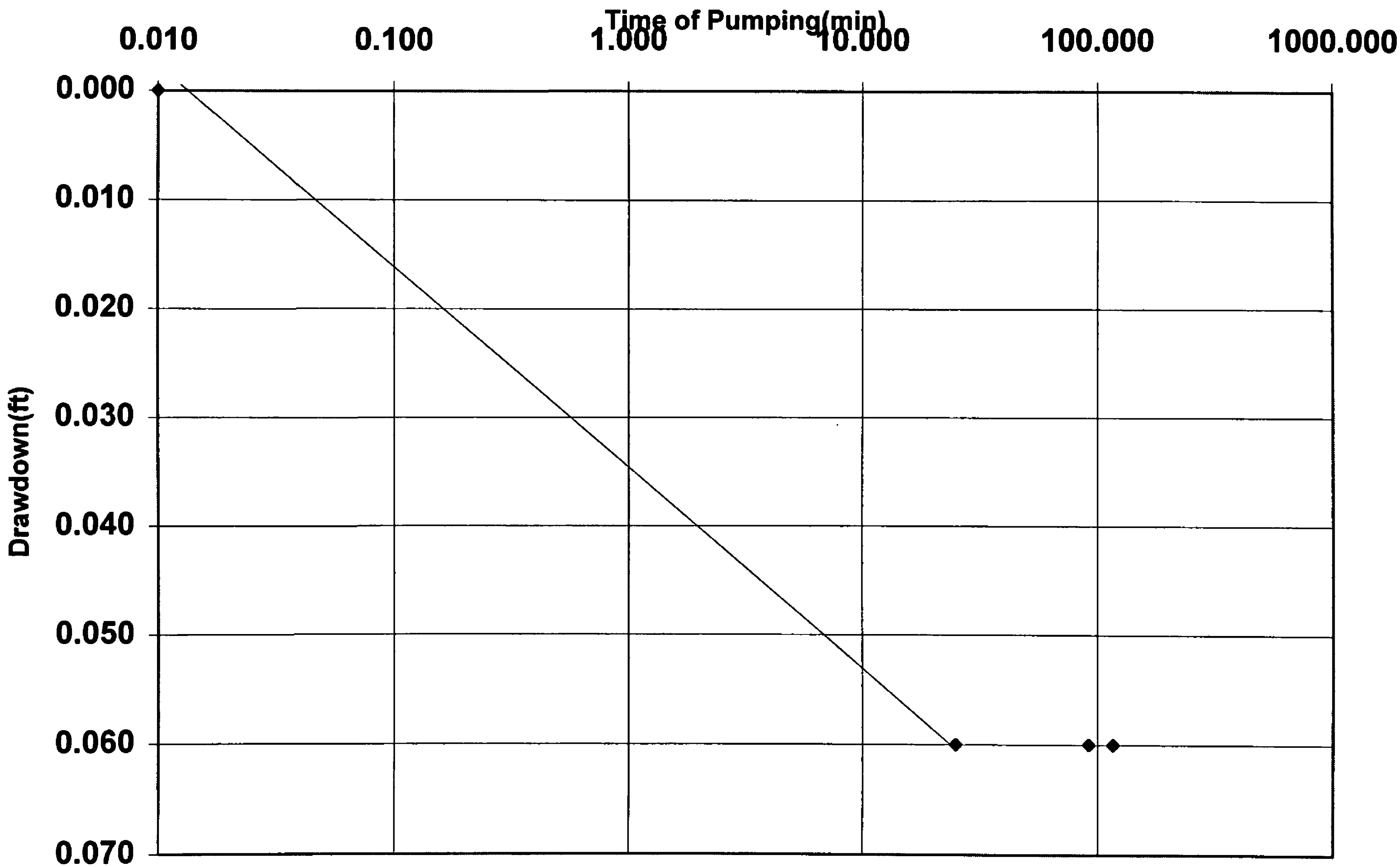

Figure B16. Time-drawdown plot observed in SP3, pumping W2.

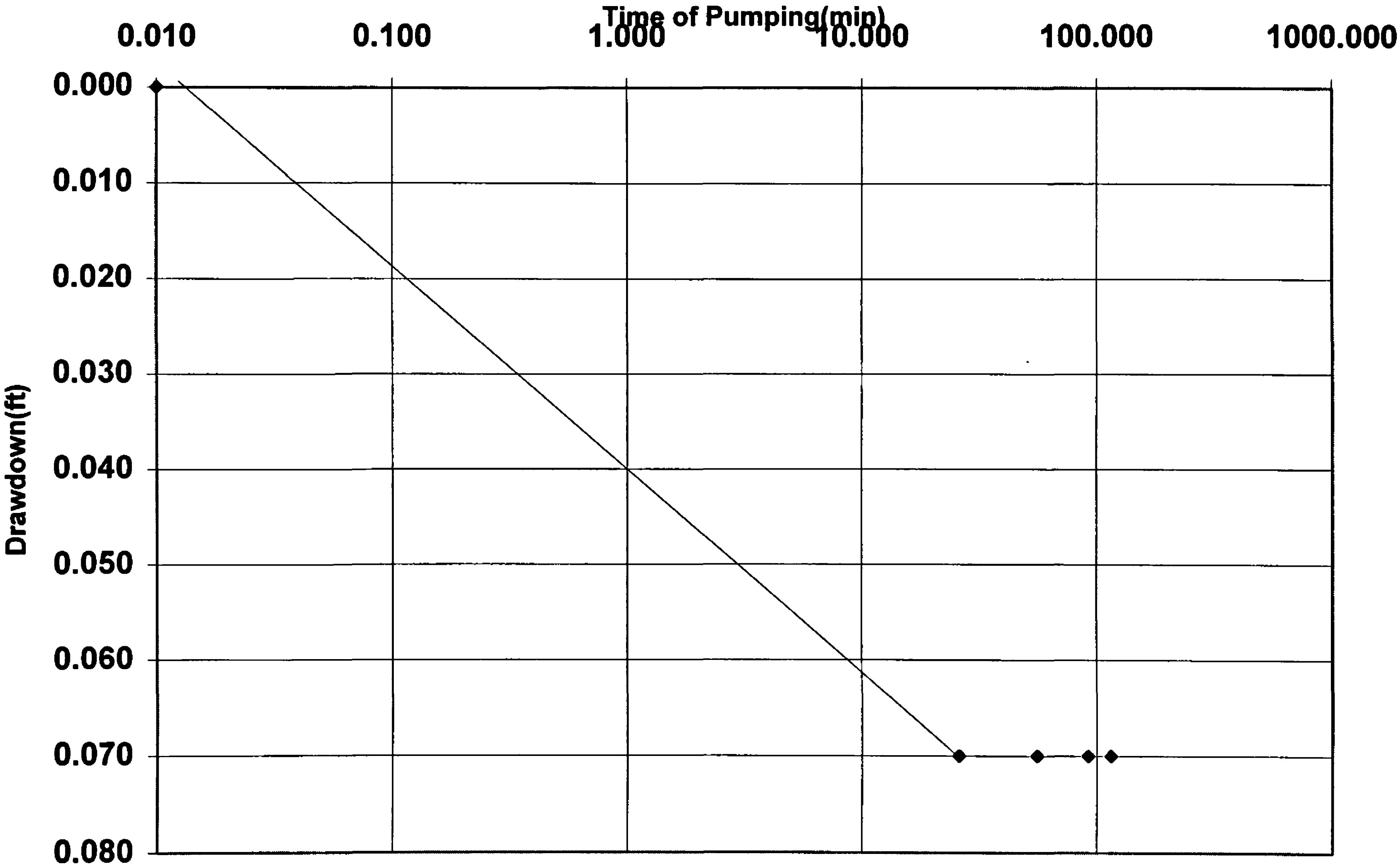

Figure B17. Time-drawdown plot observed in W1, pumping W2.

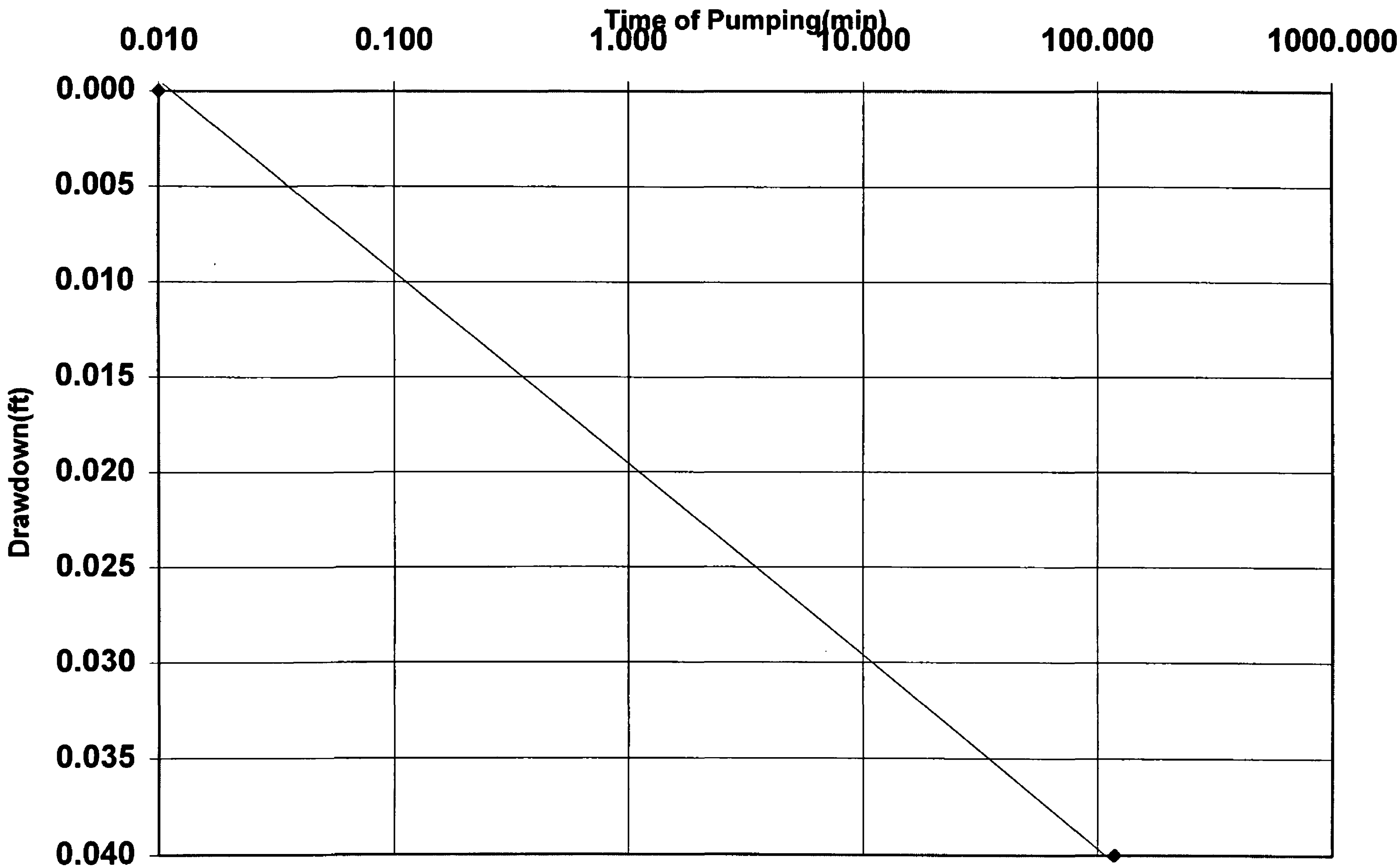

Figure B18. Time-drawdown plot observed in M10, pumping W2.

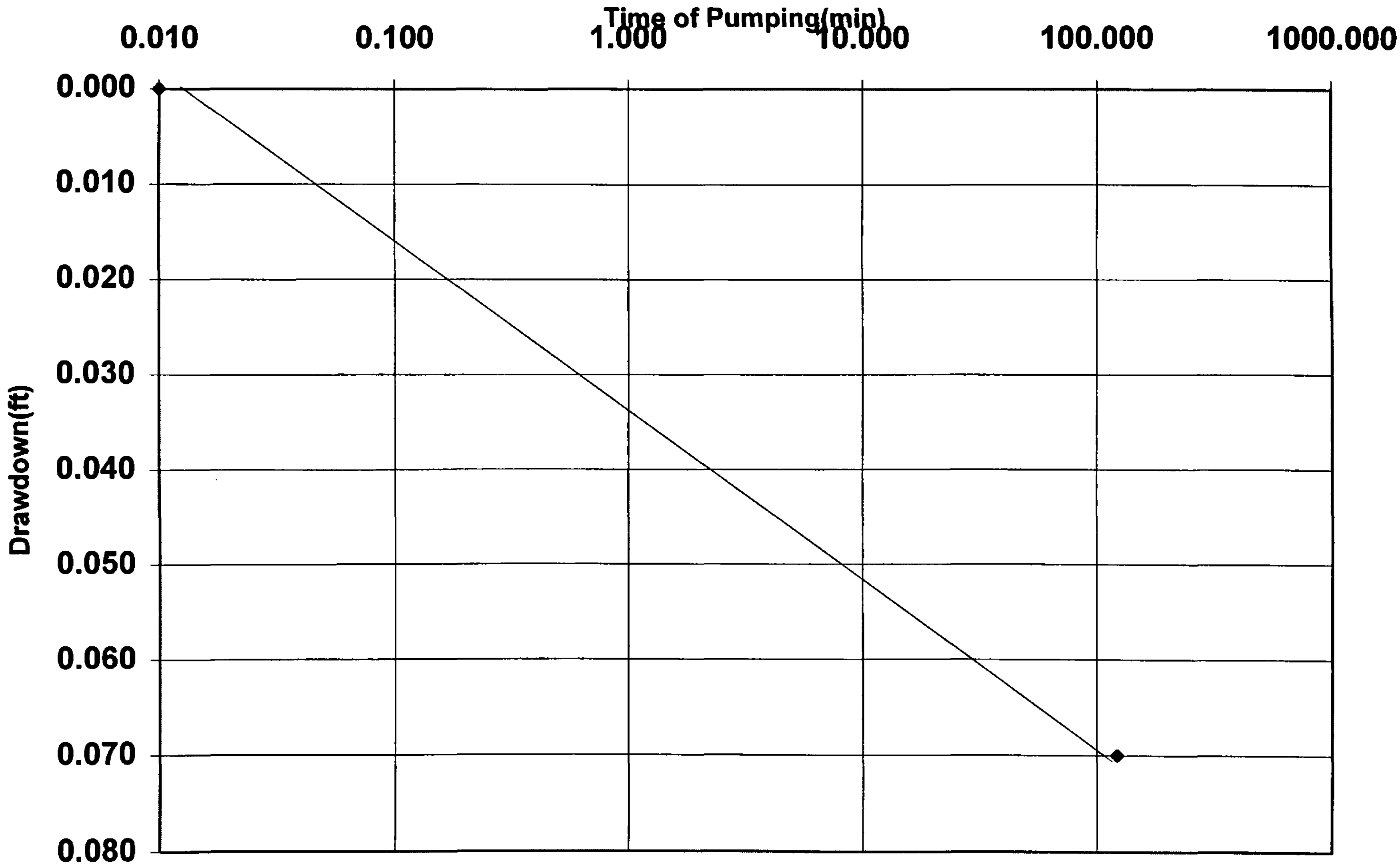

Figure B19. Time-drawdown plot observed in M11, pumping W2.

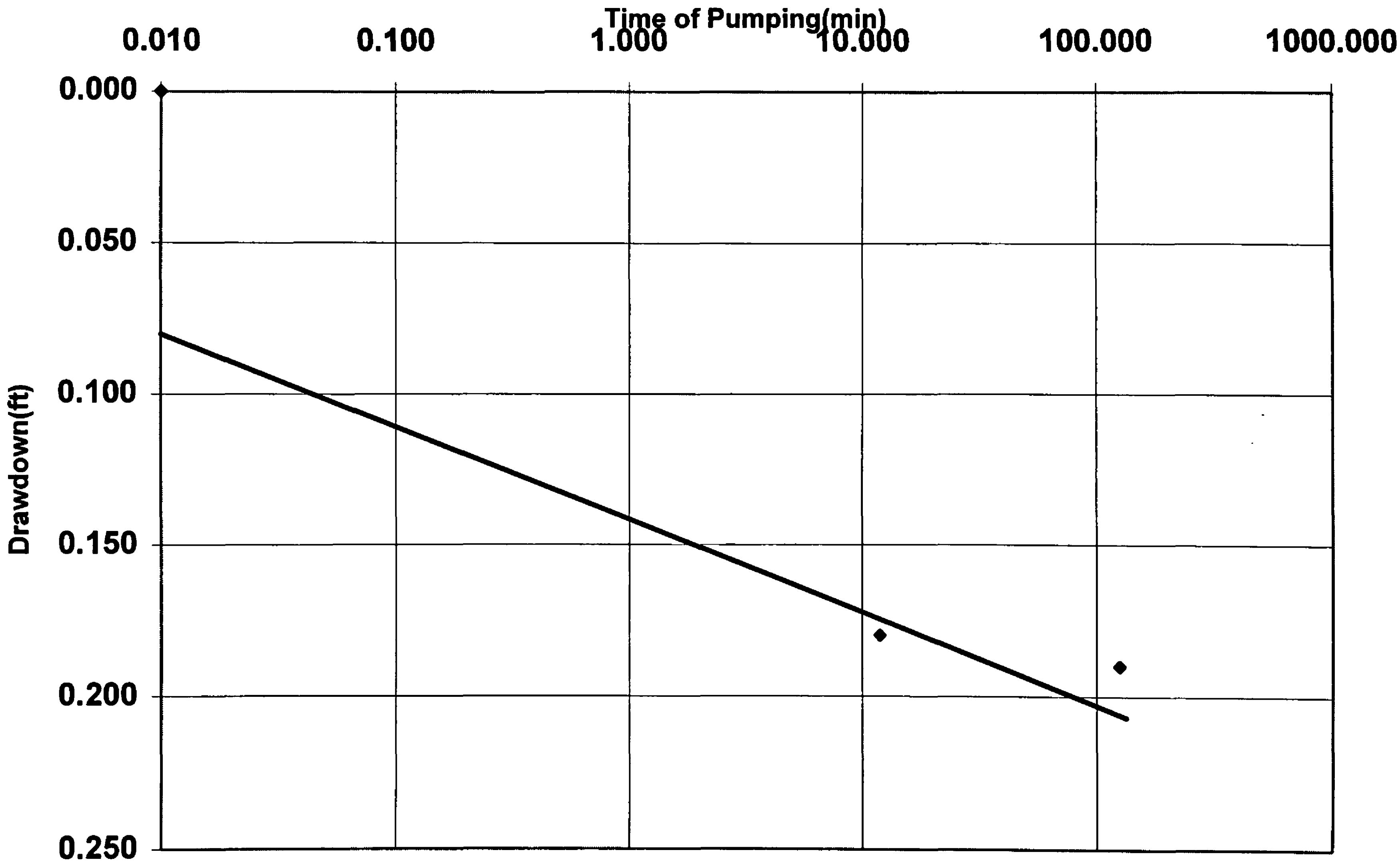

Figure B20. Time-drawdown plot observed in M12, pumping W2.

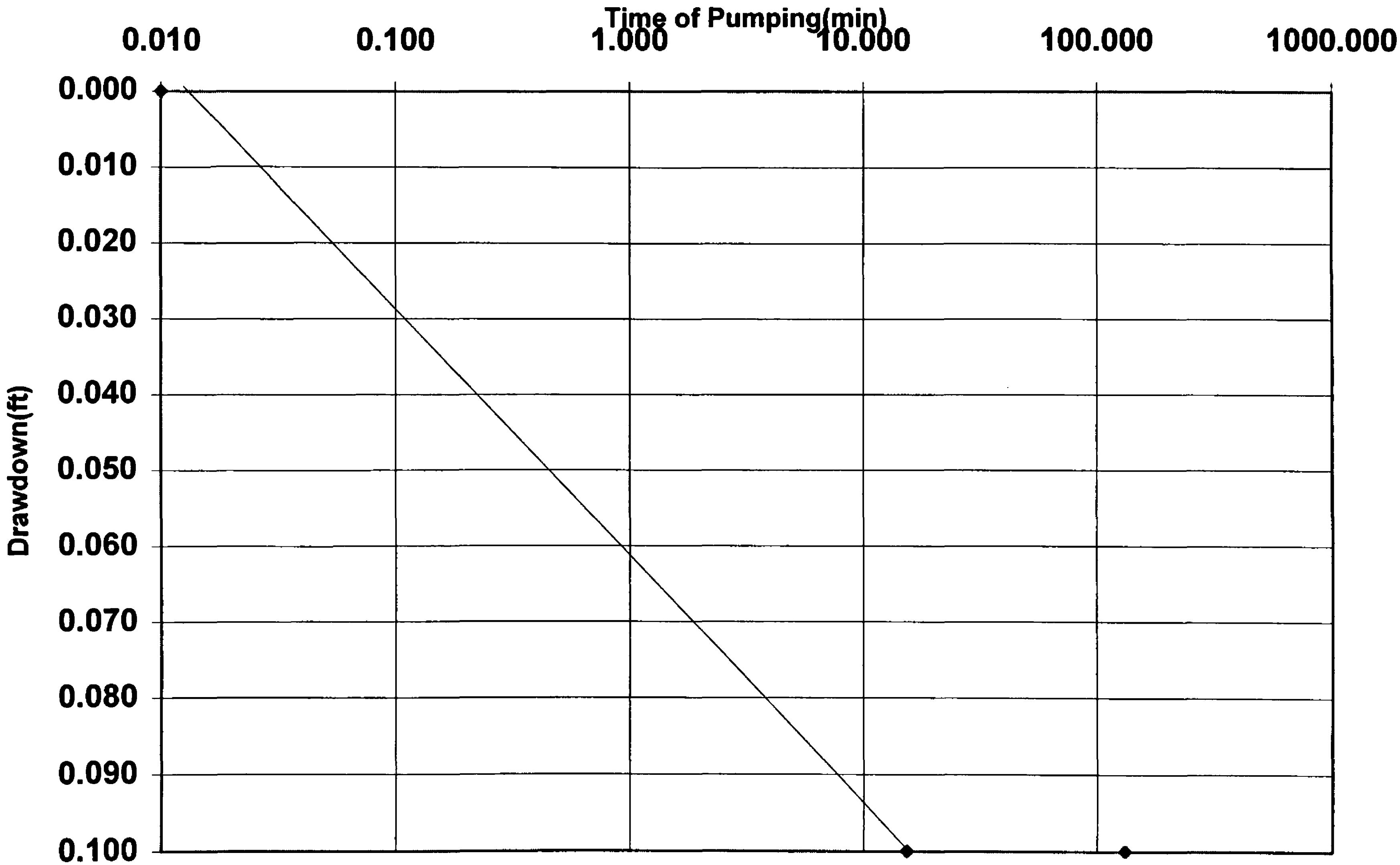

Figure B21. Time-drawdown plot observed in M13, pumping W2.

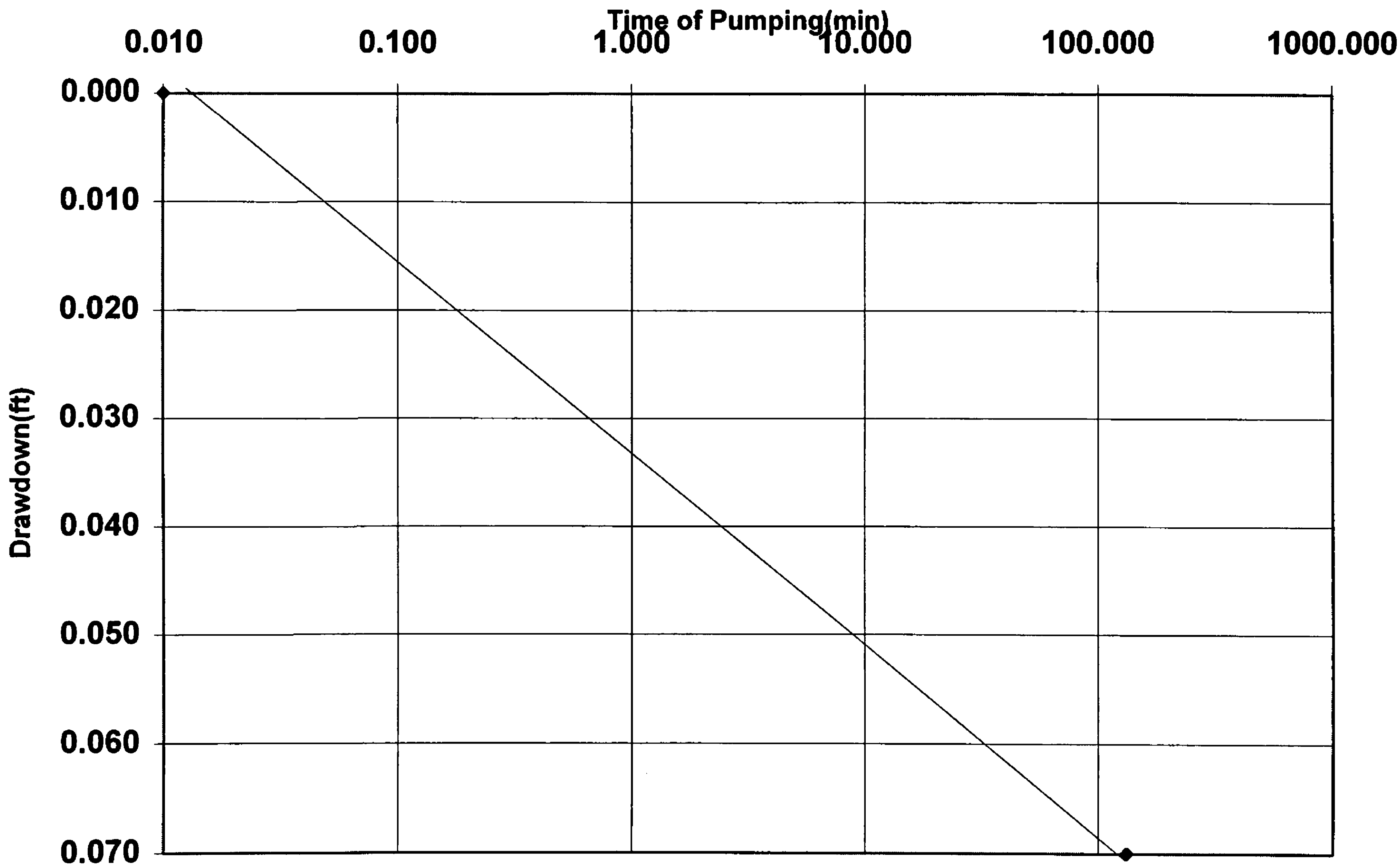

Figure B22. Time-drawdown plot observed in M14, pumping W2.

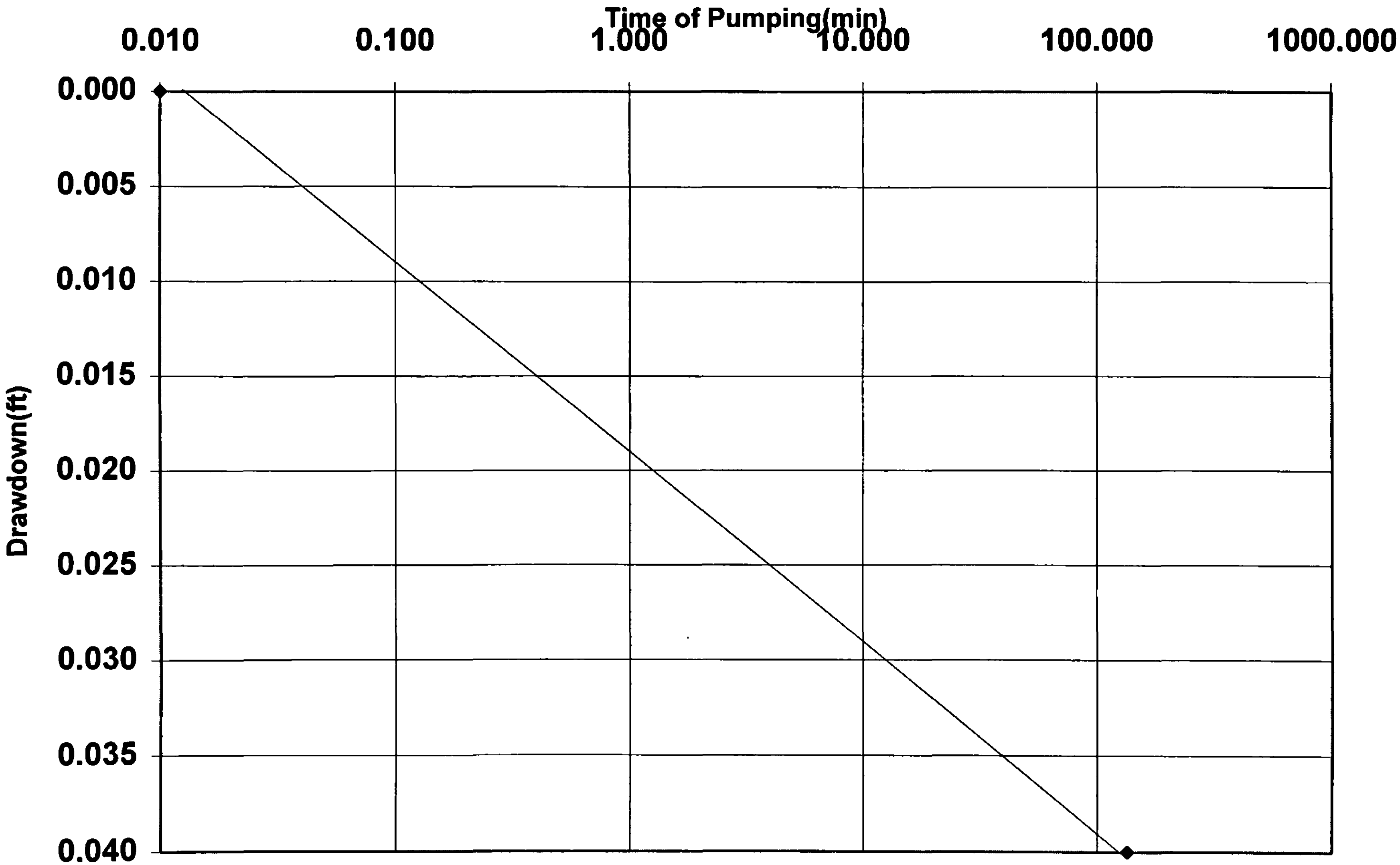

Figure B23. Time-drawdown plot observed in M15, pumping in W2.

Table B6. Time-drawdown data from aquifer test of W3.

Pumpimg W3				W3	
hrs	min	sec	t(min)	s	WL
0	0	0	0.010	0.000	6.540
0	1	30	1.500	0.330	6.870
0	3	10	3.167	0.340	6.880
0	4	0	4.000	0.340	6.880
0	5	30	5.500	0.350	6.890
0	6	30	6.500	0.350	6.890
0	13	0	13.000	0.370	6.910
0	16	30	16.500	0.370	6.910
0	21	30	21.500	0.370	6.910
0	31	30	31.500	0.380	6.920
0	46	30	46.500	0.380	6.920
0	60	30	60.500	0.380	6.920
0	90	30	90.500	0.380	6.920

W3 Pumping	
	W3
Top	101.20
Static WL	6.54
Q(gpm)	102.00
s(ft)	0.038
b(ft)	14.40
K(ft/d)	6,629.03
K(m/d)	1,988.71

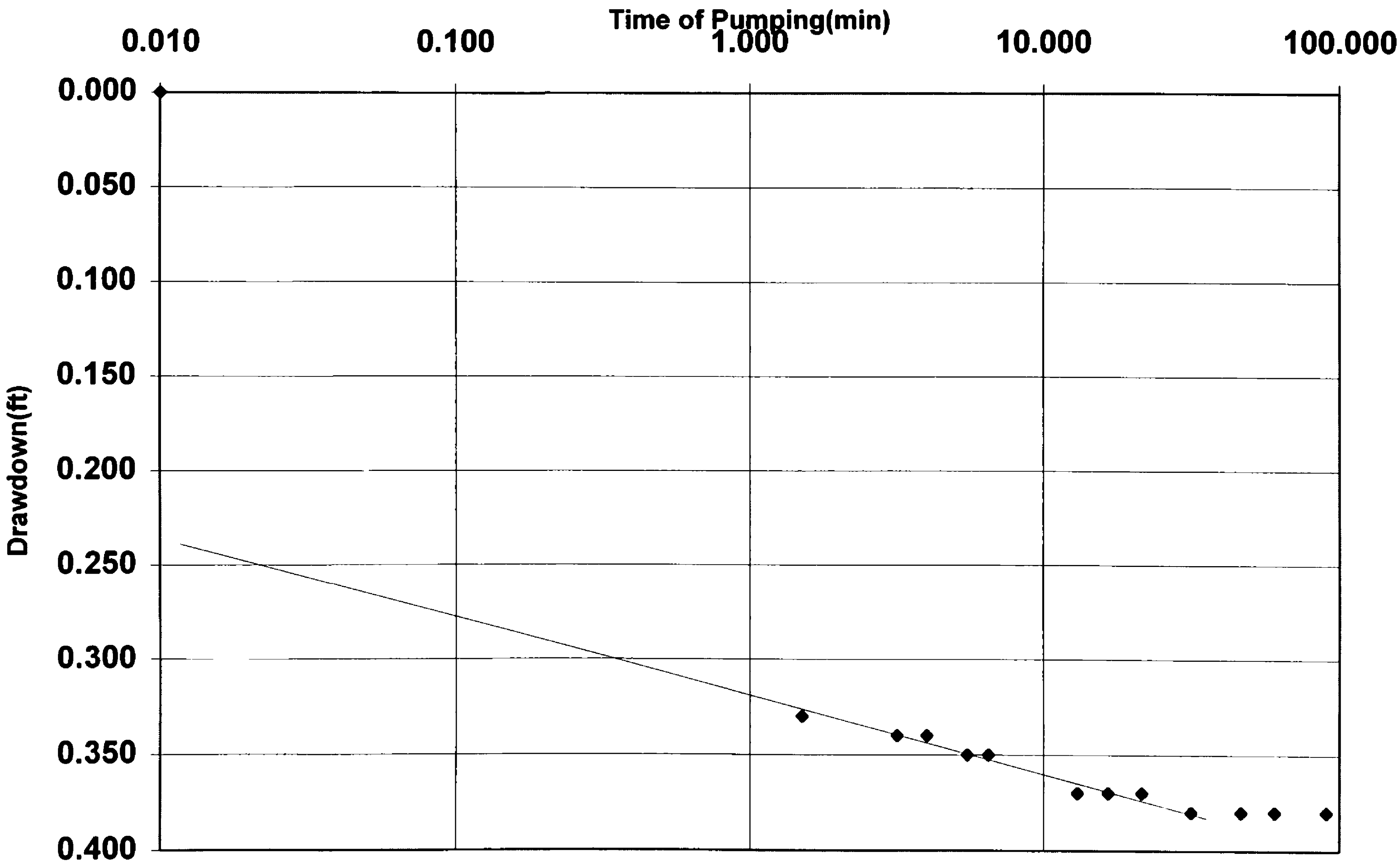

Figure B24. Time-drawdown plot observed in pumping well W3.

Appendix C

Site Instrumentation

The Erskine study site was instrumented in several stages using 5 different well designs and various placement strategies (Figure C1). The initial wells with the designation ***EE*** were installed to determine the general flow direction, depth to water, and to identify the aquifer material. These wells were installed in June 1995 using a 11.43cm diameter- hollow stem auger, and are located as in Figure C2. The ***EE*** wells are constructed of 5cm diameter PVC pipe and screened from 3 to 4.5m. The elevation of the top of the casing for each of the ***EE*** wells, and the elevation of their screened interval are relative to a 100 ft surface elevation datum (Table C1). The potentiometric map produced from water levels in the ***EE*** wells indicated a westerly groundwater flow direction.

A tracer field with 36 single level wells was constructed, the wells were driven with a jack-hammer to a depth of 2.7-3m (Figure C1) (Table C1). A 1.9cm steel pipe was driven into the ground and where possible a 1.27cm diameter PVC pipe was inserted into the steel pipe, and the steel pipe was extracted leaving a 1.27cm diameter PVC monitoring well in place. These wells were designated with a ***P***. A row of injection wells was installed with a jack-hammer. The injection wells, designated ***I***, were made from 4.4cm diameter steel pipe in 0.9m lengths, male threaded at both ends, joined by couplings. Two 0.9m sections of pipe were attached to a 0.75m sand point, screened over 0.6m. Seven tracer tests were performed in the well field (Appendix D).

To develop a more accurate knowledge of the flow path and plumes originating from the injection wells during tracer experiments, and further document the potentiometric surface, 24 sand points were installed with a Geoprobe®. These wells, labeled ***SP***, were of similar construction to the injection wells. Two 0.9m lengths of 3.18cm diameter steel pipe were attached with couplings to a 0.9m sand point of the same diameter. The sand points are screened over the entire 0.9m length (Table C1). The addition of the ***SP*** wells completed the Phase 1 well network and provided a more accurate measurement of the water table (Figure C1) (Appendix A). Although tracer movement was observed in more detail in these wells, they also identified the need to install a network of multilevel wells before conducting an extensive four virus seeding experiment.

The multilevel wells, ***M***, consisted of a 3m and 1.8m lengths of 1.27cm diameter PVC pipe attached with a PVC coupling and glue. The down hole end of this PVC was perforated for 5cm and wrapped in a screen fashioned from fine mesh paint strainers. Three lengths of 0.5cm diameter HDPE tubing, 2.1, 3.0, 3.9, and 5.1m were attached with steel wire to this main stem of PVC. The HDPE tubing was perforated and screened in the same manner as the PVC piping, over 5cm and covered with screen. To implant the multilevel sampler a drive rod was pushed to a depth of 6.75m. An interior drive rod was extracted and the multilevel sampler was inserted into the outer casing to a depth of 6.75m. The outer casing was then extracted from the hole, taking care to hold the multilevel sampler in place. The assemblage was designed to leave 0.3m of the well out of the ground positioning the sampling ports at 1.8, 2.7, 3.6, and 4.5m below the surface. Upon installing the multilevel well, a 4.8m length of HDPE tubing was inserted down the inside of the 1.27cm PVC stem to facilitate sampling. Nineteen multilevel wells were installed in arcs 7.5, 19.5, 30, and 40.5m, and one placed 0.45m from the injection well.

This Phase 2 well network was used for monitoring the transport of four viruses in a seeding experiment (Figure C2).

Four production wells were installed for use in aquifer tests and later forced gradient tracer tests. These wells, *W*, are 10.2cm diameter, 1.8m long blank steel casing attached to a 3m long, 40 slot steel screen. A well was placed up gradient to serve as a background well, at 19.5 and 30m in the Phase 2 well network, and down and cross gradient out of the known flow field.

All the wells sampled in tracer experiments had HDPE tubing dedicated to it for sampling purposes. Staff gauges were installed in low lying areas and the slough running to the south of the site to monitor surface water influences on the water table (Figure C1). The relative elevations of the top of the well casing, top and bottom of the screened interval, or sampling ports; and instrument construction details are listed in Table C1.

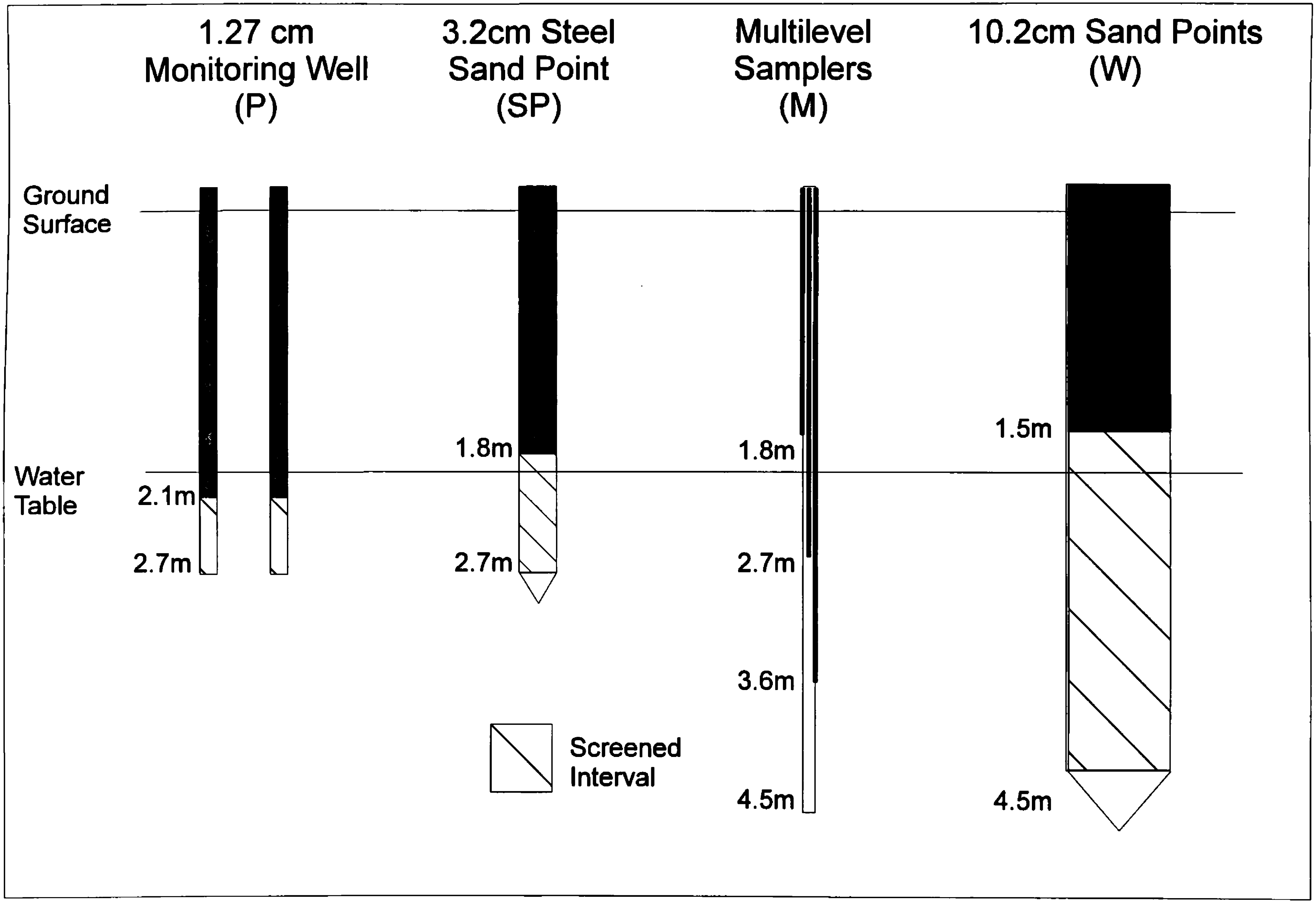

Figure C1. Well design at the Erskine site.

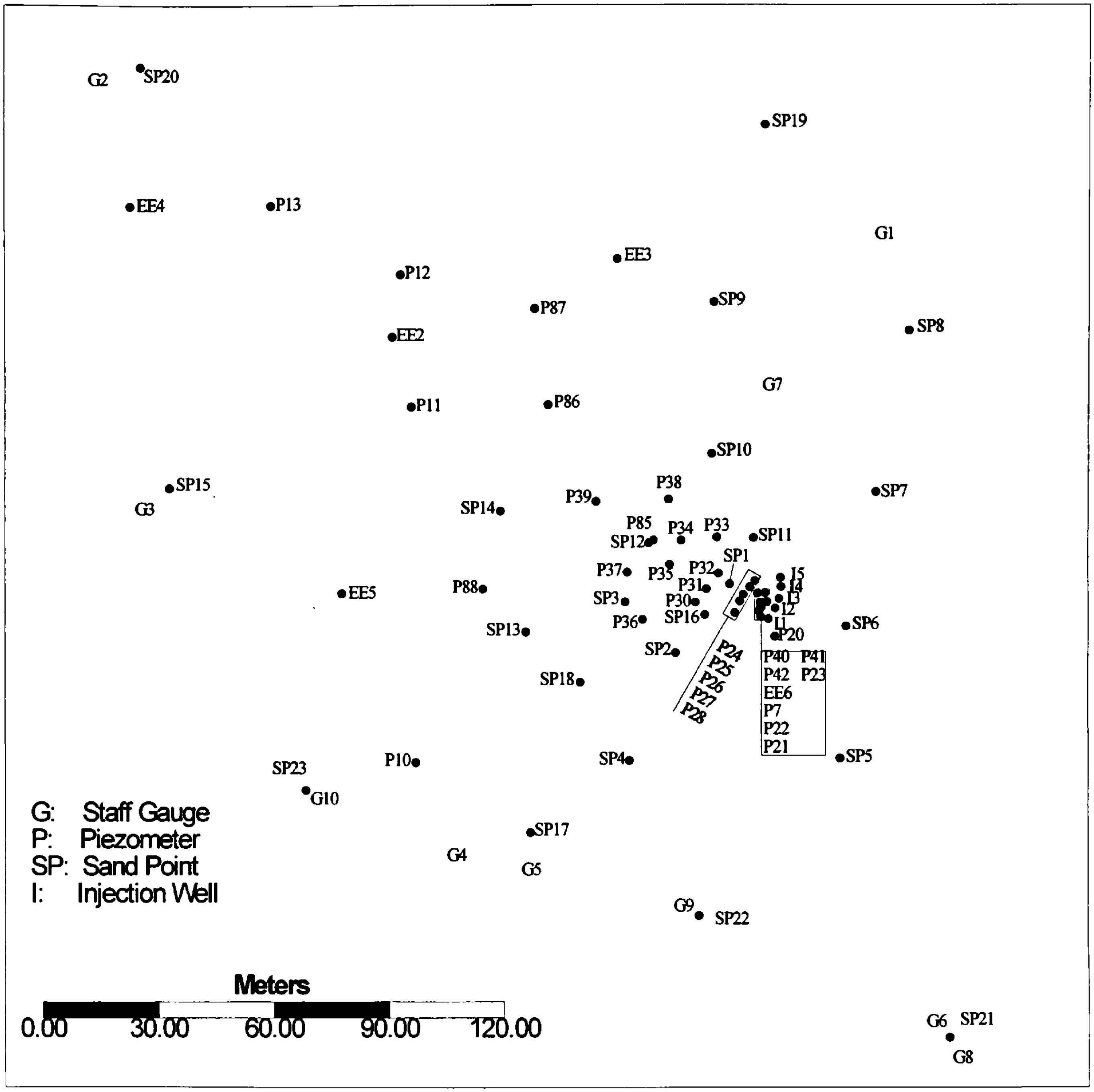

Figure C2. Phase 1 Well Network at the Erskine Study Site.

Table C1. Instrument Description

Instrument Construction Data Sheet

Well	Type	Material	Diameter
EE	Monitoring	PVC	5cm
P	Monitoring	Steel or PVC	1.9cm or 1.3cm
SP	Sand Point	Steel	3.2cm
G	Staff Gauge	Steel	
M	Multilevel	HDPE & PVC	
W	Production	Steel	10.2cm

Well	Casing Top	Screen Top	Screen Bottom
ee2	99.153	89.153	84.153
ee3	99.616	89.616	84.616
ee4	98.159	88.159	83.159
ee5	100.276	90.276	85.276
ee6	100.489	90.489	85.489
i1	101.803	94.803	92.803
i2	101.204	94.204	92.204
i3	101.011	94.011	92.011
i4	100.627	93.627	91.627
i5	100.526	93.526	91.526
p7	99.878	92.878	90.878
p10	102.141	open hole	
p11	99.718	open hole	
p12	98.862	open hole	
p13	99.251	open hole	
p20	99.953	92.953	90.953
p21	99.780	92.780	90.780
p22	99.876	92.876	90.876
p23	100.254	93.254	91.254
p24	100.110	93.110	91.110
p25	99.907	92.907	90.907
p26	99.606	92.606	90.606
p27	99.617	92.617	90.617
p28	99.713	92.713	90.713
p30	100.550	93.550	91.550
p31	100.056	93.056	91.056
p32	99.462	92.462	90.462
p33	99.896	92.896	90.896
p34	99.362	92.362	90.362
p35	100.132	93.132	91.132
p36	100.501	93.501	91.501
p37	100.697	93.697	91.697
p38	100.045	93.045	91.045
p39	99.410	92.410	90.410
p40	100.122	93.122	91.122
p41	100.356	93.356	91.356
p42	100.078	93.078	91.078
p85	101.455	open hole	
p86	100.236	open hole	
p87	99.167	open hole	
p88	101.906	open hole	
sp1	100.342	94.342	91.342
sp2	101.726	95.726	92.726
sp3	101.173	95.173	92.173
sp4	101.597	95.597	92.597
sp5	100.634	94.634	91.634
sp6	101.149	95.149	92.149
sp7	99.899	93.899	90.899
sp8	100.574	94.574	91.574
sp9	99.412	93.412	90.412
sp10	100.612	94.612	91.612
sp11	100.922	94.922	91.922
sp12	100.868	94.868	91.868
sp13	101.132	95.132	92.132
sp14	100.539	94.539	91.539
sp15	101.018	95.018	92.018
sp16	101.505	95.505	92.505
sp17	101.001	95.001	92.001
sp18	101.899	95.899	92.899
sp19	99.860	93.860	90.860
sp20	98.728	92.728	89.728
sp21	99.557	93.557	90.557
sp22	98.567	92.567	89.567
sp23	98.247	92.247	89.247
sp24	101.097	95.097	92.097
g1	97.682		
g2	96.676		
g3	99.357		
g4	98.610		
g5	98.631		
g6	98.263		
g7	97.583		
g8	97.277		
g9	96.687		
g10	96.297		
W0	101.357	95.357	85.357
W1	102.137	96.137	86.137
W2	101.907	95.907	85.907
W3	101.197	95.197	85.197

Table C1. Instrument Description

Well	Casing Top	6ft (1.8m) Port	9ft(2.7m) Port	12ft (3.6m) Port	15ft (4.5m) Port
M0	100.517	93.517	90.517	87.517	84.517
M1	100.282	93.282	90.282	87.282	84.282
M2	100.977	93.977	90.977	87.977	84.977
M3	101.307	94.307	91.307	88.307	85.307
M4	100.657	93.657	90.657	87.657	84.657
M5	101.027	94.027	91.027	88.027	85.027
M6	101.197	94.197	91.197	88.197	85.197
M7	101.427	94.427	91.427	88.427	85.427
M8	100.787	93.787	90.787	87.787	84.787
M9	100.417	93.417	90.417	87.417	84.417
M10	101.577	94.577	91.577	88.577	85.577
M11	101.777	94.777	91.777	88.777	85.777
M12	101.897	94.897	91.897	88.897	85.897
M13	101.157	94.157	91.157	88.157	85.157
M14	101.127	94.127	91.127	88.127	85.127
M15	100.907	93.907	90.907	87.907	84.907
M16	102.107	95.107	92.107	89.107	86.107
M17	100.977	93.977	90.977	87.977	84.977
M18	100.797	93.797	90.797	87.797	84.797
M19	100.337	93.337	90.337	87.337	84.337

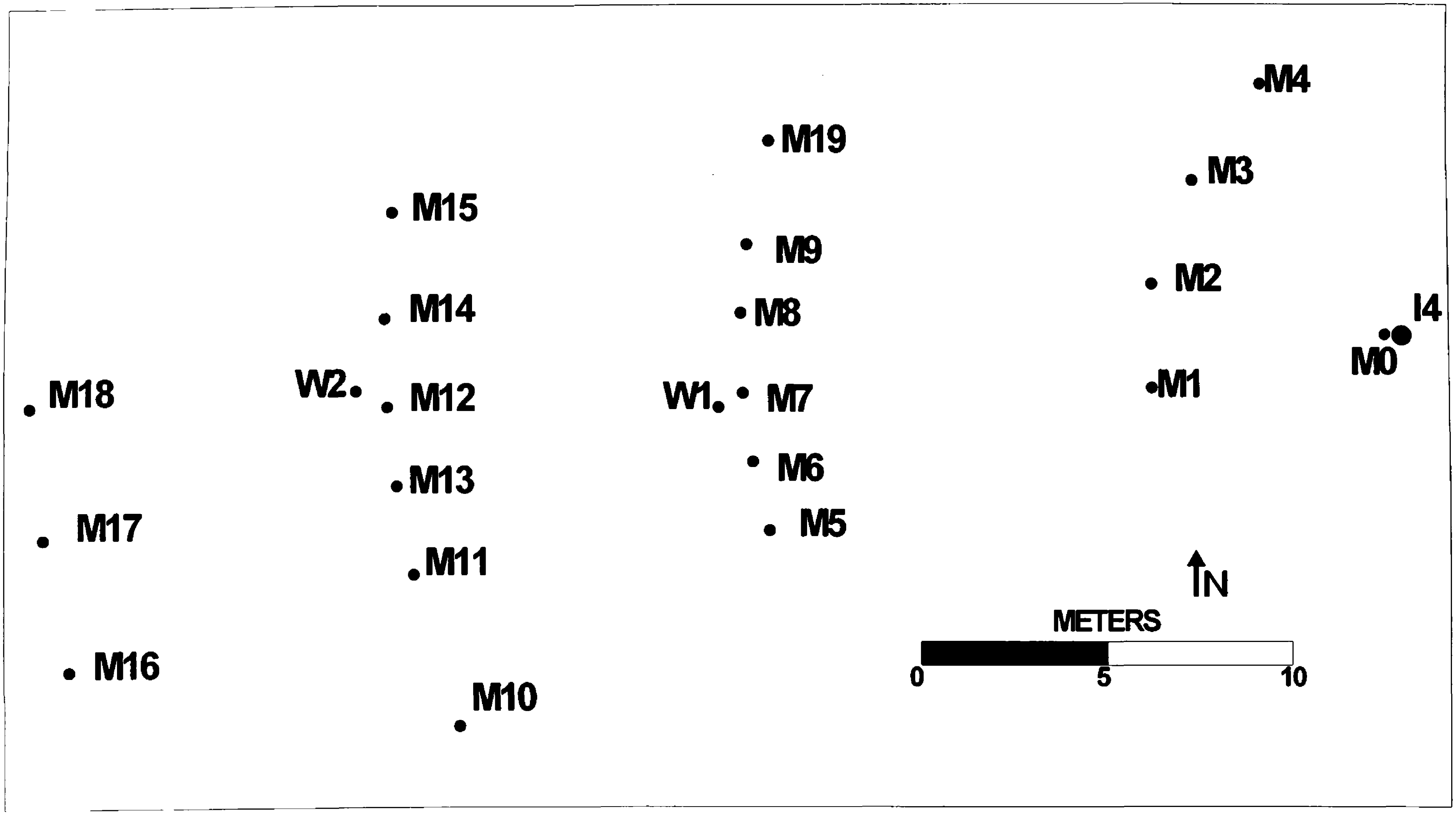

Figure C3. Phase 2 Well Network consisting og Multilevel and Production Wells

Appendix D

Rhodamine-wt

Tracer tests were the primary investigative tool used in the early stages of this research (Table D1). The fluorescent dye rhodamine-wt was used during construction of the Phase 1 well network primarily to identify flow paths from the injection wells (Figure D1). The injectate consisted of 50 to 100ml. of liquid concentrate added to 5 gallons of deionized water. Peak concentrations were observed and transport rates calculated. Rhodamine-wt and its analysis with a fluorimeter is inexpensive and quick, and for this reason it was used 5 times to determine flow paths and rates. Rhodamine-wt is an organic dye and adheres to, or stains, the aquifer material. This adsorptive process retards the transport of the tracer and underestimates average groundwater flow velocities. Another concerns in using rhodamine-wt is its organic nature. Because it is organic and bioavailabe it could possibly affect the survival of viruses once they are seeded into the system. To avoid this possibility, rhodamine-wt was not used immediately before virus seeding experiments. In general, rhodamine-wt is considered one of the most useful dyes for water tracing, and it was successfully used for that purpose in this study (Smart and Laidlaw, 1977).

Sodium Bromide

Sodium bromide, NaBr, is used as a tracer by many hydrogeologists due to its conservative nature (Davis et al, 1980). Bromide occurs naturally at low concentrations in some groundwater systems, but is not detectable at the Erskine site (<0.1mg/l). Bromide was used to determine flow direction, average groundwater velocity, and hydrologic properties of the aquifer (Figure D2) (Table B2) . To avoid density effects observed in the laboratory by Isotok et al (1995) and in field investigations by LeBlanc et al (1991), bromide was injected in concentrations ranging from 1000 to 1500 mg/l. Bromide effectively offers 4 orders of magnitude of resolution when analyzed using ion chromatography, and the high hydraulic conductivity at the Erskine site resulted in rapid dilution of the bromide plume. Due to dilution, the highest peak measured beyond the injection well was on the order of 10^1 mg/l. Low analytical sensitivity in bromide detection caused an underestimation of plume size and transport distance.

Viruses

Viruses were seeded on three separate occasions and their transport in the groundwater was monitored. To limit the risk associated with viruses, nonpathogenic viruses were used for this study. That is to say that the viruses used would not cause disease in humans. The bacteriophage MS2 was used in all three experiments. A bacteriophage is a virus that infects and reproduces only in bacteria. Unlike bromide and rhodamine-wt, MS2 offers highly sensitive analysis and large travel distances. MS2 was used to study the fate and transport of viruses in a groundwater system. The seeding of MS2 documented that its flow path was the same as bromide and rhodamine-wt. Because the analysis of viruses are very sensitive, one virus must be present in 10ml of sample to be detected, and the high concentrations injected, 10^{10} PFU/ml, the plumes could be identified over a larger breadth and width than other tracers. In order to compare the behavior of different viruses in the same groundwater system the third and final virus seeding included not only MS2, but the bacteriophages PRD1 and ∅X174, as well as poliovirus type-1 (CHAT strain). The CHAT strain of polio is attenuated and not pathogenic. It is similar to the Sabin live vaccine in that it is alive and infectious, but has been altered so as to not cause the disease poliomyelitis.

The use of viruses, and other microbial tracers, is advantageous because of the high resolution they provide. These tracers are ineffective for determining hydrologic properties because of their large size, at 20-300nm in diameter they are subject to pore size exclusion, and sorptive nature they travel at rates other than the average groundwater flow velocity. When used in conjunction with conservative tracers like bromide, virus transport can be quantified relative to the conservative agent.

Summary of Tracer and Seeding Experiments Performed

One bromide and 2 rhodamine-wt tracer tests were conducted in December, 1995. These tests defined flow path variability from the injection locations, but sampling intervals were insufficient for the determination of aquifer properties. A tracer test was performed in March, 1996, with both rhodamine-wt and bromide injected into separate injection wells using a 6 to 12 hr sampling interval. Two weeks later a second bromide tracer test, with 1 to 11 hr sampling intervals, defined the flow path through the well system and was used to design a sampling schedule for a seeding experiment using the bacteriophage MS2. The preferential flow path from injection well I4 observed during this tracer test validated the early potentiometric maps.

The March 1996 MS2 seeding experiment was a test run for future multiple virus seeding experiments (**Figure D3**). However, the large measurable variability of virus concentrations revealed the need for further instrumentation. Twenty-four, 3.2cm steel sand points, screened from 1.8-2.7m, were installed throughout the field site completing a Phase 1 well network.

Further use of rhodamine-wt and bromide injected in well I4 during June and July, 1996 confirmed the need for an extensive multilevel sampling network. Twenty multilevel samplers with sampling ports at 1.8,2.7,3.6, and 4.5m were driven into the aquifer with a Geoprobe®. After installing the first 11 multilevel samplers, a MS2 seeding experiment was conducted to determine additional well locations for the Phase 2 well network (Figure D4). MS2 was used because of its high resolution, with a detectable 11 orders of magnitude of concentration.

Upon completion of the multilevel monitoring wells, a bromide tracer test was performed. This bromide tracer test confirmed the flow path from injection well I4, and yielded the best measurement of hydrologic properties from a tracer test (Table 1). A 72hr plume was detected throughout the network of sampling wells, over an area exceeding 76.6m^2 (851ft^2) 2ft below the water table (Table D2; Figure D5-D6). The plume was not detected below the 3.6m sampling port. The results of this test also provided a conservative transport comparison to the extensive virus seeding experiment that followed. MS2, ∅X174, PRD1, and poliovirus type-1 (CHAT strain) were seeded and the rate of transport and plume distribution were observed. At the 2.7m (9ft) depth the MS2, PRD1, and ∅X174 the plumes covered area of 357.1m^2 (1190.3ft^2), 267m^2 (890ft^2), and 237m^2 (790ft^2), respectively. The initial concentrations of the tracers varied by orders of magnitude in the injected volume (Table 2). The difference in plume size for each of the viruses seeded reflect the injected volume and the behavior of the viruses in the groundwater system. Plumes were detected and plotted at the 2.7 and 3.6m depths for MS2, PRD1, and ∅X174, and the 9ft depth for polio (Tables D3-6) (Figure D7-13).

Longitudinal cross-sections were plotted for the bacteriophages using the wells along the main flow path, I4, M2, M7, M14, and M17. The similarities between these cross-sections illustrates a downward vertical gradient 30m (100ft) from I4 (Figure D14-16). The three dimensional perspective provided by combining the plume maps and the cross-sections suggests that the plume is narrow and contained during the first 19.5m (65ft) of transport, expanding volumetrically beyond 30m (100ft).

Date	Tracer	Injection Well	Test Duration (hrs)	Transport Velocities (ft/d)	Transport Velocities (m/d)
December 8, 1995	Rhodamine-wt	I1	48	plume data only	plume data only
December 15, 1996	Rhodamine-wt	I3	334	25	8
December 27, 1999	Sodium Bromide	I3	66	36	11
March 15, 1996	Rhodamine-wt	I5	48	plume data only	plume data only
	Sodium Bromide	I4	48	78	23
March 25, 1996	Sodium Bromide	I4	26	95	29
March 28, 1996	MS2	I4	636	81	54
June 25, 1996	Sodium Bromide	P31	36	not detected	not detected
July 17, 1996	Rhodamine-wt	I4	20	plume data only	plume data only
August 22, 1996	MS2	I4	72		
September 20, 1996	Sodium Bromide	I4	36	96	29
October 2, 1996	MS2	I4	72	107	32
	PRD1	I4		120	36
	Phi X174	I4		107	32
	Poliovirus type-1	I4		140	42

Table D1. Brief summary of all tracer tests at the Erskine site.

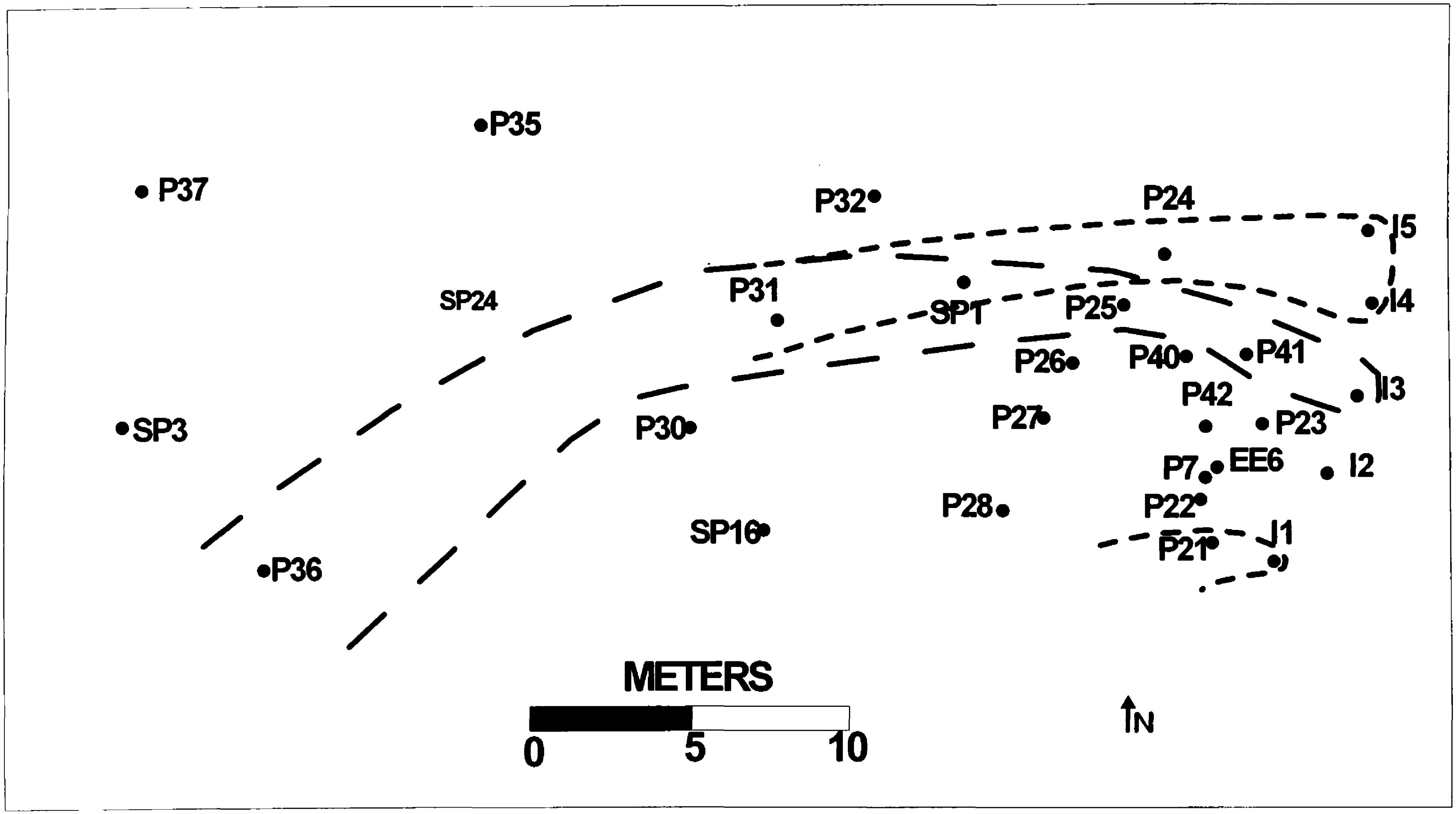

Figure D1. Rhodamine-wt plumes as detected in Phase 1 well network, flow direction to the west.

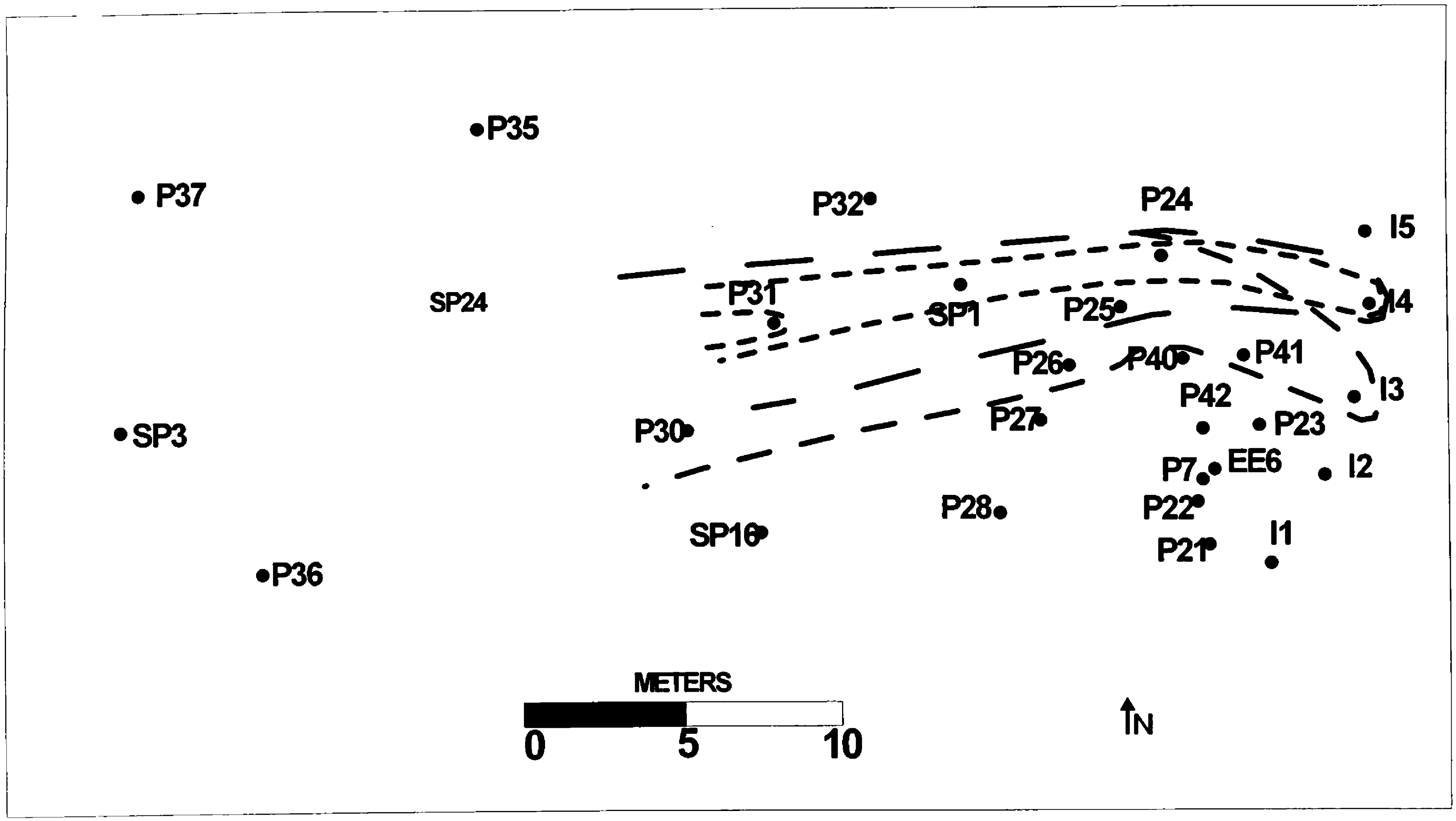

Figure D2. Bromide plumes detected in the Phase 1 well network, flow direction to the west.

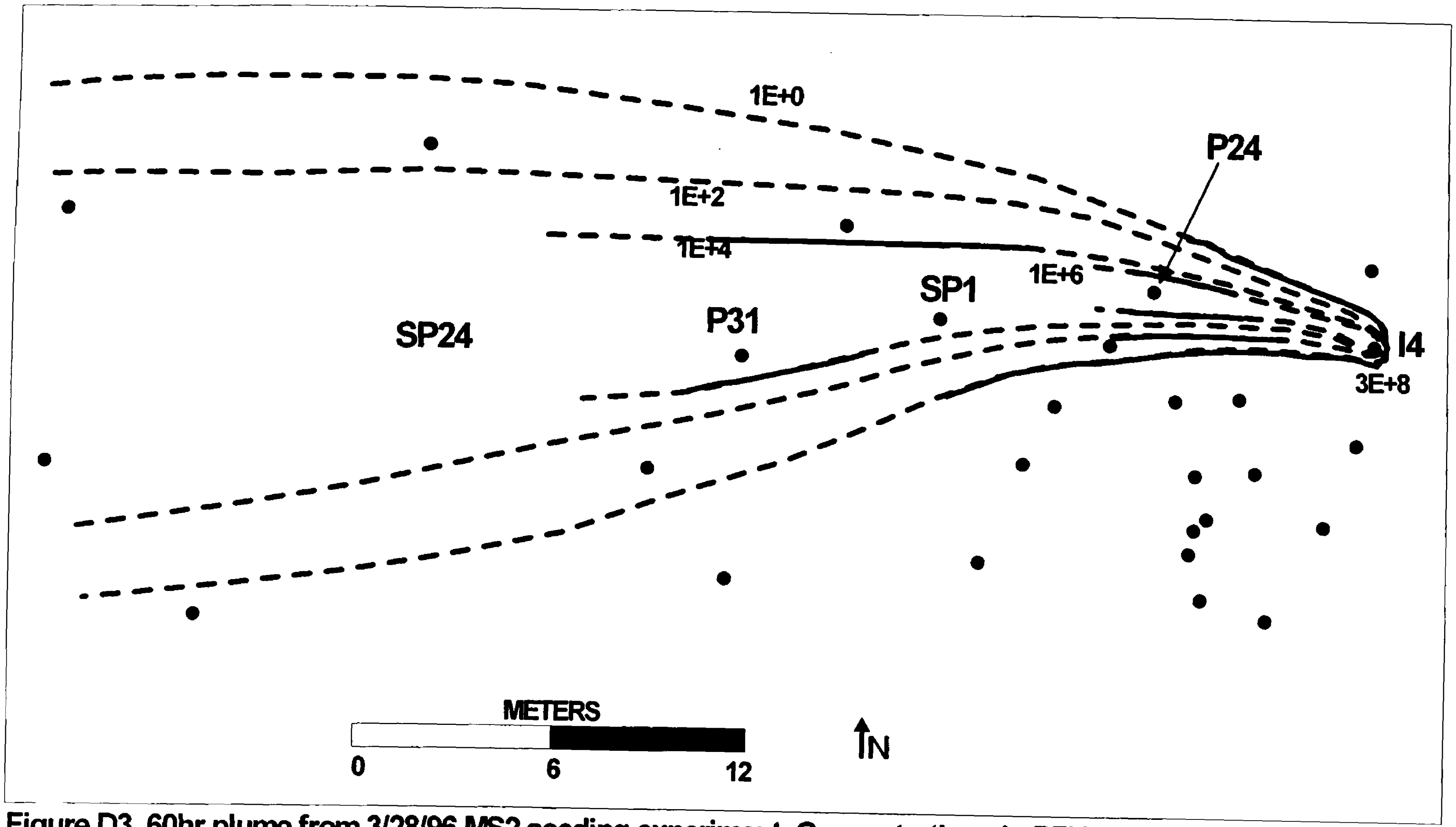

Figure D3. 60hr plume from 3/28/96 MS2 seeding experiment. Concentrations in PFU/ml, flow direction to the west.

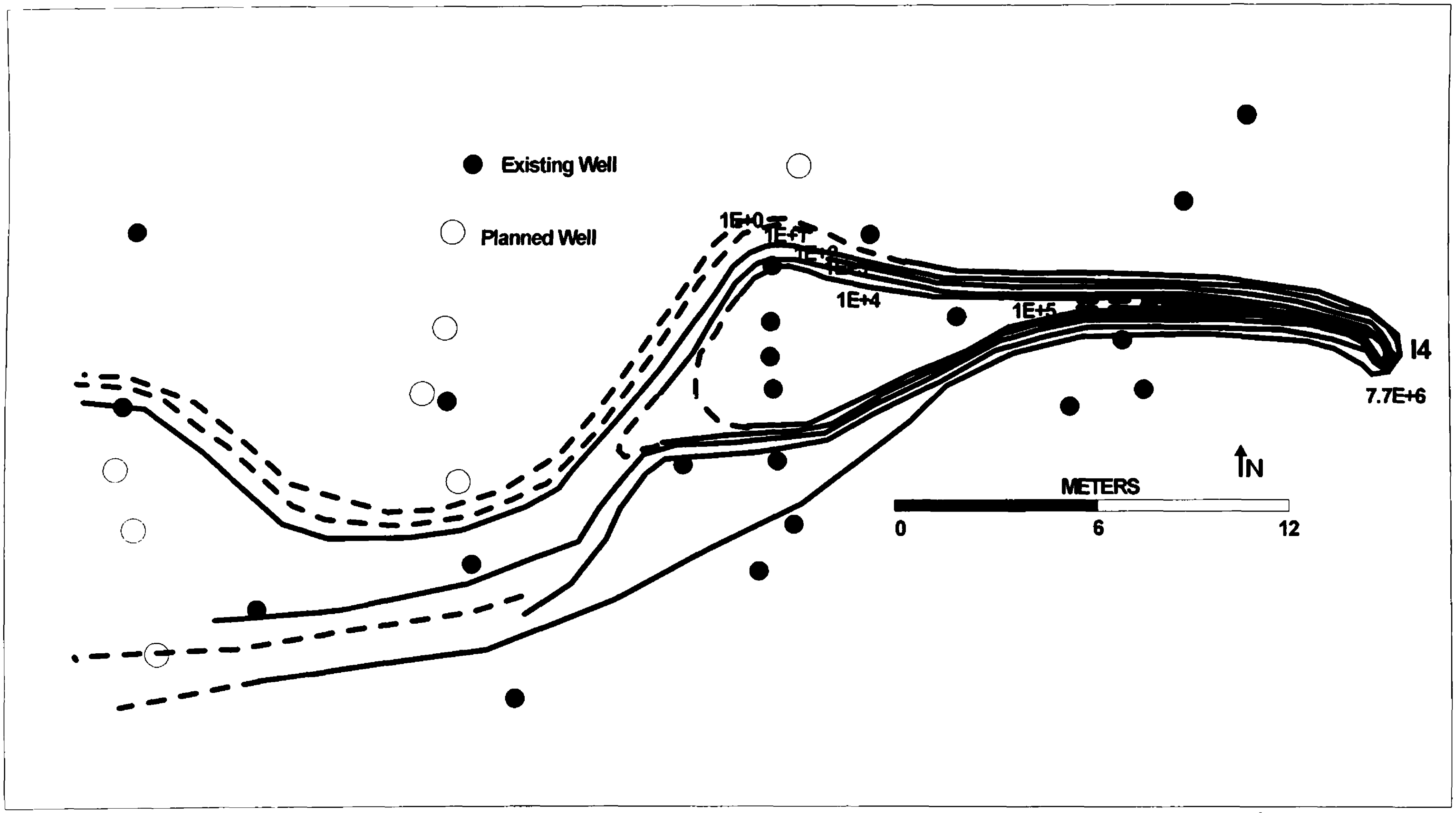

Figure D4. Plume from 8/22/96 MS2 seeding experiment. Concentrations in Log PFU/ml, flow direction to the west.

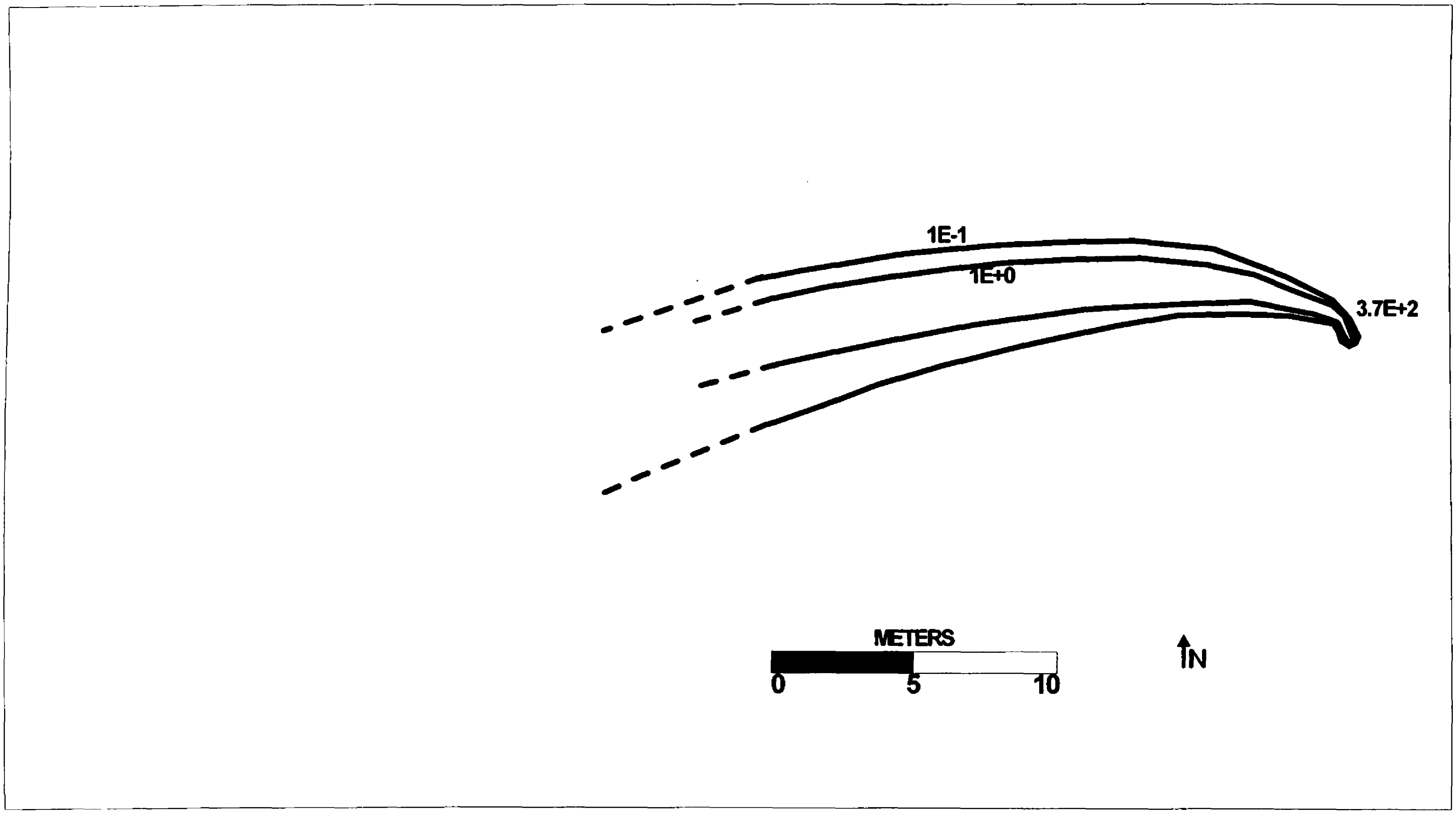

Figure D5. Bromide Plume at depth of 9ft from 9/20/96 tracer test. Concentration is in mg/l, flow direction is to the west.

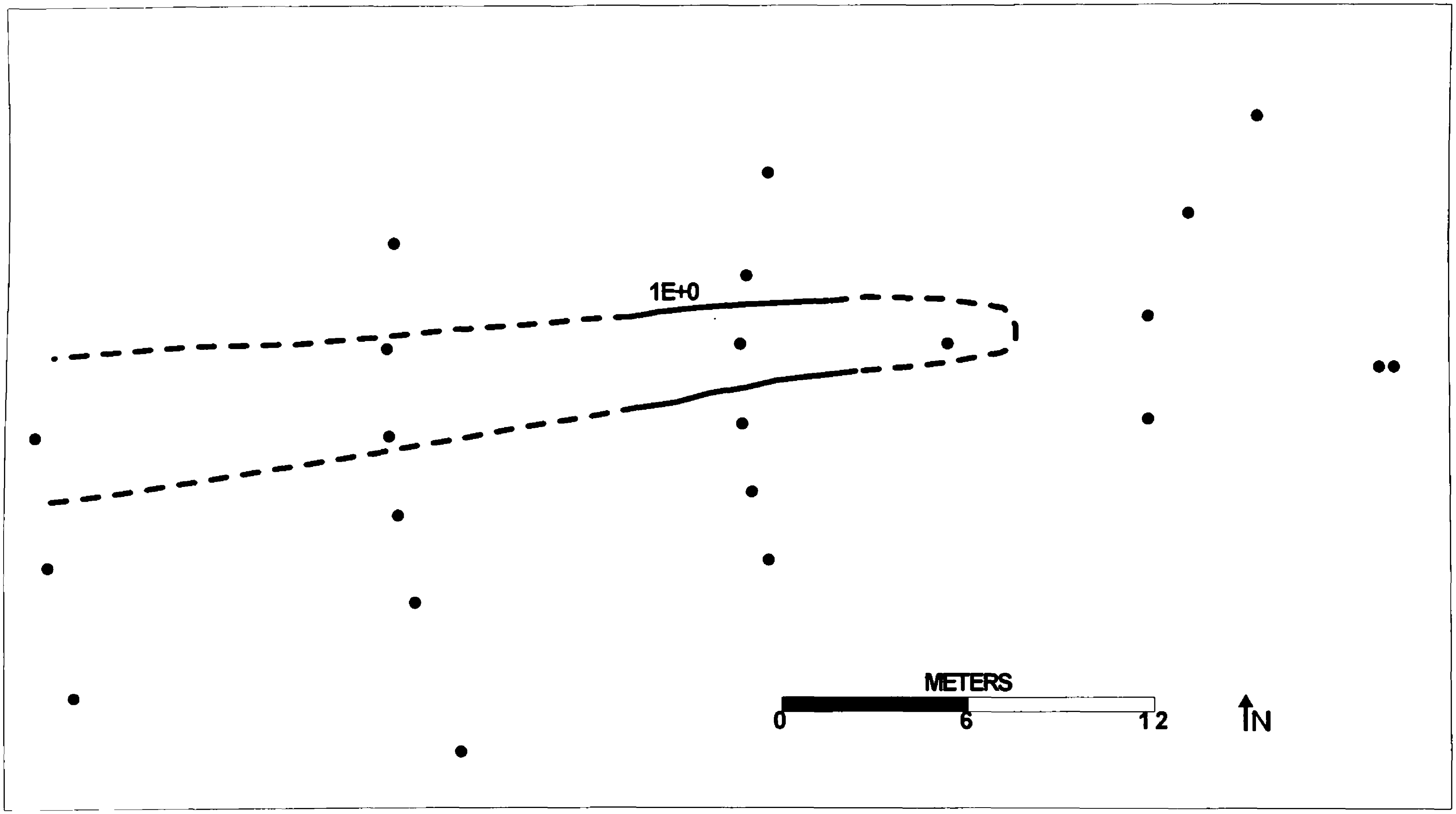

Figure D6. Bromide plume at depth of 12ft from 9/20/96 tracer test. Concentration is in mg/l, flow direction is to the west.

NA: Not Analyzed

Concentrations in mg/l

Distance from Injection well I4:			0.45m			7.5m											
Date & Time	Hour	I4	M0-9	M0-12	M0-15	M1-9	M1-12	M1-15	M2-9	M2-12	M2-15	M3-9	M3-12	M3-15	M4-9	M4-12	M4-15
09/20/96	Background	0	0	0	0	NA	NA	NA	0	0	0	NA	NA	NA	NA	NA	NA
6:00	0	1443	0	0	0												
8:00	2		0	0	0				0	0	0						
10:00	4		0	0	0				3.97	0	0						
12:00	6		0	0	0				6.26	0	0						
14:00	8	596	0	0	0	0	0	0	5.9	0	0	0	0	0	0	0	0
16:00	10								5.42	0	0						
18:00	12																
20:00	14																
22:00	16																
09/21/96																	
0:00	18																
2:00	20	426	0	0	0	0	0	0	2.2	0	0	0	0	0	0	0	0
4:00	22																
6:00	24																
8:00	26																
10:00	28																
12:00	30																
14:00	32																
16:00	34																
18:00	36	37.13	0	0	0	NA	NA	NA	1.08	0	0	NA	NA	NA	NA	NA	NA
20:00	38																
22:00	40																

Distance from Injection well I4:		13.2m	19.5m														
Date & Time	Hour	SP1	M5-9	M5-12	M5-15	M6-9	M6-12	M6-15	M7-9	M7-12	M7-15	M8-9	M8-12	M8-15	M9-9	M9-12	M9-15
09/20/96	Background	0	NA	NA	NA	NA	NA	NA	0	0	0	NA	0	NA	NA	NA	NA
6:00	0																
8:00	2																
10:00	4	0															
12:00	6	1.1															
14:00	8	2.28	0	0	0	0	0	0	0	0	0	0	0	0	0	0	0
16:00	10	3.62							0.92	0	0						
18:00	12								1.43	0	0	0	0.698	NA	NA	NA	NA
20:00	14								1.81	0	0						
22:00	16								2.1	0	0	NA	1.031	NA	NA	NA	NA
09/21/96																	
0:00	18								2.1			0.89	1.119	NA	NA	NA	NA
2:00	20	3.6	0	0	0	0	0	0	1.95	0	0	1.16	1.12	0	0	0	0
4:00	22																
6:00	24																
8:00	26																
10:00	28																
12:00	30																
14:00	32																
16:00	34																
18:00	36	2.64(1.97)	NA	NA	NA	NA	NA	NA	0.98	NA	NA	1.511	0.763	NA	NA	NA	NA
20:00	38																
22:00	40																

from Injection well I4:					30m														
Date & Time	Hour	M19-9	M19-12	M19-15	M10-9	M10-12	M10-15	M11-9	M11-12	M11-15	M12-9	M12-12	M12-15	M13-9	M13-12	M13-15	M14-9	M14-12	M14-15
09/20/96		NA	NA	NA	NA	NA	NA	0	0	0	0	0	0	NA	NA	NA	NA	NA	NA
6:00	0																		
8:00	2																		
10:00	4																		
12:00	6																		
14:00	8	0	0	0	0	0	0	0	0	0	0	0	0	0	0	0	0	0	0
16:00	10																		
18:00	12																		
20:00	14																		
22:00	16							0	0	0	0	0	0						
09/21/96																			
0:00	18																		
2:00	20	0	0	0	0	0	0	0	0	0	0	0	0	0	0	0	0	0	0
4:00	22																		
6:00	24							0	NA	NA	0	0	NA	NA	NA	NA	NA	NA	NA
8:00	26																		
10:00	28							NA	NA	NA	0	NA	NA	NA	NA	NA	NA	NA	NA
12:00	30																		
14:00	32																		
16:00	34																		
18:00	36	NA	NA	NA	NA	NA	NA	0	0	0	0	0	0	NA	NA	NA	NA	NA	NA
20:00	38																		
22:00	40							0	0	NA	0.704	0	NA	0	0.964	NA			

from Injection well I4:					40.5m								
Date & Time	Hour	M15-9	M15-12	M15-15	M16-9	M16-12	M16-15	M17-9	M17-12	M17-15	M18-9	M18-12	M18-15
09/20/96		NA	NA	NA	NA	NA	NA	NA	NA	NA	NA	NA	NA
6:00	0												
8:00	2												
10:00	4												
12:00	6												
14:00	8	0	0	0	0	0	0	0	0	0	0	0	0
16:00	10												
18:00	12												
20:00	14												
22:00	16												
09/21/96													
0:00	18												
2:00	20	0	0	0	0	0	0	0	0	0	0	0	0
4:00	22												
6:00	24												
8:00	26												
10:00	28												
12:00	30												
14:00	32												
16:00	34												
18:00	36	NA	NA	NA	NA	NA	NA	0	0	0	NA	NA	NA
20:00	38												
22:00	40					NA	NA	0.716	0	NA	0.761	0.904	NA

Table D2. Tracer test data form bromide injection into well I4, September 20, 1996.

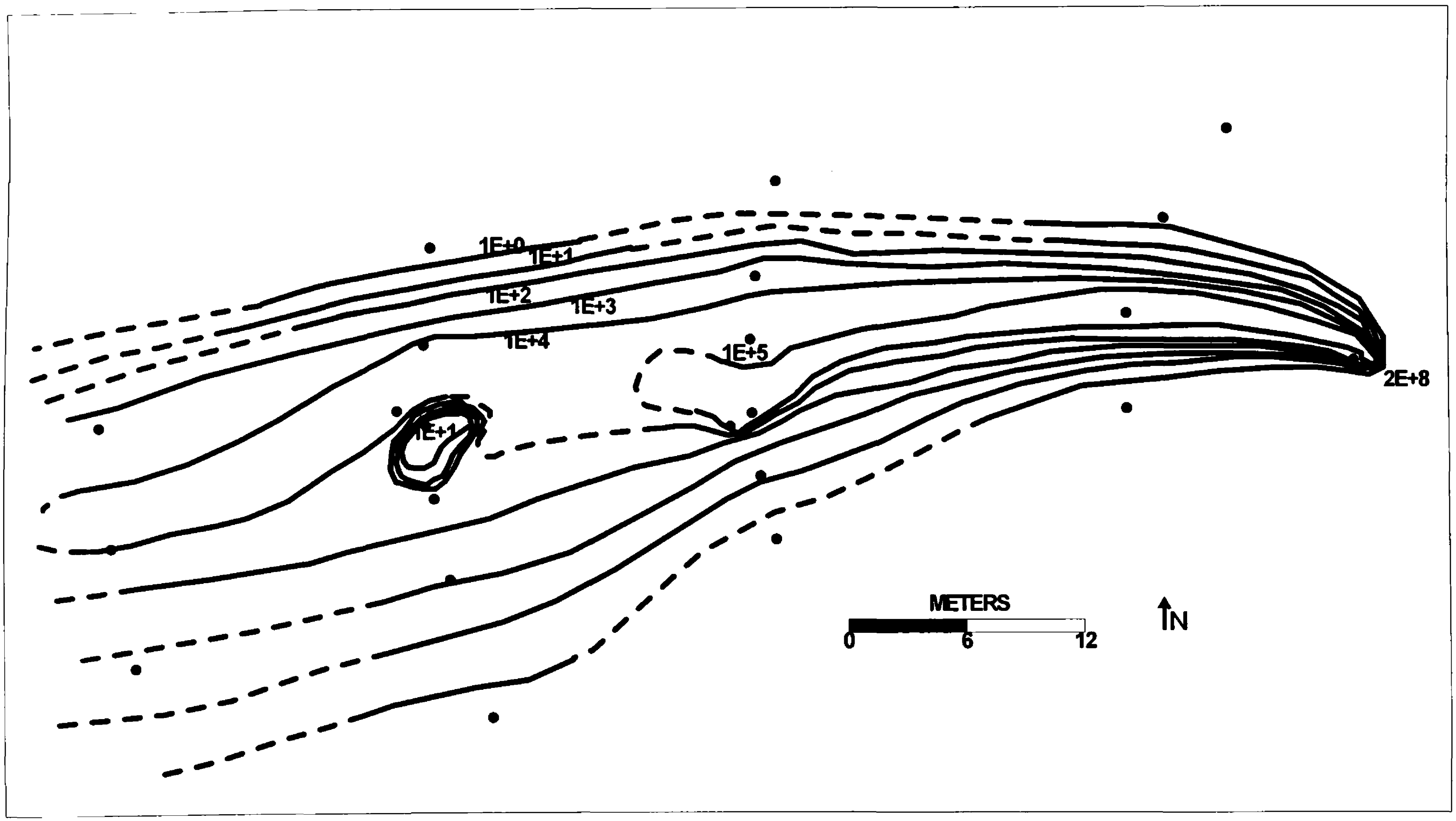

Figure D7. 72hr MS2 Plume at 9ft depth from 10/2/96 seeding experiment. Concentration in PFU/ml, flow direction to the west.

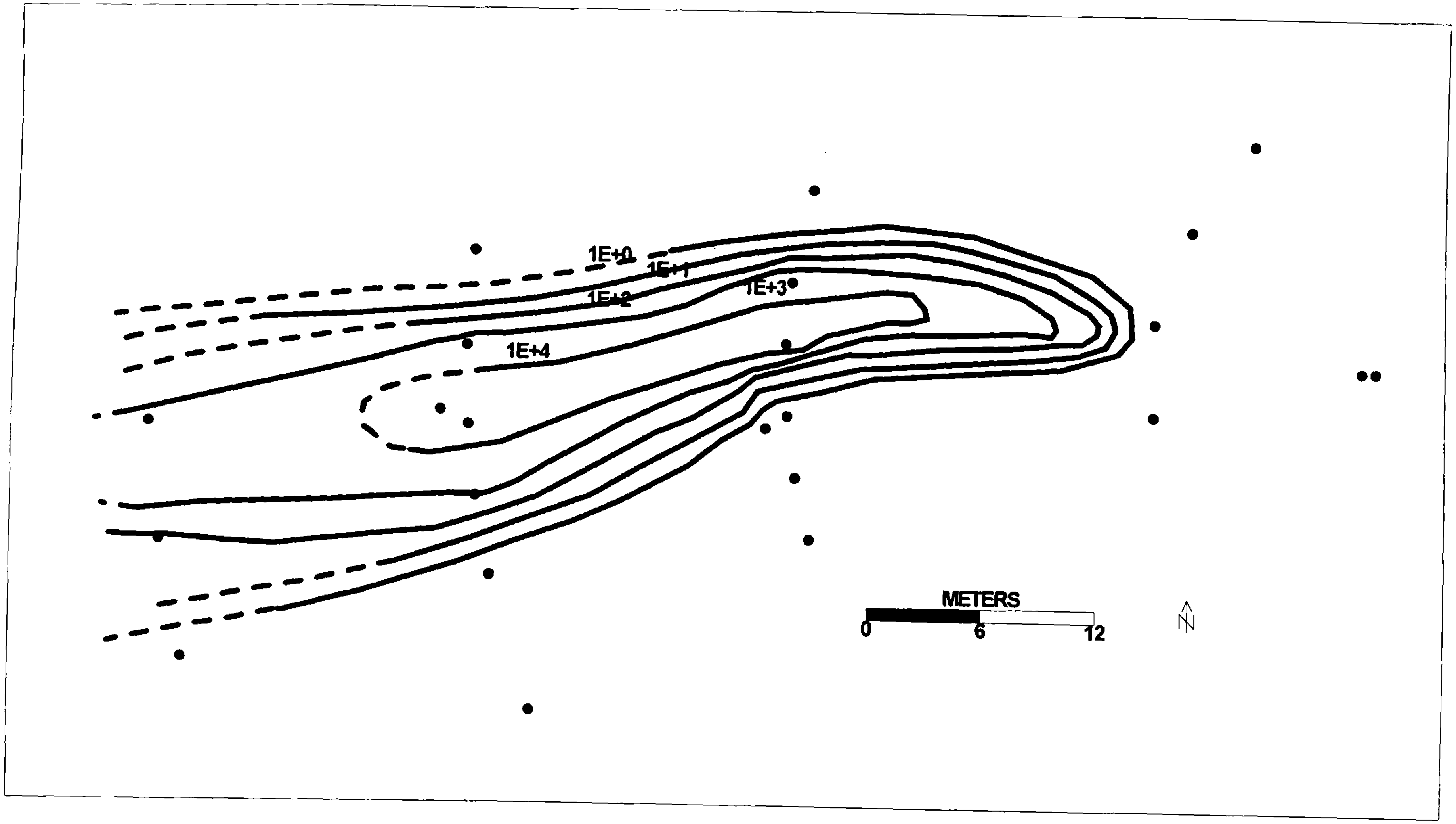

Figure D8. 72hr MS2 plume at 12ft depth from 10/2/96 seeding experiment. Concentrations in PFU/ml, flow direction to the west.

Table D3. Tracer test data from MS2 injected into well I4, October 2, 1996.

Well	Hour	PFU/ml	Well	Hour	PFU/ml	Well	Hour	PFU/ml
I4-Old	0		ML0-12	6		ML1-9	18	
I4-New	0		ML0-12	8	0.0E+00	ML1-9	20	0.0E+00
Slug	0	3.9E+10	ML0-12	10		ML1-9	24	
Injection	0	5.6E+10	ML0-12	12		ML1-9	26	
I4	0	0.0E+00	ML0-12	14		ML1-9	32	
I4	2	2.5E+10	ML0-12	16		ML1-9	36	
I4	4	1.2E+10	ML0-12	18		ML1-9	40	
I4	6		ML0-12	20	0.0E+00	ML1-9	44	
I4	8	2.5E+10	ML0-12	24		ML1-9	48	
I4	10		ML0-12	26		ML1-9	52	
I4	12		ML0-12	32		ML1-9	56	
I4	14	8.4E+09	ML0-12	36		ML1-9	60	
I4	16		ML0-12	40		ML1-9	72	1.1E-01
I4	18		ML0-12	44		ML2-9	0	1.8E+03
I4	20	4.0E+09	ML0-12	48		ML2-9	2	2.3E+04
I4	28	1.8E+09	ML0-12	52		ML2-9	4	7.9E+07
I4	32		ML0-12	56		ML2-9	6	1.6E+08
I4	36		ML0-12	60		ML2-9	8	9.6E+07
I4	40	1.5E+09	ML0-12	72	0.0E+00	ML2-9	10	8.7E+07
I4	44		ML0-15	0	9.5E+00	ML2-9	12	
I4	48	7.6E+08	ML0-15	2		ML2-9	14	5.0E+07
I4	52		ML0-15	4		ML2-9	16	
I4	56		ML0-15	6		ML2-9	18	
I4	60	3.6E+08	ML0-15	8	0.0E+00	ML2-9	20	3.9E+07
I4	72	1.9E+08	ML0-15	10		ML2-9	24	
ML0-9	0	2.5E+02	ML0-15	12		ML2-9	28	1.1E+07
ML0-9	2	9.7E+04	ML0-15	14		ML2-9	32	
ML0-9	4	8.8E+04	ML0-15	16		ML2-9	36	
ML0-9	6	6.0E+04	ML0-15	18		ML2-9	40	6.3E+06
ML0-9	8		ML0-15	20	0.0E+00	ML2-9	44	
ML0-9	10	9.2E+03	ML0-15	24		ML2-9	48	6.4E+06
ML0-9	12		ML0-15	26		ML2-9	52	
ML0-9	14		ML0-15	32		ML2-9	56	
ML0-9	16		ML0-15	36		ML2-9	60	3.7E+06
ML0-9	18		ML0-15	40		ML2-9	72	2.0E+06
ML0-9	20	1.2E+03	ML0-15	44		ML2-12	0	0.0E+00
ML0-9	24		ML0-15	48		ML2-12	2	
ML0-9	26		ML0-15	52		ML2-12	4	
ML0-9	32		ML0-15	56		ML2-12	6	
ML0-9	36		ML0-15	60		ML2-12	8	0.0E+00
ML0-9	40	8.8E+02	ML0-15	72		ML2-12	10	
ML0-9	44		ML1-9	0	1.3E+01	ML2-12	12	
ML0-9	48		ML1-9	2		ML2-12	14	
ML0-9	52		ML1-9	4		ML2-12	16	
ML0-9	56		ML1-9	6		ML2-12	18	
ML0-9	60		ML1-9	8	0.0E+00	ML2-12	20	0.0E+00
ML0-9	72	4.8E+02	ML1-9	10		ML2-12	24	
ML0-12	0	9.9E-01	ML1-9	12		ML2-12	26	
ML0-12	2		ML1-9	14		ML2-12	32	
ML0-12	4		ML1-9	16		ML2-12	36	

Table D3. Tracer test data from MS2 injected into well I4, October 2, 1996.

Well	Hour	PFU/ml	Well	Hour	PFU/ml	Well	Hour	PFU/ml
ML2-12	40		ML3-9	72	0.0E+00	ML7-12	10	
ML2-12	44		ML6-9	0	1.1E-01	ML7-12	12	
ML2-12	48		ML6-9	2		ML7-12	14	
ML2-12	52		ML6-9	4		ML7-12	16	
ML2-12	56		ML6-9	6		ML7-12	18	
ML2-12	60		ML6-9	8	0.0E+00	ML7-12	20	0.0E+00
ML2-12	72	1.1E-01	ML6-9	10		ML7-12	24	
ML2-15	0	0.0E+00	ML6-9	12		ML7-12	26	
ML2-15	2		ML6-9	14		ML7-12	32	
ML2-15	4		ML6-9	16		ML7-12	36	
ML2-15	6		ML6-9	18		ML7-12	40	
ML2-15	8	0.0E+00	ML6-9	20	0.0E+00	ML7-12	44	
ML2-15	10		ML6-9	24		ML7-12	48	
ML2-15	12		ML6-9	26		ML7-12	52	
ML2-15	14		ML6-9	32		ML7-12	56	
ML2-15	16		ML6-9	36		ML7-12	60	
ML2-15	18		ML6-9	40		ML7-12	72	3.3E-01
ML2-15	20	0.0E+00	ML6-9	44		ML7-15	0	7.7E-01
ML2-15	24		ML6-9	48		ML7-15	2	
ML2-15	26		ML6-9	52		ML7-15	4	
ML2-15	32		ML6-9	56		ML7-15	6	
ML2-15	36		ML6-9	60		ML7-15	8	0.0E+00
ML2-15	40		ML6-9	72	2.9E+01	ML7-15	10	
ML2-15	44		ML7-9	0	1.6E+03	ML7-15	12	
ML2-15	48		ML7-9	2		ML7-15	14	
ML2-15	52		ML7-9	4	6.1E+02	ML7-15	16	
ML2-15	56		ML7-9	6		ML7-15	18	
ML2-15	60		ML7-9	8	1.4E+06	ML7-15	20	0.0E+00
ML2-15	72	1.1E-01	ML7-9	10	6.1E+06	ML7-15	24	
ML3-9	0		ML7-9	12	1.3E+07	ML7-15	26	
ML3-9	2		ML7-9	14	1.6E+07	ML7-15	32	
ML3-9	4		ML7-9	16	1.4E+07	ML7-15	36	
ML3-9	6		ML7-9	18	1.2E+07	ML7-15	40	
ML3-9	8	0.0E+00	ML7-9	20	1.1E+07	ML7-15	44	
ML3-9	10		ML7-9	24		ML7-15	48	
ML3-9	12		ML7-9	28	5.6E+06	ML7-15	52	
ML3-9	14		ML7-9	32		ML7-15	56	
ML3-9	16		ML7-9	36		ML7-15	60	
ML3-9	18		ML7-9	40	2.0E+06	ML7-15	72	1.1E-01
ML3-9	20	0.0E+00	ML7-9	44		ML8-9	0	9.1E+02
ML3-9	24		ML7-9	48	1.6E+06	ML8-9	2	
ML3-9	26		ML7-9	52		ML8-9	4	
ML3-9	32		ML7-9	56		ML8-9	6	
ML3-9	36		ML7-9	60	7.2E+05	ML8-9	8	0.0E+00
ML3-9	40		ML7-9	72	4.0E+05	ML8-9	10	
ML3-9	44		ML7-12	0	0.0E+00	ML8-9	12	
ML3-9	48		ML7-12	2		ML8-9	14	
ML3-9	52		ML7-12	4		ML8-9	16	
ML3-9	56		ML7-12	6		ML8-9	18	
ML3-9	60		ML7-12	8	0.0E+00	ML8-9	20	0.0E+00

Table D3. Tracer test data from MS2 injected into well I4, October 2, 1996.

Well	Hour	PFU/ml	Well	Hour	PFU/ml	Well	Hour	PFU/ml
ML8-9	24		ML8-15	48		ML9-15	2	
ML8-9	26		ML8-15	52		ML9-15	4	
ML8-9	32		ML8-15	56		ML9-15	6	
ML8-9	36		ML8-15	60		ML9-15	8	0.0E+00
ML8-9	40		ML8-15	72	4.4E-01	ML9-15	10	
ML8-9	44		ML9-9	0	4.3E+01	ML9-15	12	
ML8-9	48		ML9-9	2		ML9-15	14	
ML8-9	52		ML9-9	4		ML9-15	16	
ML8-9	56		ML9-9	6		ML9-15	18	
ML8-9	60		ML9-9	8	0.0E+00	ML9-15	20	0.0E+00
ML8-9	72	3.9E+04	ML9-9	10		ML9-15	24	
ML8-12	0	5.3E+02	ML9-9	12		ML9-15	26	
ML8-12	2		ML9-9	14		ML9-15	32	
ML8-12	4		ML9-9	16		ML9-15	36	
ML8-12	6		ML9-9	18		ML9-15	40	
ML8-12	8	0.0E+00	ML9-9	20	0.0E+00	ML9-15	44	
ML8-12	10		ML9-9	24		ML9-15	48	
ML8-12	12		ML9-9	26		ML9-15	52	
ML8-12	14		ML9-9	32		ML9-15	56	
ML8-12	16		ML9-9	36		ML9-15	60	
ML8-12	18		ML9-9	40		ML9-15	72	4.4E-01
ML8-12	20	0.0E+00	ML9-9	44		ML19-9	0	0.0E+00
ML8-12	24		ML9-9	48		ML19-9	2	
ML8-12	26		ML9-9	52		ML19-9	4	
ML8-12	32		ML9-9	56		ML19-9	6	
ML8-12	36		ML9-9	60		ML19-9	8	0.0E+00
ML8-12	40		ML9-9	72	8.8E+03	ML19-9	10	
ML8-12	44		ML9-12	0	1.9E+02	ML19-9	12	
ML8-12	48		ML9-12	2		ML19-9	14	
ML8-12	52		ML9-12	4		ML19-9	16	
ML8-12	56		ML9-12	6		ML19-9	18	
ML8-12	60		ML9-12	8	0.0E+00	ML19-9	20	0.0E+00
ML8-12	72	9.4E+04	ML9-12	10		ML19-9	24	
ML8-15	0	0.0E+00	ML9-12	12		ML19-9	26	
ML8-15	2		ML9-12	14		ML19-9	32	
ML8-15	4		ML9-12	16		ML19-9	36	
ML8-15	6		ML9-12	18		ML19-9	40	
ML8-15	8	0.0E+00	ML9-12	20	0.0E+00	ML19-9	44	
ML8-15	10		ML9-12	24		ML19-9	48	
ML8-15	12		ML9-12	26		ML19-9	52	
ML8-15	14		ML9-12	32		ML19-9	56	
ML8-15	16		ML9-12	36		ML19-9	60	
ML8-15	18		ML9-12	40		ML19-9	72	0.0E+00
ML8-15	20	0.0E+00	ML9-12	44		ML19-12	0	8.8E-01
ML8-15	24		ML9-12	48		ML19-12	2	
ML8-15	26		ML9-12	52		ML19-12	4	
ML8-15	32		ML9-12	56		ML19-12	6	
ML8-15	36		ML9-12	60		ML19-12	8	0.0E+00
ML8-15	40		ML9-12	72	5.1E+04	ML19-12	10	
ML8-15	44		ML9-15	0	0.0E+00	ML19-12	12	

Table D3. Tracer test data from MS2 injected into well I4, October 2, 1996.

Well	Hour	PFU/ml	Well	Hour	PFU/ml	Well	Hour	PFU/ml
ML19-12	14		ML10-9	32		ML11-12	56	
ML19-12	16		ML10-9	36		ML11-12	60	
ML19-12	18		ML10-9	40		ML11-12	72	0.0E+00
ML19-12	20	0.0E+00	ML10-9	44		ML12-9	0	1.0E+01
ML19-12	24		ML10-9	48		ML12-9	2	
ML19-12	26		ML10-9	52		ML12-9	4	
ML19-12	32		ML10-9	56		ML12-9	6	
ML19-12	36		ML10-9	60		ML12-9	8	5.1E+00
ML19-12	40		ML10-9	72	0.0E+00	ML12-9	10	
ML19-12	44		ML11-9	0	8.1E+00	ML12-9	12	
ML19-12	48		ML11-9	2		ML12-9	14	7.0E+01
ML19-12	52		ML11-9	4		ML12-9	16	
ML19-12	56		ML11-9	6		ML12-9	18	
ML19-12	60		ML11-9	8	0.0E+00	ML12-9	20	1.0E+04
ML19-12	72	0.0E+00	ML11-9	10		ML12-9	24	
ML19-15	0	6.6E-01	ML11-9	12		ML12-9	28	1.1E+04
ML19-15	2		ML11-9	14		ML12-9	32	2.5E+04
ML19-15	4		ML11-9	16		ML12-9	36	2.5E+04
ML19-15	6		ML11-9	18		ML12-9	40	1.5E+04
ML19-15	8	0.0E+00	ML11-9	20	0.0E+00	ML12-9	44	1.4E+04
ML19-15	10		ML11-9	24		ML12-9	48	1.1E+04
ML19-15	12		ML11-9	26		ML12-9	52	1.2E+04
ML19-15	14		ML11-9	32		ML12-9	56	1.1E+04
ML19-15	16		ML11-9	36		ML12-9	60	3.7E+03
ML19-15	18		ML11-9	40		ML12-9	72	2.8E+03
ML19-15	20	0.0E+00	ML11-9	44		ML12-12	0	7.3E+00
ML19-15	24		ML11-9	48		ML12-12	2	
ML19-15	26		ML11-9	52		ML12-12	4	
ML19-15	32		ML11-9	56		ML12-12	6	
ML19-15	36		ML11-9	60		ML12-12	8	0.0E+00
ML19-15	40		ML11-9	72	2.2E+02	ML12-12	10	
ML19-15	44		ML11-12	0	0.0E+00	ML12-12	12	
ML19-15	48		ML11-12	2		ML12-12	14	
ML19-15	52		ML11-12	4		ML12-12	16	
ML19-15	56		ML11-12	6		ML12-12	18	
ML19-15	60		ML11-12	8	0.0E+00	ML12-12	20	0.0E+00
ML19-15	72		ML11-12	10		ML12-12	24	
ML10-9	0	2.2E+00	ML11-12	12		ML12-12	26	
ML10-9	2		ML11-12	14		ML12-12	32	
ML10-9	4		ML11-12	16		ML12-12	36	
ML10-9	6		ML11-12	18		ML12-12	40	
ML10-9	8		ML11-12	20	0.0E+00	ML12-12	44	
ML10-9	10		ML11-12	24		ML12-12	48	
ML10-9	12		ML11-12	26		ML12-12	52	
ML10-9	14		ML11-12	32		ML12-12	56	
ML10-9	16		ML11-12	36		ML12-12	60	
ML10-9	18		ML11-12	40		ML12-12	72	1.5E+03
ML10-9	20		ML11-12	44		ML12-15	0	0.0E+00
ML10-9	24		ML11-12	48		ML12-15	2	
ML10-9	26		ML11-12	52		ML12-15	4	

Table D3. Tracer test data from MS2 injected into well I4, October 2, 1996.

Well	Hour	PFU/ml	Well	Hour	PFU/ml	Well	Hour	PFU/ml
ML12-15	6		ML13-12	18		ML14-9	40	1.8E+05
ML12-15	8	0.0E+00	ML13-12	20	0.0E+00	ML14-9	44	4.8E+04
ML12-15	10		ML13-12	24		ML14-9	48	6.1E+04
ML12-15	12		ML13-12	26		ML14-9	52	2.5E+04
ML12-15	14		ML13-12	32		ML14-9	56	3.3E+04
ML12-15	16		ML13-12	36		ML14-9	60	6.8E+04
ML12-15	18		ML13-12	40		ML14-9	72	3.6E+04
ML12-15	20	0.0E+00	ML13-12	44		ML14-12	0	1.2E+01
ML12-15	24		ML13-12	48		ML14-12	2	
ML12-15	26		ML13-12	52		ML14-12	4	
ML12-15	32		ML13-12	56		ML14-12	6	
ML12-15	36		ML13-12	60		ML14-12	8	0.0E+00
ML12-15	40		ML13-12	72	2.1E+04	ML14-12	10	
ML12-15	44		ML13-15	0	1.1E+01	ML14-12	12	
ML12-15	48		ML13-15	2		ML14-12	14	0.0E+00
ML12-15	52		ML13-15	4		ML14-12	16	
ML12-15	56		ML13-15	6		ML14-12	18	
ML12-15	60		ML13-15	8	0.0E+00	ML14-12	20	0.0E+00
ML12-15	72	0.0E+00	ML13-15	10		ML14-12	24	
ML13-9	0	8.8E-01	ML13-15	12		ML14-12	26	
ML13-9	2		ML13-15	14		ML14-12	32	
ML13-9	4		ML13-15	16		ML14-12	36	
ML13-9	6		ML13-15	18		ML14-12	40	
ML13-9	8	0.0E+00	ML13-15	20	0.0E+00	ML14-12	44	
ML13-9	10		ML13-15	24		ML14-12	48	
ML13-9	12		ML13-15	26		ML14-12	52	
ML13-9	14	2.2E-01	ML13-15	32		ML14-12	56	
ML13-9	16		ML13-15	36		ML14-12	60	
ML13-9	18		ML13-15	40		ML14-12	72	7.2E+03
ML13-9	20	1.9E+00	ML13-15	44		ML14-15	0	7.3E+00
ML13-9	24		ML13-15	48		ML14-15	2	
ML13-9	28	1.7E+02	ML13-15	52		ML14-15	4	
ML13-9	32	0.0E+00	ML13-15	56		ML14-15	6	
ML13-9	36	1.6E+02	ML13-15	60		ML14-15	8	0.0E+00
ML13-9	40	2.5E+02	ML13-15	72	8.4E+03	ML14-15	10	
ML13-9	44	7.2E+01	ML14-9	0	6.8E+01	ML14-15	12	
ML13-9	48	7.5E+01	ML14-9	2		ML14-15	14	
ML13-9	52	3.8E+01	ML14-9	4		ML14-15	16	
ML13-9	56	5.4E+01	ML14-9	6		ML14-15	18	
ML13-9	60	6.1E+01	ML14-9	8	7.3E+01	ML14-15	20	0.0E+00
ML13-9	72	4.2E+00	ML14-9	10		ML14-15	24	
ML13-12	0	3.4E+01	ML14-9	12		ML14-15	26	
ML13-12	2		ML14-9	14	1.1E+04	ML14-15	32	
ML13-12	4		ML14-9	16		ML14-15	36	
ML13-12	6		ML14-9	18		ML14-15	40	
ML13-12	8	0.0E+00	ML14-9	20	4.4E+05	ML14-15	44	
ML13-12	10		ML14-9	24		ML14-15	48	
ML13-12	12		ML14-9	28	3.7E+05	ML14-15	52	
ML13-12	14		ML14-9	32	2.9E+05	ML14-15	56	
ML13-12	16		ML14-9	36	2.3E+05	ML14-15	60	

Table D3. Tracer test data from MS2 injected into well I4, October 2, 1996.

Well	Hour	PFU/ml	Well	Hour	PFU/ml	Well	Hour	PFU/ml
ML14-15	72	1.8E+03	ML18-9	10		W1	24	
ML17-9	0	1.1E-01	ML18-9	12		W1	28	
ML17-9	2		ML18-9	14		W1	32	
ML17-9	4		ML18-9	16		W1	36	
ML17-9	6		ML18-9	18		W1	40	1.8E+06
ML17-9	8	8.8E+00	ML18-9	20	3.5E+02	W1	44	
ML17-9	10		ML18-9	24		W1	48	
ML17-9	12		ML18-9	26		W1	52	
ML17-9	14		ML18-9	32		W1	56	
ML17-9	16		ML18-9	36		W1	60	
ML17-9	18		ML18-9	40	1.4E+04	W1	72	5.2E+05
ML17-9	20	4.3E+04	ML18-9	44		W2	0	
ML17-9	24		ML18-9	48		W2	2	
ML17-9	26		ML18-9	52		W2	4	0.0E+00
ML17-9	32		ML18-9	56		W2	6	
ML17-9	36		ML18-9	60		W2	8	0.0E+00
ML17-9	40	6.9E+04	ML18-9	72	3.4E+03	W2	10	
ML17-9	44		ML18-12	0	1.2E+01	W2	12	
ML17-9	48		ML18-12	2		W2	14	7.2E+00
ML17-9	52		ML18-12	4		W2	16	
ML17-9	56		ML18-12	6		W2	18	
ML17-9	60		ML18-12	8	0.0E+00	W2	20	4.7E+03
ML17-9	72	1.2E+04	ML18-12	10		W2	24	
ML17-12	0	1.3E+01	ML18-12	12		W2	26	
ML17-12	2		ML18-12	14		W2	32	
ML17-12	4		ML18-12	16		W2	36	
ML17-12	6		ML18-12	18		W2	40	
ML17-12	8	0.0E+00	ML18-12	20	0.0E+00	W2	44	
ML17-12	10		ML18-12	24		W2	48	2.5E+03
ML17-12	12		ML18-12	26		W2	52	3.2E+03
ML17-12	14		ML18-12	32		W2	56	3.5E+03
ML17-12	16		ML18-12	36		W2	60	4.4E+03
ML17-12	18		ML18-12	40		W2	72	1.8E+04
ML17-12	20	0.0E+00	ML18-12	44				
ML17-12	24		ML18-12	48				
ML17-12	26		ML18-12	52				
ML17-12	32		ML18-12	56				
ML17-12	36		ML18-12	60				
ML17-12	40		ML18-12	72	2.8E+03			
ML17-12	44		W1	0				
ML17-12	48		W1	2				
ML17-12	52		W1	4	2.2E+02			
ML17-12	56		W1	6				
ML17-12	60		W1	8	4.6E+05			
ML17-12	72	1.2E+02	W1	10				
ML18-9	0	1.7E+00	W1	12	1.5E+07			
ML18-9	2		W1	14	1.4E+07			
ML18-9	4		W1	16				
ML18-9	6		W1	18				
ML18-9	8	8.8E-01	W1	20	7.9E+06			

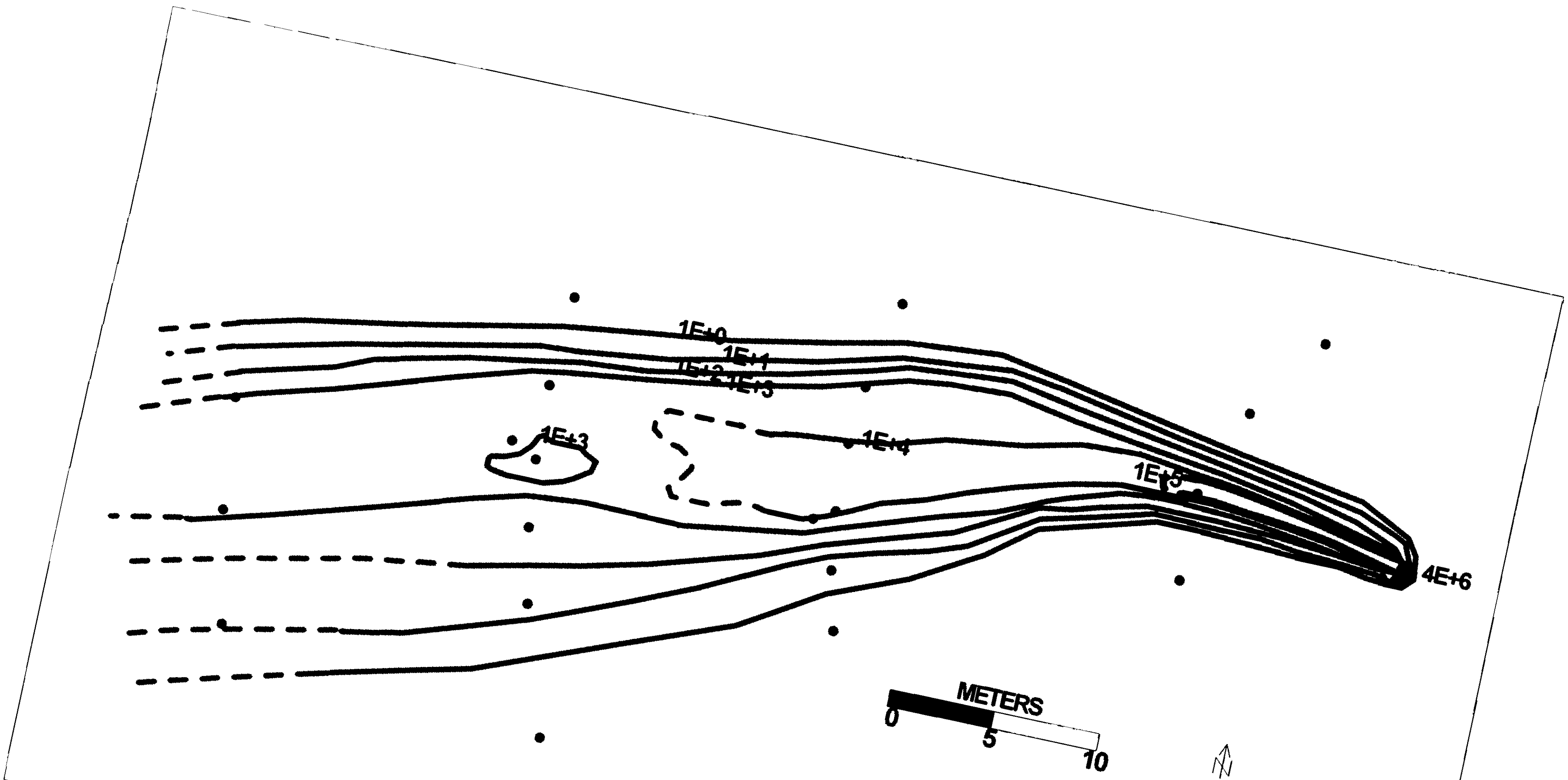

Figure D9. 72hr PRD-1 plume at 9ft depth from 10/2/96 seeding experiment. Concentration in PFU/ml, flow direction to the west.

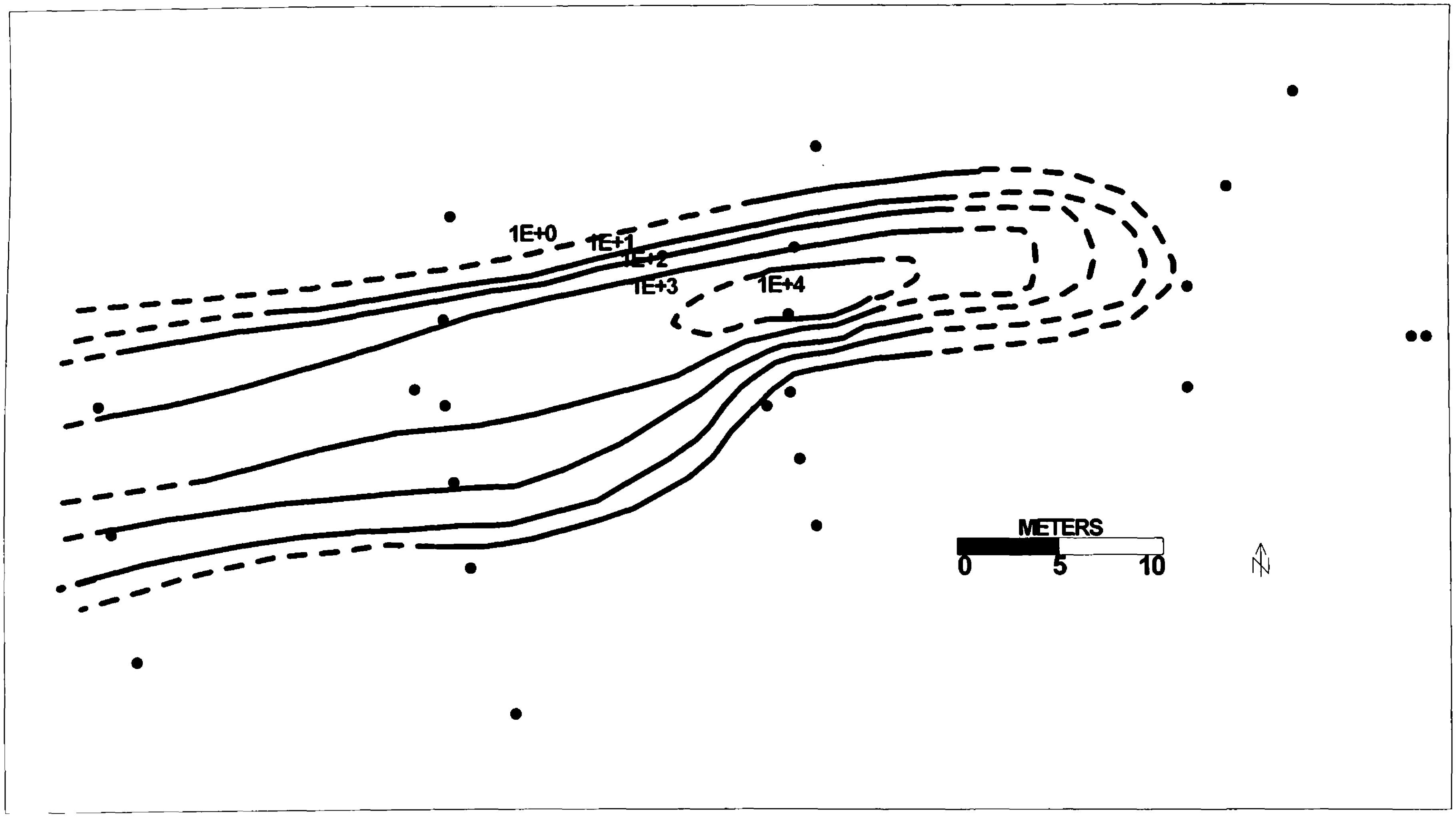

Figure D10. 72hr PRD-1 plume at 12ft depth from 10/2/96 seeding experiment. Concentration in PFU/ml, flow direction to west.

Table D4. Tracer test data from PRD1 injected into well I4, October 2, 1996.

Well	Hour	PFU/ml	Well	Hour	PFU/ml	Well	Hour	PFU/ml
I4-Old	0	0.0E+00	ML0-12	6		ML1-9	18	
I4-New	0	0.0E+00	ML0-12	8	0.0E+00	ML1-9	20	0.0E+00
Slug	0	3.7E+09	ML0-12	10		ML1-9	24	
Injection	0	5.4E+09	ML0-12	12		ML1-9	26	
I4	0	0.0E+00	ML0-12	14		ML1-9	32	
I4	2	2.1E+09	ML0-12	16		ML1-9	36	
I4	4	1.9E+09	ML0-12	18		ML1-9	40	
I4	6		ML0-12	20	0.0E+00	ML1-9	44	
I4	8	1.1E+09	ML0-12	24		ML1-9	48	
I4	10		ML0-12	26		ML1-9	52	
I4	12		ML0-12	32		ML1-9	56	
I4	14	6.7E+08	ML0-12	36		ML1-9	60	
I4	16		ML0-12	40		ML1-9	72	0.0E+00
I4	18		ML0-12	44		ML2-9	0	0.0E+00
I4	20	2.4E+08	ML0-12	48		ML2-9	2	1.0E+03
I4	28	1.8E+08	ML0-12	52		ML2-9	4	6.5E+06
I4	32		ML0-12	56		ML2-9	6	9.3E+06
I4	36		ML0-12	60		ML2-9	8	6.5E+06
I4	40	9.1E+07	ML0-12	72	0.0E+00	ML2-9	10	4.7E+06
I4	44		ML0-15	0	0.0E+00	ML2-9	12	
I4	48	4.8E+07	ML0-15	2		ML2-9	14	3.4E+06
I4	52		ML0-15	4		ML2-9	16	
I4	56		ML0-15	6		ML2-9	18	
I4	60	1.7E+07	ML0-15	8	0.0E+00	ML2-9	20	1.8E+06
I4	72	4.3E+06	ML0-15	10		ML2-9	24	
ML0-9	0	0.0E+00	ML0-15	12		ML2-9	28	7.4E+05
ML0-9	2	5.3E+03	ML0-15	14		ML2-9	32	
ML0-9	4	4.6E+03	ML0-15	16		ML2-9	36	
ML0-9	6	3.6E+03	ML0-15	18		ML2-9	40	6.0E+05
ML0-9	8		ML0-15	20	0.0E+00	ML2-9	44	
ML0-9	10	9.0E+02	ML0-15	24		ML2-9	48	4.2E+05
ML0-9	12		ML0-15	26		ML2-9	52	
ML0-9	14		ML0-15	32		ML2-9	56	
ML0-9	16		ML0-15	36		ML2-9	60	1.9E+05
ML0-9	18		ML0-15	40		ML2-9	72	1.7E+05
ML0-9	20	1.3E+02	ML0-15	44		ML2-12	0	0.0E+00
ML0-9	24		ML0-15	48		ML2-12	2	
ML0-9	26		ML0-15	52		ML2-12	4	
ML0-9	32		ML0-15	56		ML2-12	6	
ML0-9	36		ML0-15	60		ML2-12	8	0.0E+00
ML0-9	40	3.3E+01	ML0-15	72		ML2-12	10	
ML0-9	44		ML1-9	0	0.0E+00	ML2-12	12	
ML0-9	48		ML1-9	2		ML2-12	14	
ML0-9	52		ML1-9	4		ML2-12	16	
ML0-9	56		ML1-9	6		ML2-12	18	
ML0-9	60		ML1-9	8	0.0E+00	ML2-12	20	0.0E+00
ML0-9	72	1.5E+01	ML1-9	10		ML2-12	24	
ML0-12	0	0.0E+00	ML1-9	12		ML2-12	26	
ML0-12	2		ML1-9	14		ML2-12	32	
ML0-12	4		ML1-9	16		ML2-12	36	

Table D4. Tracer test data from PRD1 injected into well I4, October 2, 1996.

Well	Hour	PFU/ml
ML2-12	40	
ML2-12	44	
ML2-12	48	
ML2-12	52	
ML2-12	56	
ML2-12	60	
ML2-12	72	0.0E+00
ML2-15	0	0.0E+00
ML2-15	2	
ML2-15	4	
ML2-15	6	
ML2-15	8	0.0E+00
ML2-15	10	
ML2-15	12	
ML2-15	14	
ML2-15	16	
ML2-15	18	
ML2-15	20	0.0E+00
ML2-15	24	
ML2-15	26	
ML2-15	32	
ML2-15	36	
ML2-15	40	
ML2-15	44	
ML2-15	48	
ML2-15	52	
ML2-15	56	
ML2-15	60	
ML2-15	72	0.0E+00
ML3-9	0	
ML3-9	2	
ML3-9	4	
ML3-9	6	
ML3-9	8	0.0E+00
ML3-9	10	
ML3-9	12	
ML3-9	14	
ML3-9	16	
ML3-9	18	
ML3-9	20	0.0E+00
ML3-9	24	
ML3-9	26	
ML3-9	32	
ML3-9	36	
ML3-9	40	
ML3-9	44	
ML3-9	48	
ML3-9	52	
ML3-9	56	
ML3-9	60	

Well	Hour	PFU/ml
ML3-9	72	0.0E+00
ML6-9	0	0.0E+00
ML6-9	2	
ML6-9	4	
ML6-9	6	
ML6-9	8	0.0E+00
ML6-9	10	
ML6-9	12	
ML6-9	14	
ML6-9	16	
ML6-9	18	
ML6-9	20	0.0E+00
ML6-9	24	
ML6-9	26	
ML6-9	32	
ML6-9	36	
ML6-9	40	
ML6-9	44	
ML6-9	48	
ML6-9	52	
ML6-9	56	
ML6-9	60	
ML6-9	72	2.4E+00
ML7-9	0	0.0E+00
ML7-9	2	
ML7-9	4	0.0E+00
ML7-9	6	
ML7-9	8	9.7E+04
ML7-9	10	4.8E+05
ML7-9	12	1.3E+06
ML7-9	14	1.2E+06
ML7-9	16	9.6E+05
ML7-9	18	1.1E+06
ML7-9	20	6.5E+05
ML7-9	24	
ML7-9	28	2.6E+05
ML7-9	32	
ML7-9	36	
ML7-9	40	1.4E+05
ML7-9	44	
ML7-9	48	1.3E+05
ML7-9	52	
ML7-9	56	
ML7-9	60	9.0E+04
ML7-9	72	5.2E+04
ML7-12	0	0.0E+00
ML7-12	2	
ML7-12	4	
ML7-12	6	
ML7-12	8	0.0E+00

Well	Hour	PFU/ml
ML7-12	10	
ML7-12	12	
ML7-12	14	
ML7-12	16	
ML7-12	18	
ML7-12	20	0.0E+00
ML7-12	24	
ML7-12	26	
ML7-12	32	
ML7-12	36	
ML7-12	40	
ML7-12	44	
ML7-12	48	
ML7-12	52	
ML7-12	56	
ML7-12	60	
ML7-12	72	0.0E+00
ML7-15	0	0.0E+00
ML7-15	2	
ML7-15	4	
ML7-15	6	
ML7-15	8	0.0E+00
ML7-15	10	
ML7-15	12	
ML7-15	14	
ML7-15	16	
ML7-15	18	
ML7-15	20	0.0E+00
ML7-15	24	
ML7-15	26	
ML7-15	32	
ML7-15	36	
ML7-15	40	
ML7-15	44	
ML7-15	48	
ML7-15	52	
ML7-15	56	
ML7-15	60	
ML7-15	72	0.0E+00
ML8-9	0	0.0E+00
ML8-9	2	
ML8-9	4	
ML8-9	6	
ML8-9	8	0.0E+00
ML8-9	10	
ML8-9	12	
ML8-9	14	
ML8-9	16	
ML8-9	18	
ML8-9	20	0.0E+00

Table D4. Tracer test data from PRD1 injected into well I4, October 2, 1996.

Well	Hour	PFU/ml	Well	Hour	PFU/ml	Well	Hour	PFU/ml
ML8-9	24		ML8-15	48		ML9-15	2	
ML8-9	26		ML8-15	52		ML9-15	4	
ML8-9	32		ML8-15	56		ML9-15	6	
ML8-9	36		ML8-15	60		ML9-15	8	0.0E+00
ML8-9	40		ML8-15	72	0.0E+00	ML9-15	10	
ML8-9	44		ML9-9	0	0.0E+00	ML9-15	12	
ML8-9	48		ML9-9	2		ML9-15	14	
ML8-9	52		ML9-9	4		ML9-15	16	
ML8-9	56		ML9-9	6		ML9-15	18	
ML8-9	60		ML9-9	8	0.0E+00	ML9-15	20	0.0E+00
ML8-9	72	1.5E+04	ML9-9	10		ML9-15	24	
ML8-12	0	0.0E+00	ML9-9	12		ML9-15	26	
ML8-12	2		ML9-9	14		ML9-15	32	
ML8-12	4		ML9-9	16		ML9-15	36	
ML8-12	6		ML9-9	18		ML9-15	40	
ML8-12	8	0.0E+00	ML9-9	20	0.0E+00	ML9-15	44	
ML8-12	10		ML9-9	24		ML9-15	48	
ML8-12	12		ML9-9	26		ML9-15	52	
ML8-12	14		ML9-9	32		ML9-15	56	
ML8-12	16		ML9-9	36		ML9-15	60	
ML8-12	18		ML9-9	40		ML9-15	72	3.3E-01
ML8-12	20	0.0E+00	ML9-9	44		ML19-9	0	0.0E+00
ML8-12	24		ML9-9	48		ML19-9	2	
ML8-12	26		ML9-9	52		ML19-9	4	
ML8-12	32		ML9-9	56		ML19-9	6	
ML8-12	36		ML9-9	60		ML19-9	8	0.0E+00
ML8-12	40		ML9-9	72	1.8E+03	ML19-9	10	
ML8-12	44		ML9-12	0	0.0E+00	ML19-9	12	
ML8-12	48		ML9-12	2		ML19-9	14	
ML8-12	52		ML9-12	4		ML19-9	16	
ML8-12	56		ML9-12	6		ML19-9	18	
ML8-12	60		ML9-12	8	0.0E+00	ML19-9	20	0.0E+00
ML8-12	72	1.3E+04	ML9-12	10		ML19-9	24	
ML8-15	0	0.0E+00	ML9-12	12		ML19-9	26	
ML8-15	2		ML9-12	14		ML19-9	32	
ML8-15	4		ML9-12	16		ML19-9	36	
ML8-15	6		ML9-12	18		ML19-9	40	
ML8-15	8	0.0E+00	ML9-12	20	0.0E+00	ML19-9	44	
ML8-15	10		ML9-12	24		ML19-9	48	
ML8-15	12		ML9-12	26		ML19-9	52	
ML8-15	14		ML9-12	32		ML19-9	56	
ML8-15	16		ML9-12	36		ML19-9	60	
ML8-15	18		ML9-12	40		ML19-9	72	0.0E+00
ML8-15	20	0.0E+00	ML9-12	44		ML19-12	0	0.0E+00
ML8-15	24		ML9-12	48		ML19-12	2	
ML8-15	26		ML9-12	52		ML19-12	4	
ML8-15	32		ML9-12	56		ML19-12	6	
ML8-15	36		ML9-12	60		ML19-12	8	0.0E+00
ML8-15	40		ML9-12	72	5.2E+03	ML19-12	10	
ML8-15	44		ML9-15	0	0.0E+00	ML19-12	12	

Table D4. Tracer test data from PRD1 injected into well I4, October 2, 1996.

Well	Hour	PFU/ml	Well	Hour	PFU/ml	Well	Hour	PFU/ml
ML19-12	14		ML10-9	32		ML11-12	56	
ML19-12	16		ML10-9	36		ML11-12	60	
ML19-12	18		ML10-9	40		ML11-12	72	0.0E+00
ML19-12	20	0.0E+00	ML10-9	44		ML12-9	0	0.0E+00
ML19-12	24		ML10-9	48		ML12-9	2	
ML19-12	26		ML10-9	52		ML12-9	4	
ML19-12	32		ML10-9	56		ML12-9	6	
ML19-12	36		ML10-9	60		ML12-9	8	0.0E+00
ML19-12	40		ML10-9	72	0.0E+00	ML12-9	10	
ML19-12	44		ML11-9	0	0.0E+00	ML12-9	12	
ML19-12	48		ML11-9	2		ML12-9	14	1.4E+00
ML19-12	52		ML11-9	4		ML12-9	16	
ML19-12	56		ML11-9	6		ML12-9	18	
ML19-12	60		ML11-9	8	0.0E+00	ML12-9	20	1.2E+03
ML19-12	72	0.0E+00	ML11-9	10		ML12-9	24	
ML19-15	0	0.0E+00	ML11-9	12		ML12-9	28	4.0E+03
ML19-15	2		ML11-9	14		ML12-9	32	3.7E+03
ML19-15	4		ML11-9	16		ML12-9	36	3.7E+03
ML19-15	6		ML11-9	18		ML12-9	40	3.0E+03
ML19-15	8	0.0E+00	ML11-9	20	0.0E+00	ML12-9	44	3.0E+03
ML19-15	10		ML11-9	24		ML12-9	48	1.7E+03
ML19-15	12		ML11-9	26		ML12-9	52	1.8E+03
ML19-15	14		ML11-9	32		ML12-9	56	1.9E+03
ML19-15	16		ML11-9	36		ML12-9	60	1.9E+03
ML19-15	18		ML11-9	40		ML12-9	72	9.2E+02
ML19-15	20	0.0E+00	ML11-9	44		ML12-12	0	0.0E+00
ML19-15	24		ML11-9	48		ML12-12	2	
ML19-15	26		ML11-9	52		ML12-12	4	
ML19-15	32		ML11-9	56		ML12-12	6	
ML19-15	36		ML11-9	60		ML12-12	8	0.0E+00
ML19-15	40		ML11-9	72	4.0E+01	ML12-12	10	
ML19-15	44		ML11-12	0	0.0E+00	ML12-12	12	
ML19-15	48		ML11-12	2		ML12-12	14	
ML19-15	52		ML11-12	4		ML12-12	16	
ML19-15	56		ML11-12	6		ML12-12	18	
ML19-15	60		ML11-12	8	0.0E+00	ML12-12	20	0.0E+00
ML19-15	72		ML11-12	10		ML12-12	24	
ML10-9	0	0.0E+00	ML11-12	12		ML12-12	26	
ML10-9	2		ML11-12	14		ML12-12	32	
ML10-9	4		ML11-12	16		ML12-12	36	
ML10-9	6		ML11-12	18		ML12-12	40	
ML10-9	8		ML11-12	20	0.0E+00	ML12-12	44	
ML10-9	10		ML11-12	24		ML12-12	48	
ML10-9	12		ML11-12	26		ML12-12	52	
ML10-9	14		ML11-12	32		ML12-12	56	
ML10-9	16		ML11-12	36		ML12-12	60	
ML10-9	18		ML11-12	40		ML12-12	72	1.3E+02
ML10-9	20		ML11-12	44		ML12-15	0	0.0E+00
ML10-9	24		ML11-12	48		ML12-15	2	
ML10-9	26		ML11-12	52		ML12-15	4	

Table D4. Tracer test data from PRD1 injected into well I4, October 2, 1996.

Well	Hour	PFU/ml	Well	Hour	PFU/ml	Well	Hour	PFU/ml
ML12-15	6		ML13-12	18		ML14-9	40	1.9E+04
ML12-15	8	0.0E+00	ML13-12	20	0.0E+00	ML14-9	44	1.3E+04
ML12-15	10		ML13-12	24		ML14-9	48	1.4E+04
ML12-15	12		ML13-12	26		ML14-9	52	6.6E+03
ML12-15	14		ML13-12	32		ML14-9	56	7.9E+03
ML12-15	16		ML13-12	36		ML14-9	60	1.0E+04
ML12-15	18		ML13-12	40		ML14-9	72	7.8E+03
ML12-15	20	0.0E+00	ML13-12	44		ML14-12	0	0.0E+00
ML12-15	24		ML13-12	48		ML14-12	2	
ML12-15	26		ML13-12	52		ML14-12	4	
ML12-15	32		ML13-12	56		ML14-12	6	
ML12-15	36		ML13-12	60		ML14-12	8	0.0E+00
ML12-15	40		ML13-12	72	1.9E+03	ML14-12	10	
ML12-15	44		ML13-15	0	0.0E+00	ML14-12	12	
ML12-15	48		ML13-15	2		ML14-12	14	0.0E+00
ML12-15	52		ML13-15	4		ML14-12	16	
ML12-15	56		ML13-15	6		ML14-12	18	
ML12-15	60		ML13-15	8	0.0E+00	ML14-12	20	0.0E+00
ML12-15	72	0.0E+00	ML13-15	10		ML14-12	24	
ML13-9	0	0.0E+00	ML13-15	12		ML14-12	26	
ML13-9	2		ML13-15	14		ML14-12	32	
ML13-9	4		ML13-15	16		ML14-12	36	
ML13-9	6		ML13-15	18		ML14-12	40	
ML13-9	8	1.1E-01	ML13-15	20	0.0E+00	ML14-12	44	
ML13-9	10		ML13-15	24		ML14-12	48	
ML13-9	12		ML13-15	26		ML14-12	52	
ML13-9	14	0.0E+00	ML13-15	32		ML14-12	56	
ML13-9	16		ML13-15	36		ML14-12	60	
ML13-9	18		ML13-15	40		ML14-12	72	1.9E+03
ML13-9	20	4.4E-01	ML13-15	44		ML14-15	0	0.0E+00
ML13-9	24		ML13-15	48		ML14-15	2	
ML13-9	28	2.9E+01	ML13-15	52		ML14-15	4	
ML13-9	32	0.0E+00	ML13-15	56		ML14-15	6	
ML13-9	36	3.1E+01	ML13-15	60		ML14-15	8	0.0E+00
ML13-9	40	4.8E+01	ML13-15	72	9.9E+02	ML14-15	10	
ML13-9	44	1.8E+01	ML14-9	0	0.0E+00	ML14-15	12	
ML13-9	48	1.3E+01	ML14-9	2		ML14-15	14	
ML13-9	52	1.1E+01	ML14-9	4		ML14-15	16	
ML13-9	56	1.6E+01	ML14-9	6		ML14-15	18	
ML13-9	60	2.3E+01	ML14-9	8	0.0E+00	ML14-15	20	0.0E+00
ML13-9	72	3.4E+00	ML14-9	10		ML14-15	24	
ML13-12	0	0.0E+00	ML14-9	12		ML14-15	26	
ML13-12	2		ML14-9	14	1.2E+03	ML14-15	32	
ML13-12	4		ML14-9	16		ML14-15	36	
ML13-12	6		ML14-9	18		ML14-15	40	
ML13-12	8	0.0E+00	ML14-9	20	5.5E+04	ML14-15	44	
ML13-12	10		ML14-9	24		ML14-15	48	
ML13-12	12		ML14-9	28	3.2E+04	ML14-15	52	
ML13-12	14		ML14-9	32	2.9E+04	ML14-15	56	
ML13-12	16		ML14-9	36	2.8E+04	ML14-15	60	

Table D4. Tracer test data from PRD1 injected into well I4, October 2, 1996.

Well	Hour	PFU/ml
ML14-15	72	3.1E+02
ML17-9	0	0.0E+00
ML17-9	2	
ML17-9	4	
ML17-9	6	
ML17-9	8	0.0E+00
ML17-9	10	
ML17-9	12	
ML17-9	14	
ML17-9	16	
ML17-9	18	
ML17-9	20	5.3E+03
ML17-9	24	
ML17-9	26	
ML17-9	32	
ML17-9	36	
ML17-9	40	8.0E+03
ML17-9	44	
ML17-9	48	
ML17-9	52	
ML17-9	56	
ML17-9	60	
ML17-9	72	2.5E+03
ML17-12	0	0.0E+00
ML17-12	2	
ML17-12	4	
ML17-12	6	
ML17-12	8	0.0E+00
ML17-12	10	
ML17-12	12	
ML17-12	14	
ML17-12	16	
ML17-12	18	
ML17-12	20	0.0E+00
ML17-12	24	
ML17-12	26	
ML17-12	32	
ML17-12	36	
ML17-12	40	
ML17-12	44	
ML17-12	48	
ML17-12	52	
ML17-12	56	
ML17-12	60	
ML17-12	72	7.5E+01
ML18-9	0	0.0E+00
ML18-9	2	
ML18-9	4	
ML18-9	6	
ML18-9	8	0.0E+00
ML18-9	10	
ML18-9	12	
ML18-9	14	
ML18-9	16	
ML18-9	18	
ML18-9	20	6.4E+01
ML18-9	24	
ML18-9	26	
ML18-9	32	
ML18-9	36	
ML18-9	40	3.9E+03
ML18-9	44	
ML18-9	48	
ML18-9	52	
ML18-9	56	
ML18-9	60	
ML18-9	72	1.1E+03
ML18-12	0	0.0E+00
ML18-12	2	
ML18-12	4	
ML18-12	6	
ML18-12	8	0.0E+00
ML18-12	10	
ML18-12	12	
ML18-12	14	
ML18-12	16	
ML18-12	18	
ML18-12	20	0.0E+00
ML18-12	24	
ML18-12	26	
ML18-12	32	
ML18-12	36	
ML18-12	40	
ML18-12	44	
ML18-12	48	
ML18-12	52	
ML18-12	56	
ML18-12	60	
ML18-12	72	1.3E+03
W1	0	
W1	2	
W1	4	0.0E+00
W1	6	
W1	8	4.4E+04
W1	10	
W1	12	1.5E+06
W1	14	1.2E+06
W1	16	
W1	18	
W1	20	7.2E+05
W1	24	
W1	28	
W1	32	
W1	36	
W1	40	1.4E+05
W1	44	
W1	48	
W1	52	
W1	56	
W1	60	
W1	72	4.5E+04
W2	0	
W2	2	
W2	4	0.0E+00
W2	6	
W2	8	0.0E+00
W2	10	
W2	12	
W2	14	0.0E+00
W2	16	
W2	18	
W2	20	2.2E+03
W2	24	
W2	28	
W2	32	
W2	36	
W2	40	2.0E+04
W2	44	1.7E+04
W2	48	
W2	52	7.3E+03
W2	56	5.1E+03
W2	60	6.7E+03
W2	72	7.0E+03

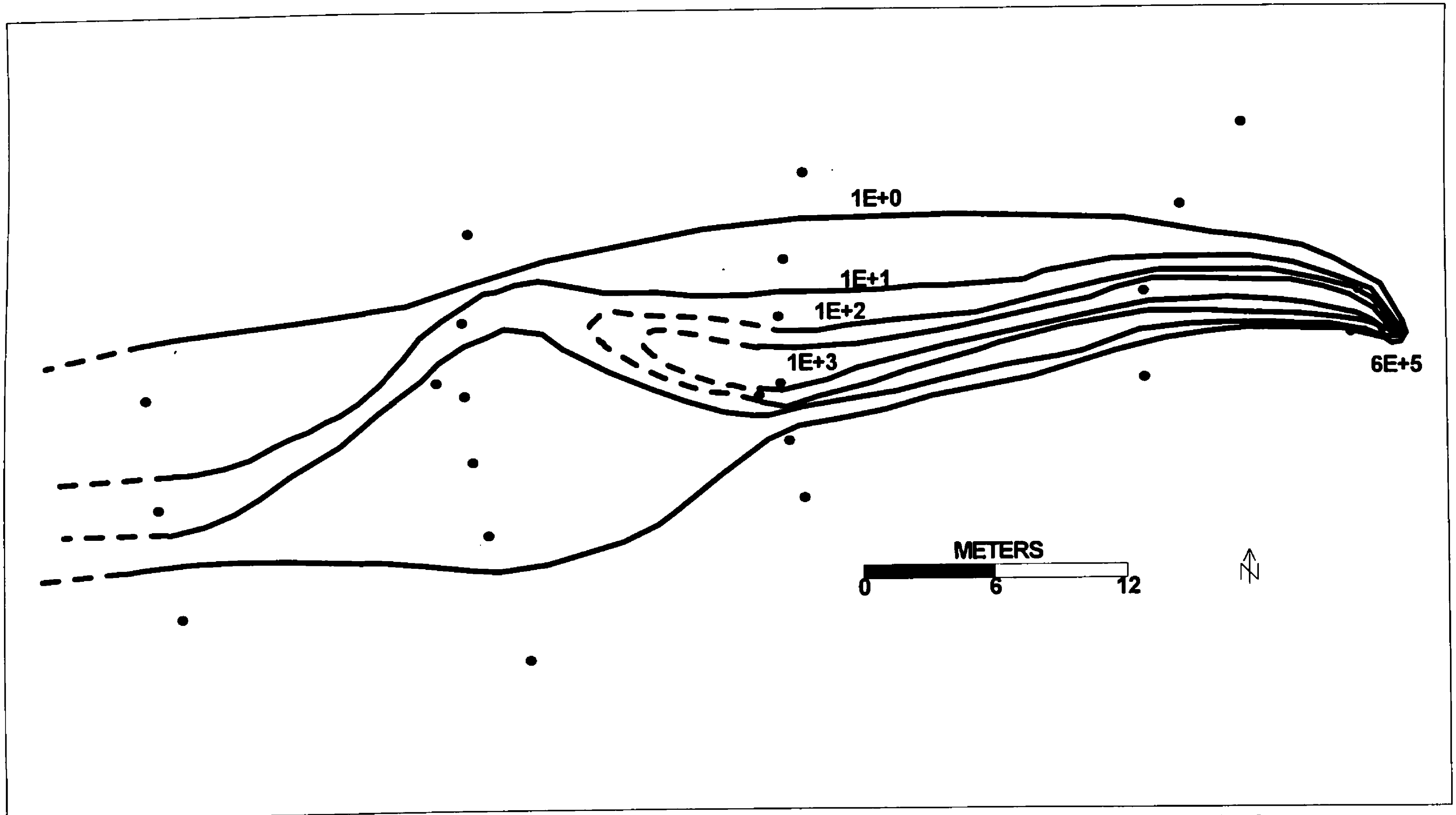

Figure D11. 72hr Phi X174 plume at 9ft from 10/2/96 seeding experiment. Concentration in PFU/ml, flow direction to the west.

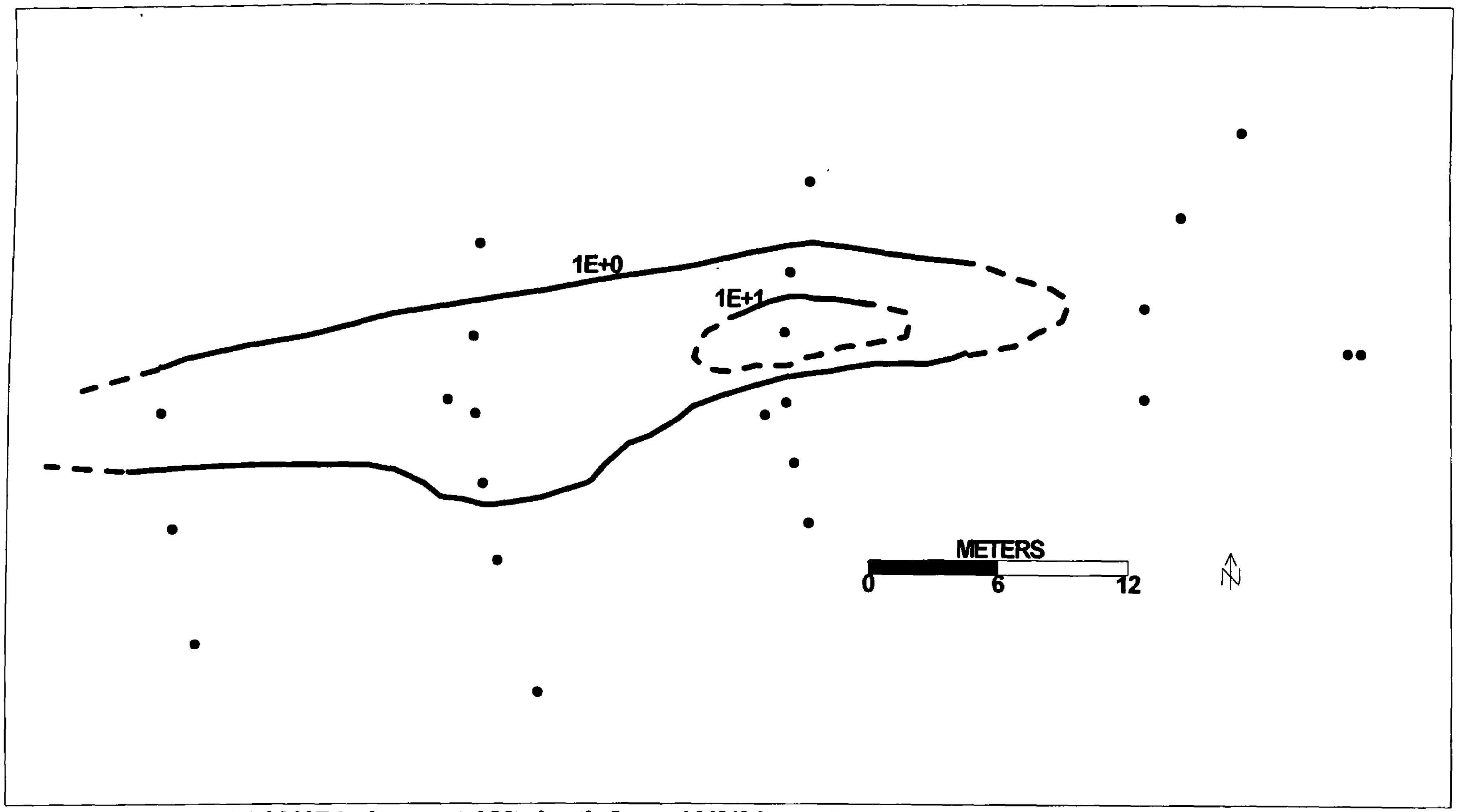

Figure D12. 72hr Phi X174 plume at 12ft depth from 10/2/96 seeding experiment. Concentration in PFU/ml, flow direction to the west.

Table D5. Tracer test data from ∅X174 injected into well I4, October 2, 1996.

Well	Hour	PFU/ml	Well	Hour	PFU/ml	Well	Hour	PFU/ml
I4-Old	0		ML0-12	6		ML1-9	18	
I4-New	0		ML0-12	8	0.0E+00	ML1-9	20	0.0E+00
Slug	0	4.1E+07	ML0-12	10		ML1-9	24	
Injection	0	2.9E+07	ML0-12	12		ML1-9	26	
I4	0	0.0E+00	ML0-12	14		ML1-9	32	
I4	2	2.1E+07	ML0-12	16		ML1-9	36	
I4	4	1.5E+07	ML0-12	18		ML1-9	40	
I4	6		ML0-12	20	0.0E+00	ML1-9	44	
I4	8	6.4E+06	ML0-12	24		ML1-9	48	
I4	10		ML0-12	26		ML1-9	52	
I4	12		ML0-12	32		ML1-9	56	
I4	14	3.6E+06	ML0-12	36		ML1-9	60	
I4	16		ML0-12	40		ML1-9	72	0.0E+00
I4	18		ML0-12	44		ML2-9	0	0.0E+00
I4	20	1.7E+06	ML0-12	48		ML2-9	2	1.1E+01
I4	28	1.1E+06	ML0-12	52		ML2-9	4	3.7E+04
I4	32		ML0-12	56		ML2-9	6	5.6E+04
I4	36		ML0-12	60		ML2-9	8	2.9E+04
I4	40	1.4E+06	ML0-12	72	0.0E+00	ML2-9	10	2.0E+04
I4	44		ML0-15	0		ML2-9	12	
I4	48	1.1E+06	ML0-15	2		ML2-9	14	1.1E+04
I4	52		ML0-15	4		ML2-9	16	
I4	56		ML0-15	6		ML2-9	18	
I4	60	8.8E+05	ML0-15	8	0.0E+00	ML2-9	20	8.0E+03
I4	72	5.6E+05	ML0-15	10		ML2-9	24	
ML0-9	0	3.3E-01	ML0-15	12		ML2-9	28	4.5E+03
ML0-9	2	3.3E+01	ML0-15	14		ML2-9	32	
ML0-9	4	3.9E+01	ML0-15	16		ML2-9	36	
ML0-9	6	1.1E+01	ML0-15	18		ML2-9	40	5.6E+03
ML0-9	8		ML0-15	20	0.0E+00	ML2-9	44	
ML0-9	10	3.1E+00	ML0-15	24		ML2-9	48	7.6E+03
ML0-9	12		ML0-15	26		ML2-9	52	
ML0-9	14		ML0-15	32		ML2-9	56	
ML0-9	16		ML0-15	36		ML2-9	60	6.8E+03
ML0-9	18		ML0-15	40		ML2-9	72	7.0E+03
ML0-9	20	1.3E+00	ML0-15	44		ML2-12	0	0.0E+00
ML0-9	24		ML0-15	48		ML2-12	2	
ML0-9	26		ML0-15	52		ML2-12	4	
ML0-9	32		ML0-15	56		ML2-12	6	
ML0-9	36		ML0-15	60		ML2-12	8	0.0E+00
ML0-9	40	8.8E-01	ML0-15	72		ML2-12	10	
ML0-9	44		ML1-9	0	0.0E+00	ML2-12	12	
ML0-9	48		ML1-9	2		ML2-12	14	
ML0-9	52		ML1-9	4		ML2-12	16	
ML0-9	56		ML1-9	6		ML2-12	18	
ML0-9	60		ML1-9	8	0.0E+00	ML2-12	20	0.0E+00
ML0-9	72	9.9E-01	ML1-9	10		ML2-12	24	
ML0-12	0	0.0E+00	ML1-9	12		ML2-12	26	
ML0-12	2		ML1-9	14		ML2-12	32	
ML0-12	4		ML1-9	16		ML2-12	36	

Table D5. Tracer test data from ∅X174 injected into well I4, October 2, 1996.

Well	Hour	PFU/ml	Well	Hour	PFU/ml	Well	Hour	PFU/ml
ML2-12	40		ML3-9	72	0.0E+00	ML7-12	10	
ML2-12	44		ML6-9	0	0.0E+00	ML7-12	12	
ML2-12	48		ML6-9	2		ML7-12	14	
ML2-12	52		ML6-9	4		ML7-12	16	
ML2-12	56		ML6-9	6		ML7-12	18	
ML2-12	60		ML6-9	8	0.0E+00	ML7-12	20	0.0E+00
ML2-12	72	0.0E+00	ML6-9	10		ML7-12	24	
ML2-15	0	0.0E+00	ML6-9	12		ML7-12	26	
ML2-15	2		ML6-9	14		ML7-12	32	
ML2-15	4		ML6-9	16		ML7-12	36	
ML2-15	6		ML6-9	18		ML7-12	40	
ML2-15	8	0.0E+00	ML6-9	20	0.0E+00	ML7-12	44	
ML2-15	10		ML6-9	24		ML7-12	48	
ML2-15	12		ML6-9	26		ML7-12	52	
ML2-15	14		ML6-9	32		ML7-12	56	
ML2-15	16		ML6-9	36		ML7-12	60	
ML2-15	18		ML6-9	40		ML7-12	72	0.0E+00
ML2-15	20	0.0E+00	ML6-9	44		ML7-15	0	0.0E+00
ML2-15	24		ML6-9	48		ML7-15	2	
ML2-15	26		ML6-9	52		ML7-15	4	
ML2-15	32		ML6-9	56		ML7-15	6	
ML2-15	36		ML6-9	60		ML7-15	8	0.0E+00
ML2-15	40		ML6-9	72	0.0E+00	ML7-15	10	
ML2-15	44		ML7-9	0	0.0E+00	ML7-15	12	
ML2-15	48		ML7-9	2		ML7-15	14	
ML2-15	52		ML7-9	4	0.0E+00	ML7-15	16	
ML2-15	56		ML7-9	6		ML7-15	18	
ML2-15	60		ML7-9	8	5.9E+02	ML7-15	20	0.0E+00
ML2-15	72	0.0E+00	ML7-9	10	2.3E+03	ML7-15	24	
ML3-9	0		ML7-9	12	3.6E+03	ML7-15	26	
ML3-9	2		ML7-9	14	3.6E+03	ML7-15	32	
ML3-9	4		ML7-9	16	2.5E+03	ML7-15	36	
ML3-9	6		ML7-9	18	2.3E+03	ML7-15	40	
ML3-9	8	0.0E+00	ML7-9	20	1.9E+03	ML7-15	44	
ML3-9	10		ML7-9	24		ML7-15	48	
ML3-9	12		ML7-9	28	7.2E+02	ML7-15	52	
ML3-9	14		ML7-9	32		ML7-15	56	
ML3-9	16		ML7-9	36		ML7-15	60	
ML3-9	18		ML7-9	40	6.8E+02	ML7-15	72	0.0E+00
ML3-9	20	0.0E+00	ML7-9	44		ML8-9	0	0.0E+00
ML3-9	24		ML7-9	48	7.3E+02	ML8-9	2	
ML3-9	26		ML7-9	52		ML8-9	4	
ML3-9	32		ML7-9	56		ML8-9	6	
ML3-9	36		ML7-9	60	6.8E+02	ML8-9	8	0.0E+00
ML3-9	40		ML7-9	72	1.0E+03	ML8-9	10	
ML3-9	44		ML7-12	0	0.0E+00	ML8-9	12	
ML3-9	48		ML7-12	2		ML8-9	14	
ML3-9	52		ML7-12	4		ML8-9	16	
ML3-9	56		ML7-12	6		ML8-9	18	
ML3-9	60		ML7-12	8	0.0E+00	ML8-9	20	0.0E+00

Table D5. Tracer test data from ∅X174 Injected into well I4, October 2, 1996.

Well	Hour	PFU/ml	Well	Hour	PFU/ml	Well	Hour	PFU/ml
ML8-9	24		ML8-15	48		ML9-15	2	
ML8-9	26		ML8-15	52		ML9-15	4	
ML8-9	32		ML8-15	56		ML9-15	6	
ML8-9	36		ML8-15	60		ML9-15	8	0.0E+00
ML8-9	40		ML8-15	72	0.0E+00	ML9-15	10	
ML8-9	44		ML9-9	0	0.0E+00	ML9-15	12	
ML8-9	48		ML9-9	2		ML9-15	14	
ML8-9	52		ML9-9	4		ML9-15	16	
ML8-9	56		ML9-9	6		ML9-15	18	
ML8-9	60		ML9-9	8	0.0E+00	ML9-15	20	0.0E+00
ML8-9	72	2.1E+01	ML9-9	10		ML9-15	24	
ML8-12	0	0.0E+00	ML9-9	12		ML9-15	26	
ML8-12	2		ML9-9	14		ML9-15	32	
ML8-12	4		ML9-9	16		ML9-15	36	
ML8-12	6		ML9-9	18		ML9-15	40	
ML8-12	8	0.0E+00	ML9-9	20	0.0E+00	ML9-15	44	
ML8-12	10		ML9-9	24		ML9-15	48	
ML8-12	12		ML9-9	26		ML9-15	52	
ML8-12	14		ML9-9	32		ML9-15	56	
ML8-12	16		ML9-9	36		ML9-15	60	
ML8-12	18		ML9-9	40		ML9-15	72	0.0E+00
ML8-12	20	0.0E+00	ML9-9	44		ML19-9	0	0.0E+00
ML8-12	24		ML9-9	48		ML19-9	2	
ML8-12	26		ML9-9	52		ML19-9	4	
ML8-12	32		ML9-9	56		ML19-9	6	
ML8-12	36		ML9-9	60		ML19-9	8	0.0E+00
ML8-12	40		ML9-9	72	5.5E+00	ML19-9	10	
ML8-12	44		ML9-12	0	0.0E+00	ML19-9	12	
ML8-12	48		ML9-12	2		ML19-9	14	
ML8-12	52		ML9-12	4		ML19-9	16	
ML8-12	56		ML9-12	6		ML19-9	18	
ML8-12	60		ML9-12	8	0.0E+00	ML19-9	20	0.0E+00
ML8-12	72	1.7E+02	ML9-12	10		ML19-9	24	
ML8-15	0	0.0E+00	ML9-12	12		ML19-9	26	
ML8-15	2		ML9-12	14		ML19-9	32	
ML8-15	4		ML9-12	16		ML19-9	36	
ML8-15	6		ML9-12	18		ML19-9	40	
ML8-15	8	0.0E+00	ML9-12	20	0.0E+00	ML19-9	44	
ML8-15	10		ML9-12	24		ML19-9	48	
ML8-15	12		ML9-12	26		ML19-9	52	
ML8-15	14		ML9-12	32		ML19-9	56	
ML8-15	16		ML9-12	36		ML19-9	60	
ML8-15	18		ML9-12	40		ML19-9	72	0.0E+00
ML8-15	20	0.0E+00	ML9-12	44		ML19-12	0	0.0E+00
ML8-15	24		ML9-12	48		ML19-12	2	
ML8-15	26		ML9-12	52		ML19-12	4	
ML8-15	32		ML9-12	56		ML19-12	6	
ML8-15	36		ML9-12	60		ML19-12	8	0.0E+00
ML8-15	40		ML9-12	72	7.5E+01	ML19-12	10	
ML8-15	44		ML9-15	0	0.0E+00	ML19-12	12	

Table D5. Tracer test data from ∅X174 injected into well I4, October 2, 1996.

Well	Hour	PFU/ml
ML19-12	14	
ML19-12	16	
ML19-12	18	
ML19-12	20	0.0E+00
ML19-12	24	
ML19-12	26	
ML19-12	32	
ML19-12	36	
ML19-12	40	
ML19-12	44	
ML19-12	48	
ML19-12	52	
ML19-12	56	
ML19-12	60	
ML19-12	72	0.0E+00
ML19-15	0	0.0E+00
ML19-15	2	
ML19-15	4	
ML19-15	6	
ML19-15	8	0.0E+00
ML19-15	10	
ML19-15	12	
ML19-15	14	
ML19-15	16	
ML19-15	18	
ML19-15	20	0.0E+00
ML19-15	24	
ML19-15	26	
ML19-15	32	
ML19-15	36	
ML19-15	40	
ML19-15	44	
ML19-15	48	
ML19-15	52	
ML19-15	56	
ML19-15	60	
ML19-15	72	
ML10-9	0	0.0E+00
ML10-9	2	
ML10-9	4	
ML10-9	6	
ML10-9	8	
ML10-9	10	
ML10-9	12	
ML10-9	14	
ML10-9	16	
ML10-9	18	
ML10-9	20	
ML10-9	24	
ML10-9	26	
ML10-9	32	
ML10-9	36	
ML10-9	40	
ML10-9	44	
ML10-9	48	
ML10-9	52	
ML10-9	56	
ML10-9	60	
ML10-9	72	0.0E+00
ML11-9	0	0.0E+00
ML11-9	2	
ML11-9	4	
ML11-9	6	
ML11-9	8	0.0E+00
ML11-9	10	
ML11-9	12	
ML11-9	14	
ML11-9	16	
ML11-9	18	
ML11-9	20	0.0E+00
ML11-9	24	
ML11-9	26	
ML11-9	32	
ML11-9	36	
ML11-9	40	
ML11-9	44	
ML11-9	48	
ML11-9	52	
ML11-9	56	
ML11-9	60	
ML11-9	72	5.3E+00
ML11-12	0	0.0E+00
ML11-12	2	
ML11-12	4	
ML11-12	6	
ML11-12	8	0.0E+00
ML11-12	10	
ML11-12	12	
ML11-12	14	
ML11-12	16	
ML11-12	18	
ML11-12	20	0.0E+00
ML11-12	24	
ML11-12	26	
ML11-12	32	
ML11-12	36	
ML11-12	40	
ML11-12	44	
ML11-12	48	
ML11-12	52	
ML11-12	56	
ML11-12	60	
ML11-12	72	0.0E+00
ML12-9	0	0.0E+00
ML12-9	2	
ML12-9	4	
ML12-9	6	
ML12-9	8	0.0E+00
ML12-9	10	
ML12-9	12	
ML12-9	14	0.0E+00
ML12-9	16	
ML12-9	18	
ML12-9	20	3.1E+00
ML12-9	24	
ML12-9	28	3.0E+00
ML12-9	32	5.0E+00
ML12-9	36	2.4E+00
ML12-9	40	2.2E+00
ML12-9	44	1.4E+00
ML12-9	48	1.1E+00
ML12-9	52	1.8E+00
ML12-9	56	1.9E+00
ML12-9	60	4.0E+00
ML12-9	72	9.9E-01
ML12-12	0	0.0E+00
ML12-12	2	
ML12-12	4	
ML12-12	6	
ML12-12	8	0.0E+00
ML12-12	10	
ML12-12	12	
ML12-12	14	
ML12-12	16	
ML12-12	18	
ML12-12	20	0.0E+00
ML12-12	24	
ML12-12	26	
ML12-12	32	
ML12-12	36	
ML12-12	40	
ML12-12	44	
ML12-12	48	
ML12-12	52	
ML12-12	56	
ML12-12	60	
ML12-12	72	2.2E+00
ML12-15	0	0.0E+00
ML12-15	2	
ML12-15	4	

Table D5. Tracer test data from ∅X174 injected into well I4, October 2, 1996.

Well	Hour	PFU/ml	Well	Hour	PFU/ml	Well	Hour	PFU/ml
ML12-15	6		ML13-12	18		ML14-9	40	3.0E+01
ML12-15	8	0.0E+00	ML13-12	20	0.0E+00	ML14-9	44	1.7E+01
ML12-15	10		ML13-12	24		ML14-9	48	1.2E+01
ML12-15	12		ML13-12	26		ML14-9	52	9.7E+00
ML12-15	14		ML13-12	32		ML14-9	56	1.2E+01
ML12-15	16		ML13-12	36		ML14-9	60	9.5E+00
ML12-15	18		ML13-12	40		ML14-9	72	1.1E+01
ML12-15	20	0.0E+00	ML13-12	44		ML14-12	0	0.0E+00
ML12-15	24		ML13-12	48		ML14-12	2	
ML12-15	26		ML13-12	52		ML14-12	4	
ML12-15	32		ML13-12	56		ML14-12	6	
ML12-15	36		ML13-12	60		ML14-12	8	0.0E+00
ML12-15	40		ML13-12	72	4.0E+00	ML14-12	10	
ML12-15	44		ML13-15	0	0.0E+00	ML14-12	12	
ML12-15	48		ML13-15	2		ML14-12	14	0.0E+00
ML12-15	52		ML13-15	4		ML14-12	16	
ML12-15	56		ML13-15	6		ML14-12	18	
ML12-15	60		ML13-15	8	0.0E+00	ML14-12	20	0.0E+00
ML12-15	72	0.0E+00	ML13-15	10		ML14-12	24	
ML13-9	0	0.0E+00	ML13-15	12		ML14-12	26	
ML13-9	2		ML13-15	14		ML14-12	32	
ML13-9	4		ML13-15	16		ML14-12	36	
ML13-9	6		ML13-15	18		ML14-12	40	
ML13-9	8	0.0E+00	ML13-15	20	0.0E+00	ML14-12	44	
ML13-9	10		ML13-15	24		ML14-12	48	
ML13-9	12		ML13-15	26		ML14-12	52	
ML13-9	14	0.0E+00	ML13-15	32		ML14-12	56	
ML13-9	16		ML13-15	36		ML14-12	60	
ML13-9	18		ML13-15	40		ML14-12	72	2.0E+00
ML13-9	20	0.0E+00	ML13-15	44		ML14-15	0	0.0E+00
ML13-9	24		ML13-15	48		ML14-15	2	
ML13-9	28	0.0E+00	ML13-15	52		ML14-15	4	
ML13-9	32		ML13-15	56		ML14-15	6	
ML13-9	36	0.0E+00	ML13-15	60		ML14-15	8	0.0E+00
ML13-9	40	1.1E-01	ML13-15	72	2.1E+00	ML14-15	10	
ML13-9	44	0.0E+00	ML14-9	0	0.0E+00	ML14-15	12	
ML13-9	48	0.0E+00	ML14-9	2		ML14-15	14	
ML13-9	52	0.0E+00	ML14-9	4		ML14-15	16	
ML13-9	56	0.0E+00	ML14-9	6		ML14-15	18	
ML13-9	60	0.0E+00	ML14-9	8	0.0E+00	ML14-15	20	0.0E+00
ML13-9	72	0.0E+00	ML14-9	10		ML14-15	24	
ML13-12	0	0.0E+00	ML14-9	12		ML14-15	26	
ML13-12	2		ML14-9	14	4.6E+00	ML14-15	32	
ML13-12	4		ML14-9	16		ML14-15	36	
ML13-12	6		ML14-9	18		ML14-15	40	
ML13-12	8	0.0E+00	ML14-9	20	3.8E+01	ML14-15	44	
ML13-12	10		ML14-9	24		ML14-15	48	
ML13-12	12		ML14-9	28	2.1E+01	ML14-15	52	
ML13-12	14		ML14-9	32	1.9E+01	ML14-15	56	
ML13-12	16		ML14-9	36	1.4E+01	ML14-15	60	

Table D5. Tracer test data from ∅X174 injected into well I4, October 2, 1996.

Well	Hour	PFU/ml
ML14-15	72	1.1E-01
ML17-9	0	0.0E+00
ML17-9	2	
ML17-9	4	
ML17-9	6	
ML17-9	8	0.0E+00
ML17-9	10	
ML17-9	12	
ML17-9	14	
ML17-9	16	
ML17-9	18	
ML17-9	20	7.9E+00
ML17-9	24	
ML17-9	26	
ML17-9	32	
ML17-9	36	
ML17-9	40	9.5E+00
ML17-9	44	
ML17-9	48	
ML17-9	52	
ML17-9	56	
ML17-9	60	
ML17-9	72	1.0E+01
ML17-12	0	0.0E+00
ML17-12	2	
ML17-12	4	
ML17-12	6	
ML17-12	8	0.0E+00
ML17-12	10	
ML17-12	12	
ML17-12	14	
ML17-12	16	
ML17-12	18	
ML17-12	20	0.0E+00
ML17-12	24	
ML17-12	26	
ML17-12	32	
ML17-12	36	
ML17-12	40	
ML17-12	44	
ML17-12	48	
ML17-12	52	
ML17-12	56	
ML17-12	60	
ML17-12	72	0.0E+00
ML18-9	0	0.0E+00
ML18-9	2	
ML18-9	4	
ML18-9	6	
ML18-9	8	0.0E+00
ML18-9	10	
ML18-9	12	
ML18-9	14	
ML18-9	16	
ML18-9	18	
ML18-9	20	0.0E+00
ML18-9	24	
ML18-9	26	
ML18-9	32	
ML18-9	36	
ML18-9	40	8.8E-01
ML18-9	44	
ML18-9	48	
ML18-9	52	
ML18-9	56	
ML18-9	60	
ML18-9	72	1.3E+00
ML18-12	0	0.0E+00
ML18-12	2	
ML18-12	4	
ML18-12	6	
ML18-12	8	0.0E+00
ML18-12	10	
ML18-12	12	
ML18-12	14	
ML18-12	16	
ML18-12	18	
ML18-12	20	0.0E+00
ML18-12	24	
ML18-12	26	
ML18-12	32	
ML18-12	36	
ML18-12	40	
ML18-12	44	
ML18-12	48	
ML18-12	52	
ML18-12	56	
ML18-12	60	
ML18-12	72	9.9E-01
W1	0	
W1	2	
W1	4	0.0E+00
W1	6	
W1	8	3.9E+02
W1	10	
W1	12	5.2E+03
W1	14	4.5E+03
W1	16	
W1	18	
W1	20	2.4E+03
W1	24	
W1	28	
W1	32	
W1	36	
W1	40	9.0E+02
W1	44	
W1	48	
W1	52	
W1	56	
W1	60	
W1	72	1.3E+03
W2	0	0.0E+00
W2	2	
W2	4	0.0E+00
W2	6	
W2	8	0.0E+00
W2	10	
W2	12	
W2	14	0.0E+00
W2	16	
W2	18	
W2	20	1.5E+01
W2	24	
W2	26	
W2	32	
W2	36	
W2	40	1.4E+01
W2	44	1.2E+01
W2	48	8.8E+00
W2	52	7.5E+00
W2	56	8.1E+00
W2	60	8.0E+00
W2	72	8.0E+00

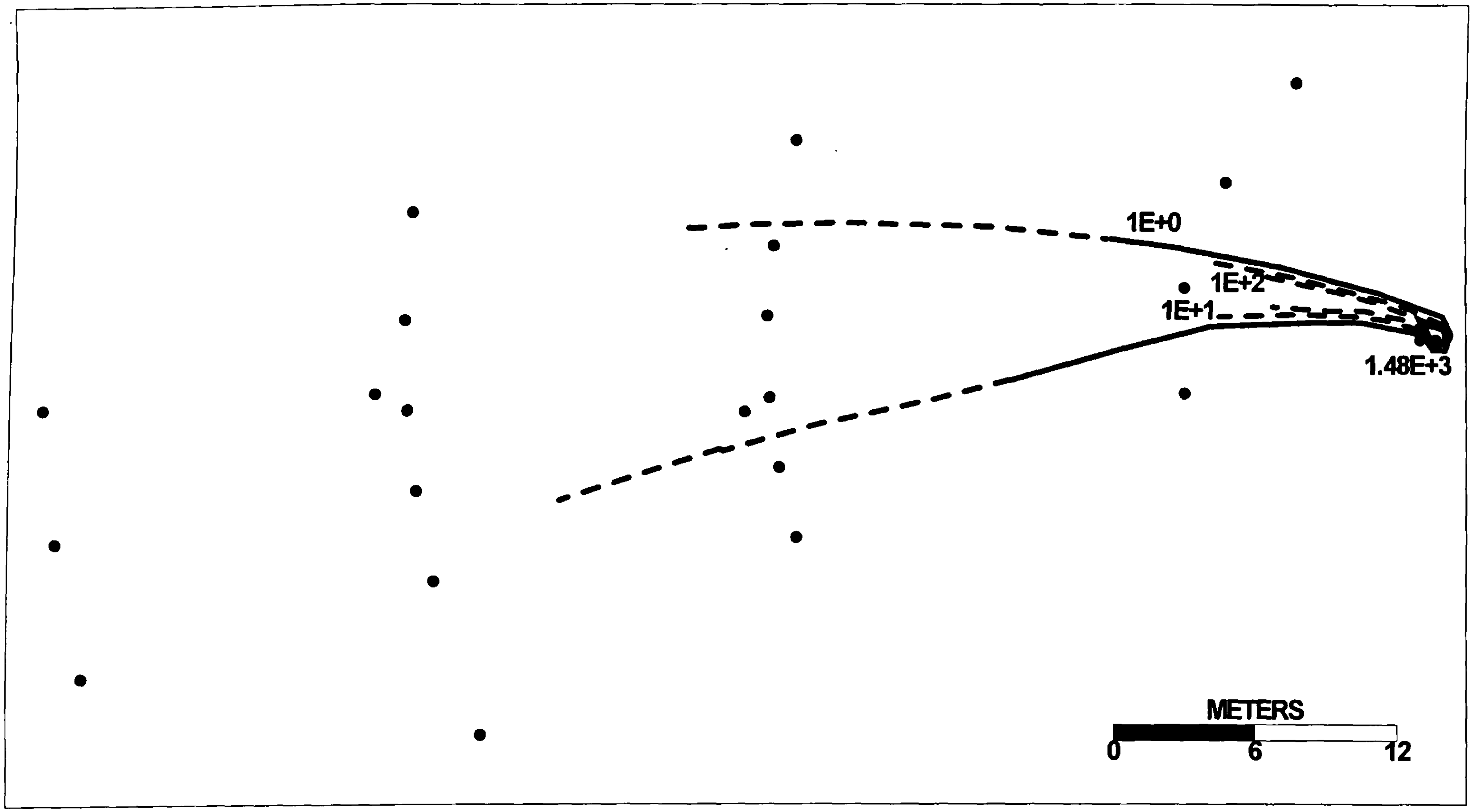

Figure D13. 72hr Poliovirus Plume at 9ft depth from 10/2/96 seeding experiment. Concentrations in PFU/ml, flow direction to the west.

Table D6. Tracer test data from poliovirus type-1 injected into well I4, October 2, 1996.

Well	Hour	PFU/ml	Well	Hour	PFU/ml	Well	Hour	PFU/ml
I4-Old	0		ML0-12	6		ML1-9	18	
I4-New	0		ML0-12	8		ML1-9	20	
Slug	0	5.9E+01	ML0-12	10		ML1-9	24	
Injection	0	4.9E+01	ML0-12	12		ML1-9	26	
I4	0	3.4E+06	ML0-12	14		ML1-9	32	
I4	2	1.3E+06	ML0-12	16		ML1-9	36	
I4	4		ML0-12	18		ML1-9	40	
I4	6		ML0-12	20		ML1-9	44	
I4	8	8.0E+04	ML0-12	24		ML1-9	48	
I4	10		ML0-12	26		ML1-9	52	
I4	12		ML0-12	32		ML1-9	56	
I4	14		ML0-12	36		ML1-9	60	
I4	16		ML0-12	40		ML1-9	72	
I4	18		ML0-12	44		ML2-9	0	
I4	20	4.0E+04	ML0-12	48		ML2-9	2	4.0E+00
I4	28		ML0-12	52		ML2-9	4	3.8E+02
I4	32		ML0-12	56		ML2-9	6	1.6E+02
I4	36		ML0-12	60		ML2-9	8	2.1E+01
I4	40	2.0E+03	ML0-12	72		ML2-9	10	1.2E+01
I4	44		ML0-15	0		ML2-9	12	
I4	48		ML0-15	2		ML2-9	14	1.0E+00
I4	52		ML0-15	4		ML2-9	16	
I4	56		ML0-15	6		ML2-9	18	
I4	60		ML0-15	8		ML2-9	20	2.0E+00
I4	72	1.5E+03	ML0-15	10		ML2-9	24	
ML0-9	0		ML0-15	12		ML2-9	28	
ML0-9	2	0.0E+00	ML0-15	14		ML2-9	32	
ML0-9	4	1.0E+00	ML0-15	16		ML2-9	36	
ML0-9	6	0.0E+00	ML0-15	18		ML2-9	40	0.0E+00
ML0-9	8	0.0E+00	ML0-15	20		ML2-9	44	
ML0-9	10	0.0E+00	ML0-15	24		ML2-9	48	
ML0-9	12		ML0-15	26		ML2-9	52	
ML0-9	14		ML0-15	32		ML2-9	56	
ML0-9	16		ML0-15	36		ML2-9	60	
ML0-9	18		ML0-15	40		ML2-9	72	4.0E+00
ML0-9	20	0.0E+00	ML0-15	44		ML2-12	0	
ML0-9	24		ML0-15	48		ML2-12	2	
ML0-9	26		ML0-15	52		ML2-12	4	
ML0-9	32		ML0-15	56		ML2-12	6	
ML0-9	36		ML0-15	60		ML2-12	8	
ML0-9	40	0.0E+00	ML0-15	72		ML2-12	10	
ML0-9	44		ML1-9	0		ML2-12	12	
ML0-9	48		ML1-9	2		ML2-12	14	
ML0-9	52		ML1-9	4		ML2-12	16	
ML0-9	56		ML1-9	6		ML2-12	18	
ML0-9	60	0.0E+00	ML1-9	8		ML2-12	20	
ML0-9	72	0.0E+00	ML1-9	10		ML2-12	24	
ML0-12	0		ML1-9	12		ML2-12	26	
ML0-12	2		ML1-9	14		ML2-12	32	
ML0-12	4		ML1-9	16		ML2-12	36	

Table D6. Tracer test data from poliovirus type-1 injected into well I4, October 2, 1996.

Well	Hour	PFU/ml	Well	Hour	PFU/ml	Well	Hour	PFU/ml
ML2-12	40		ML3-9	72		ML7-12	10	
ML2-12	44		ML6-9	0		ML7-12	12	
ML2-12	48		ML6-9	2		ML7-12	14	
ML2-12	52		ML6-9	4		ML7-12	16	
ML2-12	56		ML6-9	6		ML7-12	18	
ML2-12	60		ML6-9	8		ML7-12	20	
ML2-12	72		ML6-9	10		ML7-12	24	
ML2-15	0		ML6-9	12		ML7-12	26	
ML2-15	2		ML6-9	14		ML7-12	32	
ML2-15	4		ML6-9	16		ML7-12	36	
ML2-15	6		ML6-9	18		ML7-12	40	
ML2-15	8		ML6-9	20		ML7-12	44	
ML2-15	10		ML6-9	24		ML7-12	48	
ML2-15	12		ML6-9	26		ML7-12	52	
ML2-15	14		ML6-9	32		ML7-12	56	
ML2-15	16		ML6-9	36		ML7-12	60	
ML2-15	18		ML6-9	40		ML7-12	72	
ML2-15	20		ML6-9	44		ML7-15	0	
ML2-15	24		ML6-9	48		ML7-15	2	
ML2-15	26		ML6-9	52		ML7-15	4	
ML2-15	32		ML6-9	56		ML7-15	6	
ML2-15	36		ML6-9	60		ML7-15	8	
ML2-15	40		ML6-9	72		ML7-15	10	
ML2-15	44		ML7-9	0		ML7-15	12	
ML2-15	48		ML7-9	2		ML7-15	14	
ML2-15	52		ML7-9	4	0.0E+00	ML7-15	16	
ML2-15	56		ML7-9	6		ML7-15	18	
ML2-15	60		ML7-9	8	1.5E+01	ML7-15	20	
ML2-15	72		ML7-9	10	2.5E+01	ML7-15	24	
ML3-9	0		ML7-9	12	2.6E+01	ML7-15	26	
ML3-9	2		ML7-9	14	1.0E+01	ML7-15	32	
ML3-9	4		ML7-9	16	1.0E+00	ML7-15	36	
ML3-9	6		ML7-9	18		ML7-15	40	
ML3-9	8		ML7-9	20	0.0E+00	ML7-15	44	
ML3-9	10		ML7-9	24		ML7-15	48	
ML3-9	12		ML7-9	28		ML7-15	52	
ML3-9	14		ML7-9	32		ML7-15	56	
ML3-9	16		ML7-9	36		ML7-15	60	
ML3-9	18		ML7-9	40	0.0E+00	ML7-15	72	
ML3-9	20		ML7-9	44		ML8-9	0	
ML3-9	24		ML7-9	48		ML8-9	2	
ML3-9	26		ML7-9	52		ML8-9	4	
ML3-9	32		ML7-9	56		ML8-9	6	
ML3-9	36		ML7-9	60		ML8-9	8	
ML3-9	40		ML7-9	72	0.0E+00	ML8-9	10	
ML3-9	44		ML7-12	0		ML8-9	12	
ML3-9	48		ML7-12	2		ML8-9	14	
ML3-9	52		ML7-12	4		ML8-9	16	
ML3-9	56		ML7-12	6		ML8-9	18	
ML3-9	60		ML7-12	8		ML8-9	20	

Table D6. Tracer test data from poliovirus type-1 injected into well I4, October 2, 1996.

Well	Hour	PFU/ml	Well	Hour	PFU/ml	Well	Hour	PFU/ml
ML8-9	24		ML8-15	48		ML9-15	2	
ML8-9	26		ML8-15	52		ML9-15	4	
ML8-9	32		ML8-15	56		ML9-15	6	
ML8-9	36		ML8-15	60		ML9-15	8	
ML8-9	40		ML8-15	72		ML9-15	10	
ML8-9	44		ML9-9	0		ML9-15	12	
ML8-9	48		ML9-9	2		ML9-15	14	
ML8-9	52		ML9-9	4		ML9-15	16	
ML8-9	56		ML9-9	6		ML9-15	18	
ML8-9	60		ML9-9	8		ML9-15	20	
ML8-9	72		ML9-9	10		ML9-15	24	
ML8-12	0		ML9-9	12		ML9-15	26	
ML8-12	2		ML9-9	14		ML9-15	32	
ML8-12	4		ML9-9	16		ML9-15	36	
ML8-12	6		ML9-9	18		ML9-15	40	
ML8-12	8		ML9-9	20		ML9-15	44	
ML8-12	10		ML9-9	24		ML9-15	48	
ML8-12	12		ML9-9	26		ML9-15	52	
ML8-12	14		ML9-9	32		ML9-15	56	
ML8-12	16		ML9-9	36		ML9-15	60	
ML8-12	18		ML9-9	40		ML9-15	72	
ML8-12	20		ML9-9	44		ML19-9	0	
ML8-12	24		ML9-9	48		ML19-9	2	
ML8-12	26		ML9-9	52		ML19-9	4	
ML8-12	32		ML9-9	56		ML19-9	6	
ML8-12	36		ML9-9	60		ML19-9	8	
ML8-12	40		ML9-9	72		ML19-9	10	
ML8-12	44		ML9-12	0		ML19-9	12	
ML8-12	48		ML9-12	2		ML19-9	14	
ML8-12	52		ML9-12	4		ML19-9	16	
ML8-12	56		ML9-12	6		ML19-9	18	
ML8-12	60		ML9-12	8		ML19-9	20	
ML8-12	72		ML9-12	10		ML19-9	24	
ML8-15	0		ML9-12	12		ML19-9	26	
ML8-15	2		ML9-12	14		ML19-9	32	
ML8-15	4		ML9-12	16		ML19-9	36	
ML8-15	6		ML9-12	18		ML19-9	40	
ML8-15	8		ML9-12	20		ML19-9	44	
ML8-15	10		ML9-12	24		ML19-9	48	
ML8-15	12		ML9-12	26		ML19-9	52	
ML8-15	14		ML9-12	32		ML19-9	56	
ML8-15	16		ML9-12	36		ML19-9	60	
ML8-15	18		ML9-12	40		ML19-9	72	
ML8-15	20		ML9-12	44		ML19-12	0	
ML8-15	24		ML9-12	48		ML19-12	2	
ML8-15	26		ML9-12	52		ML19-12	4	
ML8-15	32		ML9-12	56		ML19-12	6	
ML8-15	36		ML9-12	60		ML19-12	8	
ML8-15	40		ML9-12	72		ML19-12	10	
ML8-15	44		ML9-15	0		ML19-12	12	

Table D6. Tracer test data from poliovirus type-1 injected into well I4, October 2, 1996.

Well	Hour	PFU/ml	Well	Hour	PFU/ml	Well	Hour	PFU/ml
ML19-12	14		ML10-9	32		ML11-12	56	
ML19-12	16		ML10-9	36		ML11-12	60	
ML19-12	18		ML10-9	40		ML11-12	72	
ML19-12	20		ML10-9	44		ML12-9	0	
ML19-12	24		ML10-9	48		ML12-9	2	
ML19-12	26		ML10-9	52		ML12-9	4	
ML19-12	32		ML10-9	56		ML12-9	6	
ML19-12	36		ML10-9	60		ML12-9	8	0.0E+00
ML19-12	40		ML10-9	72		ML12-9	10	
ML19-12	44		ML11-9	0		ML12-9	12	
ML19-12	48		ML11-9	2		ML12-9	14	0.0E+00
ML19-12	52		ML11-9	4		ML12-9	16	
ML19-12	56		ML11-9	6		ML12-9	18	
ML19-12	60		ML11-9	8		ML12-9	20	0.0E+00
ML19-12	72		ML11-9	10		ML12-9	24	
ML19-15	0		ML11-9	12		ML12-9	28	0.0E+00
ML19-15	2		ML11-9	14		ML12-9	32	0.0E+00
ML19-15	4		ML11-9	16		ML12-9	36	0.0E+00
ML19-15	6		ML11-9	18		ML12-9	40	0.0E+00
ML19-15	8		ML11-9	20		ML12-9	44	
ML19-15	10		ML11-9	24		ML12-9	48	
ML19-15	12		ML11-9	26		ML12-9	52	
ML19-15	14		ML11-9	32		ML12-9	56	0.0E+00
ML19-15	16		ML11-9	36		ML12-9	60	0.0E+00
ML19-15	18		ML11-9	40		ML12-9	72	0.0E+00
ML19-15	20		ML11-9	44		ML12-12	0	
ML19-15	24		ML11-9	48		ML12-12	2	
ML19-15	26		ML11-9	52		ML12-12	4	
ML19-15	32		ML11-9	56		ML12-12	6	
ML19-15	36		ML11-9	60		ML12-12	8	
ML19-15	40		ML11-9	72		ML12-12	10	
ML19-15	44		ML11-12	0		ML12-12	12	
ML19-15	48		ML11-12	2		ML12-12	14	
ML19-15	52		ML11-12	4		ML12-12	16	
ML19-15	56		ML11-12	6		ML12-12	18	
ML19-15	60		ML11-12	8		ML12-12	20	
ML19-15	72		ML11-12	10		ML12-12	24	
ML10-9	0		ML11-12	12		ML12-12	26	
ML10-9	2		ML11-12	14		ML12-12	32	
ML10-9	4		ML11-12	16		ML12-12	36	
ML10-9	6		ML11-12	18		ML12-12	40	
ML10-9	8		ML11-12	20		ML12-12	44	
ML10-9	10		ML11-12	24		ML12-12	48	
ML10-9	12		ML11-12	26		ML12-12	52	
ML10-9	14		ML11-12	32		ML12-12	56	
ML10-9	16		ML11-12	36		ML12-12	60	
ML10-9	18		ML11-12	40		ML12-12	72	
ML10-9	20		ML11-12	44		ML12-15	0	
ML10-9	24		ML11-12	48		ML12-15	2	
ML10-9	26		ML11-12	52		ML12-15	4	

Table D6. Tracer test data from poliovirus type-1 injected into well I4, October 2, 1996.

Well	Hour	PFU/ml
ML12-15	6	
ML12-15	8	
ML12-15	10	
ML12-15	12	
ML12-15	14	
ML12-15	16	
ML12-15	18	
ML12-15	20	
ML12-15	24	
ML12-15	26	
ML12-15	32	
ML12-15	36	
ML12-15	40	
ML12-15	44	
ML12-15	48	
ML12-15	52	
ML12-15	56	
ML12-15	60	
ML12-15	72	
ML13-9	0	
ML13-9	2	
ML13-9	4	
ML13-9	6	
ML13-9	8	0.0E+00
ML13-9	10	
ML13-9	12	
ML13-9	14	
ML13-9	16	
ML13-9	18	
ML13-9	20	0.0E+00
ML13-9	24	
ML13-9	28	
ML13-9	32	0.0E+00
ML13-9	36	
ML13-9	40	0.0E+00
ML13-9	44	
ML13-9	48	
ML13-9	52	0.0E+00
ML13-9	56	
ML13-9	60	
ML13-9	72	0.0E+00
ML13-12	0	
ML13-12	2	
ML13-12	4	
ML13-12	6	
ML13-12	8	
ML13-12	10	
ML13-12	12	
ML13-12	14	
ML13-12	16	
ML13-12	18	
ML13-12	20	
ML13-12	24	
ML13-12	26	
ML13-12	32	
ML13-12	36	
ML13-12	40	
ML13-12	44	
ML13-12	48	
ML13-12	52	
ML13-12	56	
ML13-12	60	
ML13-12	72	
ML13-15	0	
ML13-15	2	
ML13-15	4	
ML13-15	6	
ML13-15	8	
ML13-15	10	
ML13-15	12	
ML13-15	14	
ML13-15	16	
ML13-15	18	
ML13-15	20	
ML13-15	24	
ML13-15	26	
ML13-15	32	
ML13-15	36	
ML13-15	40	
ML13-15	44	
ML13-15	48	
ML13-15	52	
ML13-15	56	
ML13-15	60	
ML13-15	72	
ML14-9	0	
ML14-9	2	
ML14-9	4	
ML14-9	6	
ML14-9	8	0.0E+00
ML14-9	10	
ML14-9	12	
ML14-9	14	1.0E+00
ML14-9	16	
ML14-9	18	
ML14-9	20	1.0E+00
ML14-9	24	
ML14-9	28	0.0E+00
ML14-9	32	0.0E+00
ML14-9	36	
ML14-9	40	0.0E+00
ML14-9	44	
ML14-9	48	
ML14-9	52	0.0E+00
ML14-9	56	
ML14-9	60	0.0E+00
ML14-9	72	0.0E+00
ML14-12	0	
ML14-12	2	
ML14-12	4	
ML14-12	6	
ML14-12	8	
ML14-12	10	
ML14-12	12	
ML14-12	14	
ML14-12	16	
ML14-12	18	
ML14-12	20	
ML14-12	24	
ML14-12	26	
ML14-12	32	
ML14-12	36	
ML14-12	40	
ML14-12	44	
ML14-12	48	
ML14-12	52	
ML14-12	56	
ML14-12	60	
ML14-12	72	
ML14-15	0	
ML14-15	2	
ML14-15	4	
ML14-15	6	
ML14-15	8	
ML14-15	10	
ML14-15	12	
ML14-15	14	
ML14-15	16	
ML14-15	18	
ML14-15	20	
ML14-15	24	
ML14-15	26	
ML14-15	32	
ML14-15	36	
ML14-15	40	
ML14-15	44	
ML14-15	48	
ML14-15	52	
ML14-15	56	
ML14-15	60	

Table D6. Tracer test data from poliovirus type-1 injected into well I4, October 2, 1996.

Well	Hour	PFU/ml	Well	Hour	PFU/ml	Well	Hour	PFU/ml
ML14-15	72		ML18-9	10		W1	24	
ML17-9	0	0.0E+00	ML18-9	12		W1	28	
ML17-9	2		ML18-9	14		W1	32	
ML17-9	4		ML18-9	16		W1	36	
ML17-9	6		ML18-9	18		W1	40	3.0E+00
ML17-9	8	0.0E+00	ML18-9	20	1.0E+00	W1	44	
ML17-9	10		ML18-9	24		W1	48	
ML17-9	12		ML18-9	26		W1	52	
ML17-9	14		ML18-9	32		W1	56	
ML17-9	16		ML18-9	36		W1	60	
ML17-9	18		ML18-9	40	0.0E+00	W1	72	0.0E+00
ML17-9	20	1.0E+00	ML18-9	44		W2	0	
ML17-9	24		ML18-9	48		W2	2	
ML17-9	26		ML18-9	52		W2	4	
ML17-9	32		ML18-9	56		W2	6	
ML17-9	36		ML18-9	60		W2	8	0.0E+00
ML17-9	40	1.0E+00	ML18-9	72	0.0E+00	W2	10	
ML17-9	44		ML18-12	0		W2	12	
ML17-9	48		ML18-12	2		W2	14	0.0E+00
ML17-9	52		ML18-12	4		W2	16	
ML17-9	56		ML18-12	6		W2	18	
ML17-9	60		ML18-12	8		W2	20	0.0E+00
ML17-9	72	0.0E+00	ML18-12	10		W2	24	
ML17-12	0		ML18-12	12		W2	26	
ML17-12	2		ML18-12	14		W2	32	
ML17-12	4		ML18-12	16		W2	36	
ML17-12	6		ML18-12	18		W2	40	
ML17-12	8		ML18-12	20		W2	44	
ML17-12	10		ML18-12	24		W2	48	
ML17-12	12		ML18-12	26		W2	52	
ML17-12	14		ML18-12	32		W2	56	
ML17-12	16		ML18-12	36		W2	60	
ML17-12	18		ML18-12	40		W2	72	
ML17-12	20		ML18-12	44				
ML17-12	24		ML18-12	48				
ML17-12	26		ML18-12	52				
ML17-12	32		ML18-12	56				
ML17-12	36		ML18-12	60				
ML17-12	40		ML18-12	72				
ML17-12	44		W1	0				
ML17-12	48		W1	2				
ML17-12	52		W1	4	0.0E+00			
ML17-12	56		W1	6				
ML17-12	60		W1	8	1.3E+01			
ML17-12	72		W1	10				
ML18-9	0		W1	12	3.1E+01			
ML18-9	2		W1	14	1.0E+01			
ML18-9	4		W1	16				
ML18-9	6		W1	18				
ML18-9	8	0.0E+00	W1	20	0.0E+00			

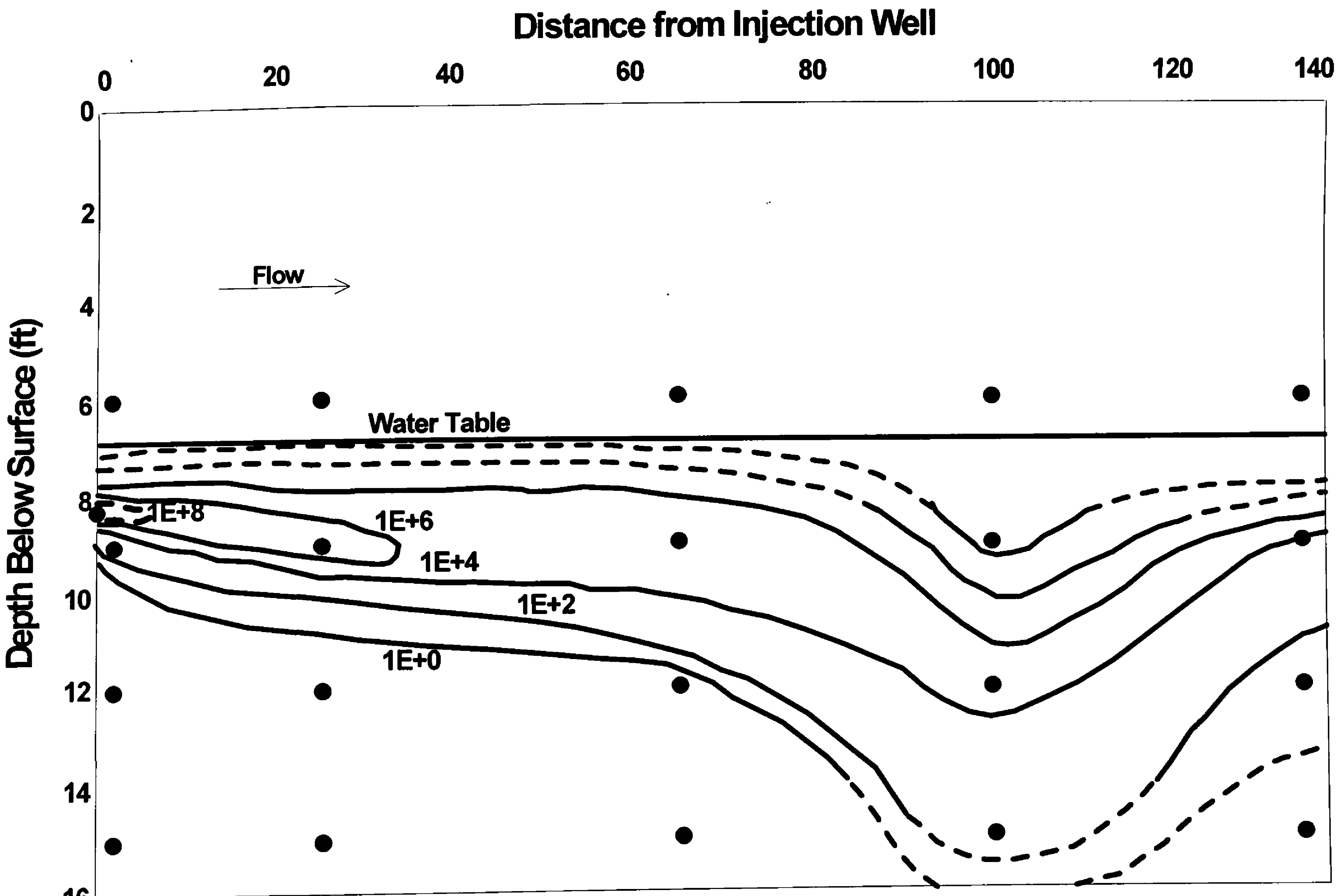

Figure D14. 72hr Cross-section of MS2 plume from 10/2/96 seeding experiment. Concentrations in PFU/ml, flow direction to the west.

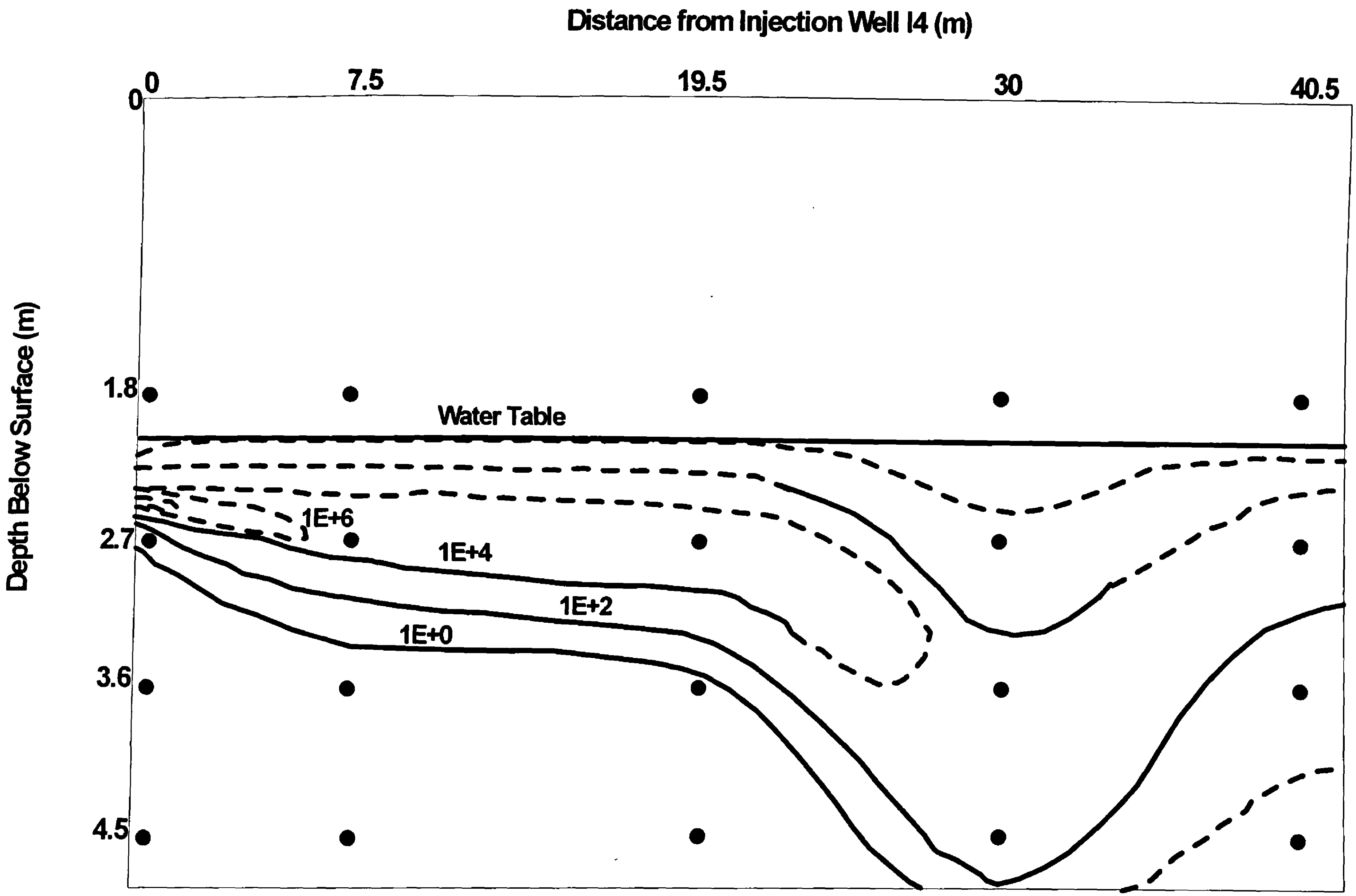

Figure D15. 72hr Cross-section of PRD1 from 10/2/96 seeding experiment. Concentrations in PFU/ml, flow direction to the west.

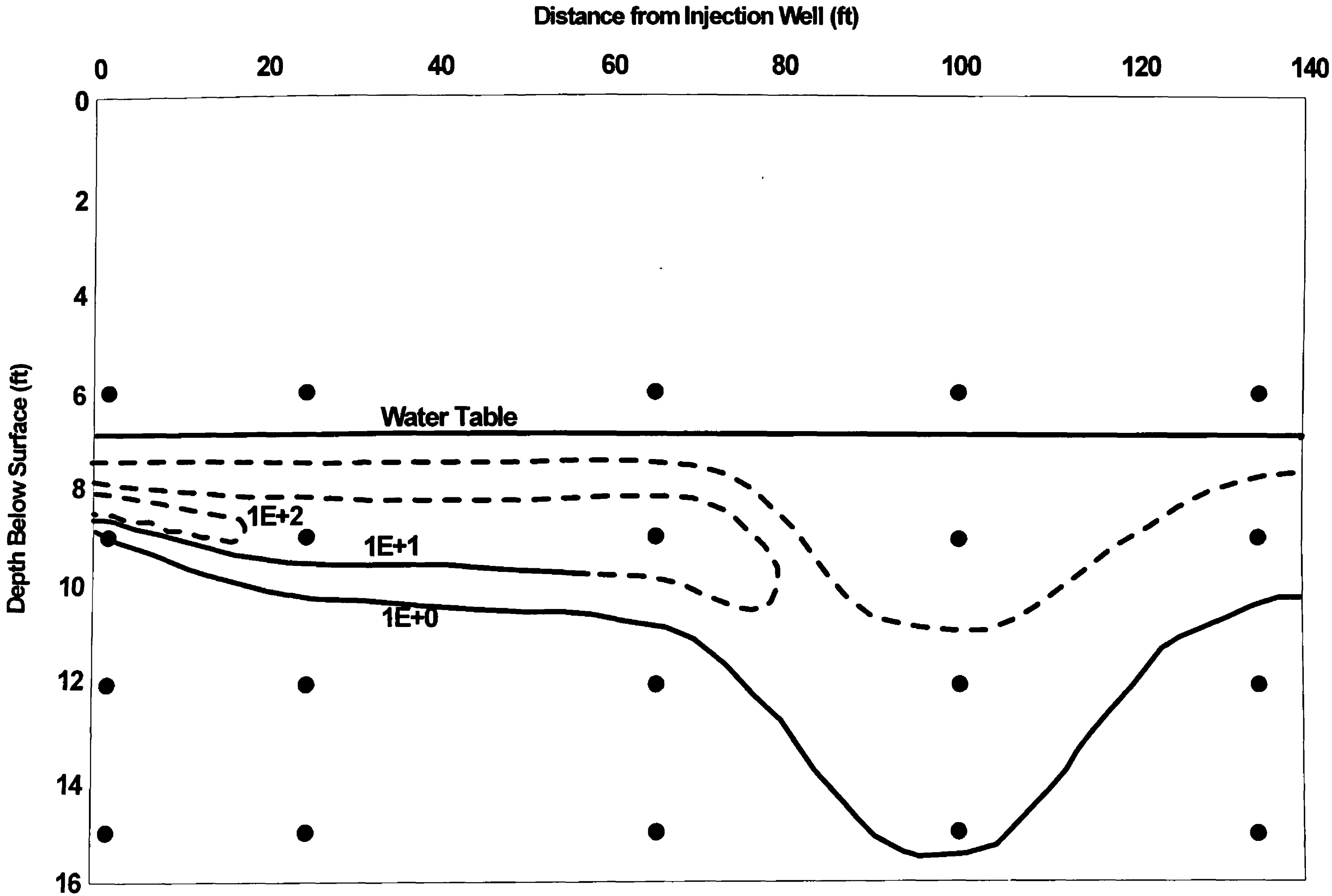

Figure D16. 72hr Cross-section of PRD1 from 10/02/96 seeding experiment. Concentration in PFU/ml, flow direction to the west.